

國立臺灣大學工學院化學工程學系

碩士論文

Department of Chemical Engineering

College of Engineering


National Taiwan University

Master Thesis

己烷噻吩-己烷氧噻吩共聚物(P3HT-P3HOT)

之合成機制探討與性質鑑定

Synthesis, Characterization and Mechanism Investigation
of Poly(3-hexylthiophene-co-3-hexyloxythiophene)
via Grignard Metathesis



吳俊慶

Chun-Ching Wu

指導教授：戴子安 博士

Advisor: Chi-An Dai, Ph.D.

中華民國 97 年 7 月

July, 2008

謝辭

兩年過去了，彷彿是一轉眼的事，首先我第一個要感謝的人就是我的指導教授戴子安老師，老師不僅在實驗上給了我很多的建議與鼓勵，也讓我了解到對於追求學術研究上應有的方法，永遠都要有追求真理的態度，感謝老師讓我了解到如何讓一份研究從無到有，以及處理事情的方法，這兩年真是辛苦您了。

感謝口試委員—芮祥鵬老師、程耀毅老師、王立義老師、邱文英老師對於我論文方面的指導，點出我沒注意到的細節與寫作邏輯的技巧，也給予我很多建議與未來可行的工作，在此非常感謝。

在實驗生活方面，感謝惟哲學長的教導，使我在合成方面碰到的問題得以解決；感謝鈞傑、宜桓學長對於我研究上的幫助，使我的論文更加多采多姿；感謝昂志、安呈、世豪，這兩年我們互相扶持、互相交流，最後大家都一起順利的畢業了。感謝學弟妹偉鈞、莉庭、世鈞、嘉鴻、伯盛的幫助，很多事情如果沒有你們的幫助，我的實驗不會那麼順利。還有化工 206 的學長姐及同學們平常的照顧，讓我在有時很枯燥的實驗中，還可以很開心的繼續努力，另外我們在實驗上的經驗討論，使我節省了很多摸索實驗的時間，謝謝你們。

最後我要特別感謝我的女朋友黃莉雯，平常時對我的照顧，幫我整理家裡，陪我聊天，讓我不寂寞，最後幾個月的那段時間，如果沒有你的打氣以及陪伴，我一定會非常難熬的，我能完成這本論文有一半是你的功勞。另外我要謝謝我的爸爸、媽媽，感謝你們這兩年對我的關心，雖然我們一個禮拜只見一次面，但我每天都可以感受到你們對我的關心，以及無私的付出，我能有今天都是因為你們。

感謝大家的幫忙，讓我能在全球最高學府順利完成我的求學歷程，這一直是我的夢想，如今終於實現，謝謝你們，我對你們每一個人都充滿了無限的感激。

吳俊慶 民國 97 年 7 月 17 日

中文摘要

用格林納反應 (Grignard Reaction) 原理為基礎，然後以鎳 (Ni) 的錯合物當作觸媒合成出一系列同時具有烷基和烷氧基側鏈的噻吩共聚物(P3HT-P3HOT)，接著利用觸媒與分子量的關係實驗，發現共聚物由於受到了溶解度的影響，觸媒與分子量的相關性只限於某個分子量之內，而過了此分子量之值後，減少觸媒的量將再也不能提高共聚物的分子量。此外，我們也利用對於兩個單體不同的進料比例與實際比例實驗中，發現不管在任何不同比例下，烷氧基的噻吩的實際比例皆高於進料比例6~10%。後來再更進一步的實驗中，發現原來是因為烷氧基噻吩再形成格林納反應中間物時，具有比較好的化學選擇性，可以在反應時產生較多的可聚合中間物，而造成這個現象。最後我們利用了共聚公式，將我們的實驗結果回推我們的反應係數，得到 r_1 為1.2， r_2 為0.8， r_1r_2 的乘積為0.96，得到此反應屬於一個高度隨機共聚的行為(random copolymerization)，而不是交互共聚(alternating copolymerization)或是塊狀共聚(block copolymerization)。最後我們將不同比例的烷基和烷氧基側鏈的噻吩共聚物(P3HT-P3HOT)進行紫外-可見光譜(UV-vis)、螢光光譜(PL)、熱裂解分析(TGA)、循環伏安法(CV)、X光散射(XRD)和元件測試，元件效率等一系列的光電性質以及熱性質測試，發覺當烷氧基側鏈的噻吩在共聚物中比例增加時，光譜吸收會產生紅移的現象，再配合循環伏安法

的測試，發覺加入烷氧基側鏈的噻吩會使其最高填滿軌域(HOMO)上升，整體能隙(band gap)下降，也了解到可以藉由控制烷氧基側鏈的噻吩在共聚物的內部比例來控制其最高填滿軌域以及能隙。此外我們發現由於烷氧基較易被氧化的關係，加入含烷氧基側鏈的噻吩會使熱穩定性變差，且經由X光散射的實驗發現加入烷氧基側鏈的噻吩會使整體的結晶性下降，最後，我們將此材料應用於太陽能電池中的活性層上面，發覺雖然降低能隙可以使原件吸收更多的光子，但由於最高填滿軌域的上升，造成元件的開路電壓(Voc)下降而影響元件的效率。

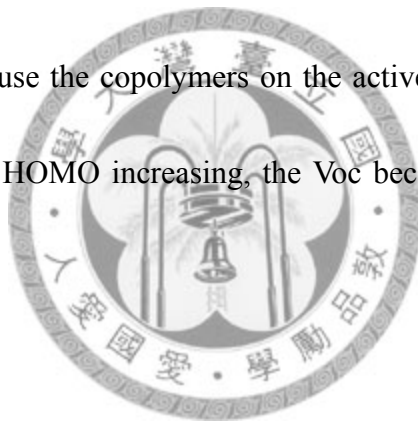


關鍵字: 格林納反應、烷基、烷氧基、噻吩共聚物、隨機共聚物、低能隙共聚物、推電子性質高分子

Abstract

Poly(3-hexylthiophene-co-3-hexyloxythiophene) (P3HT-P3HOT) was synthesized using Grignard reaction, and confirm the inert structure by H NMR. And we do a series of experiments about the relationship of catalyst and molecular weight to study the mechanism of copolymerization, due to the effect of solubility, we find that the copolymerization only obey the GRIM chain-growth phenomenon below certain molecular weight, after is number the molecular won't grow up even you reduce the amount of catalyst. And we find the real ratio of 3-alkoxythiophene is always 6~10% higher than feed ratio in different molar fraction of comonomer experiment. And we assume the phenomenon is because of the 3-alkoxythiophene has well degree of regiocontrol than 3-alkylthiophene. That is, 3-alkoxythiophene will form more react Grignard intermediate than 3-alkylthiophene. And we also use copolymerization equation and our result to calculate the monomer reactivity ratios r_1 and r_2 , and r_1 is equal to 1.2 and r_2 is equal to 0.8, the multiple of r_1 and r_2 is equal to 0.96, indirectly prove the copolymerization is a random copolymerization rather than alternating or block copolymerization. We choose five different fraction of copolymers and detect in UV-vis, photoluminescence(PL), cyclic voltammetry(CV), thermal gravimetric analysis(TGA), X-ray diffraction(XRD) and solar device. And when we add

alkoxythiophene into our copolymer, it will be red shift in optical absorption because of the electro-donation property of alkoxythiophene, and the highest occupied molecule orbital (HOMO) increase and the band gap decrease when we increase the mole fraction of alkoxythiophene, in other words, we can control the HOMO and the band gap by controlling the mole fraction of alkoxythiophene. In TGA test of thermal stability, because the alkoxy is more oxidize, the thermal stability become worse when we increase the mole fraction of alkoxythiophene, and also the crystallinity in the copolymers. Finally , we use the copolymers on the active layer of the organic solar cell, due to the reason of HOMO increasing, the Voc become smaller and lower the efficiency.



Keywords: Poly(3-hexylthiophene-co-3-hexyloxythiophene)·P3HT-P3HOT·Grignard reaction·random copolymer·alkoxy-substituted thiophene·low band gap copolymer.

Index

Chapter 1 General introduction 1

- 1.1 The origin of semiconducting behavior[6] 1
- 1.2 History and synthesis of Poly(alkyl-thiophene)..... 4
- 1.3 Configuration of Poly(alkyl-thiophene)..... 5
- 1.4 Mechanism of the Nickel-Initiated Grignard reaction 8
- 1.5 Photovoltaic properties of poly(3-alkyl thiophene) 10
- 1.6 Working principles of organic solar cell[6] 11
- 1.7 Solar cell performance of P3HT-PCBM bulk heterojunction system..... 14
- 1.8 Development on poly(3-alkoxythiophene) 16
- 1.9 Development on poly(alkoxythiophene-co-alkylthiophene) 17

Chapter 2 Experimental Part 19

- 2.1 Experiment materials 19
- 2.2 Experiment instrument..... 20
- 2.3 Synthesis of 3-hexylthiophene 21
- 2.4 Synthesis of 2,5-dibromo-3-hexylthiophene 22
- 2.5 Synthesis of 3-hexyloxythiophene 23
- 2.6 Synthesis of 2,5-dibromo-3-hexyloxythiophene 24
- 2.7 Synthesis of poly(-3-hexylthiophene)-co-poly (-3-hexyloxy thiophene) by the Grignard Metathesis method..... 25
- 2.8 Experiment in the different feed ratio of 2,5,Br-3HOT and add the same molar ratio of catalyst. 26
- 2.9 Experiment of different molar ratio of catalyst in equal molar fraction of two monomers system (P3HT-P3HOT[5:5]) 27
- 2.10 Quenching result of Grignard metathesis reaction of 2,5,dibromo-3-hexylthiophene and 2,5,dibromo-3-hexyloxythiophene 28

Chapter 3 Result and discussion 30

- 3.1 Synthesis of 3-hexylthiophene 30
- 3.2 Synthesis of 2,5-dibromo-3-hexylthiophene 30
- 3.3 Synthesis of 3-hexyloxythiophene..... 31
- 3.4 Synthesis of 2,5-dibromo-3-hexyloxythiophene 31
- 3.5 Experiment in the different feed ratio of 2,5,Br-3HOT and add the same molar ratio of catalyst. 31

3.6	Experiment of different molar ratio of catalyst in equal molar fraction of two monomers system (P3HT-P3HOT[5:5])	32
3.7	Quenching experiment of Grignard metathesis reaction of 2,5,dibromo-3-hexylthiophene and 2,5,dibromo-3-hexyloxythiophene	35
3.8	Adjustment of the ideal molecular calculation in P3HT-P3HOT[5:5] system based on the quenching experiments	36
3.9	Mechanism prediction of P3HT-P3HOT[5:5] system	37
3.10	Calculation of the reactivity ratio in 2,5,Br-3-HT and 2,5,Br-3- HOT copolymerization base on the copolymerization equation.....	38
3.11	Characteristic of five different molar fraction of P3HT-P3HOT	40
3.12	Appearance	40
3.13	UV-Visible Absorption of P3HT-P3HOT in different molar fraction	41
3.14	Electrochemical Characterization of P3HT-P3HOT in different molar fraction	42
3.15	X-ray diffraction (XRD) of P3HT-P3HOT in different molar fraction	44
3.16	Thermal analysis (TGA)	45
3.17	FT IR.....	46
3.18	Organic solar cell performance	47
Chapter4 Conclusion.....		48
Chapter5 Reference.....		50

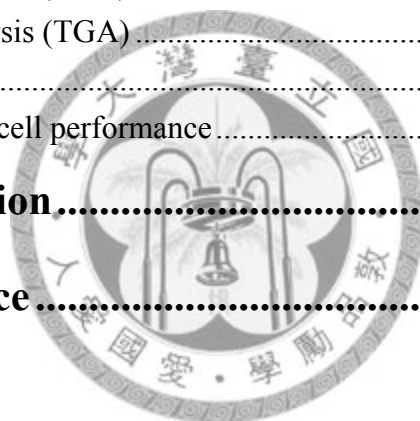


Table index

Table 2.1 Experiment in the different feed ratio of 2,5,Br-3HOT and add the same molar ratio of catalyst.	81
Table 2.2 Experiment of different molar ratio of catalyst in equal molar fraction of two monomers system.....	82
Table 3.1 Summary of five different molar fraction of 3-HT and 3-HOT experiment	83
Table 3.2 Summary of the different ratio of monomer to Ni(dppp)Cl ₂ experiment results in equal molar fraction of 3HT and 3HOT system(P3HT-P3HOT[5:5])	84
Table 3.3 Photovoltaic and thermal properties of five different molar fraction of 3-HT and 3-HOT copolymer	85
Table 3.4 X-ray diffraction 2 θ positions and calculated d spacing of P3HT-P3HOT...	86
Table 3.5 Summary of P3HT-P3HOT/PCBM bulk heterojunction solar cell performance	87
Table 3.6 All experiments of the relationship between mole percentage and derived Mn.....	88

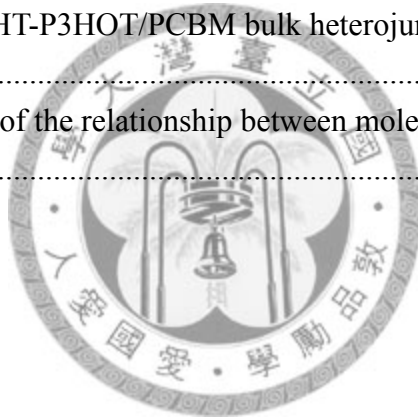


Figure index

Figure 3.1	H NMR of 3-hexyl thiophene.....	53
Figure 3.2	H NMR of 2,5,dibromo-3-hexyl thiophene.....	54
Figure 3.3	H NMR of 3-hexyloxy thiophene.....	55
Figure 3.4	H NMR of 2,5,dibromo-3-hexyloxy thiophene.....	56
Figure 3.5	H NMR of poly(3-hexyl thiophene).....	57
Figure 3.6	H NMR of poly(3-hexyl thiophene)-co-poly(3-hexyloxy thiophene) Feed ratio: 7:3.....	58
Figure 3.7	H NMR of poly(3-hexyl thiophene)-co-poly(3-hexyloxy thiophene) Feed ratio: 5:5.....	59
Figure 3.8	H NMR of poly(3-hexyl thiophene)-co-poly(3-hexyloxy thiophene) Feed ratio: 3:7.....	60
Figure 3.9	H NMR of poly(3-hexyloxy thiophene).....	61
Figure 3.10	Different ratio of monomer to Ni(dppp)Cl ₂ results in equal molar of 3HT and 3HOT system(P3HT-P3HOT[5:5]).....	62
Figure 3.11	Five GPC peak of different ratio of monomer to Ni(dppp)Cl ₂ results in equal molar of 3HT and 3HOT system(P3HT-P3HOT[5:5]).....	63
Figure 3.12	The relationship of Mn and [monomer]/[Ni(dppp)Cl ₂] in different molar ratio of P3HT-P3HOT.....	64
Figure 3.13	Quenching result of Grignard metathesis reaction of 3-hexylthiophene..	65
Figure 3.14	Quenching result of Grignard metathesis reaction of 3-hexyloxythiophene.....	66
Figure 3.15	Different ratio of monomer to Ni(dppp)Cl ₂ results in equal molar of 3HT and 3HOT system(P3HT-P3HOT[5:5]).....	67
Figure 3.16	Mechanism prediction of equal molar of 3-HT and 3-HOT copolymerization(P3HT-P3HOT[5:5]).....	68
Figure 3.17	The relationship between the molar fraction of 3-HOT in comonomer feed(f ₁) and the molar fraction of 3-HOT in copolymer(F ₁).....	69
Figure 3.18	Outlook of five different molar fraction of P3HT-P3HOT, from left to right are (a)P3HOT, (b)P3HT-P3HOT[3:7], (c)P3HT-P3HOT[5:5], (d)P3HT-P3HOT[7:3], (e)P3HT respectively.....	70
Figure 3.19	UV-absorption of five copolymers in chloroform solution.....	71
Figure 3.20	UV-absorption of five copolymers in thin film state.....	72
Figure 3.21	X-ray diffraction patterns of five polymer films cast from chloroform solutions.....	73

Figure 3.22 (a) simulate arrangement inside P3HT	74
Figure 3.23 TGA curve of five polymer	75
Figure 3.24 Cyclic voltammograms diagram(CV) of five different molar fraction of P3HT-P3HOT(A)P3HOT (B)P3HT-P3HOT[3:7] (C)P3HT-P3HOT[5:5] (D)P3HT-P3HOT[7:3] (E)P3HT.....	76
Figure3.25 Energy-level diagram of five different molar fraction of P3HT-P3HOT ..	77
Figure 3.26 FT-IR of five different molar fraction of P3HT-P3HOT	78
Figure 3.27 The current-voltage characteristics of a P3HT-P3HOT/PCBM bulk heterojunction solar cell.....	79
Figure 3.28 UV-vis of five different molar fraction of P3HT-P3HOT blend with PCBM in equal mole.....	80



Chapter 1 General introduction

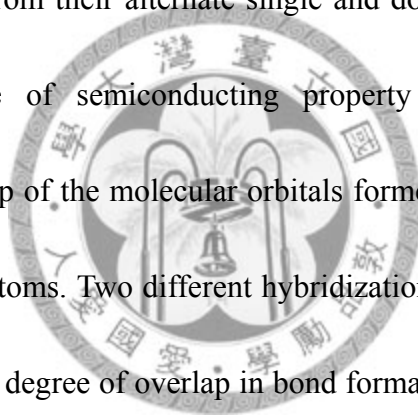
The conjugated polymer-based electronics has rapidly investigating wherever the advantages of low cost, flexibility and lightweight is desirable. In the recently, conjugated polymers have a lot of applications such as photovoltaic devices[1, 2], integrated electronic circuits based on field effect transistors[3, 4] and the polymer-based light emitting diodes. To fulfill the energy need in the future. Flexible and cheap polymer solar cells are considered as the most significant devices[5]. The best performing polymer solar cell was made by bulk heterojunction to an active layer, which is blend with each other and use spin coating method to form a thin film, was polymer/molecule blends thin film on active layer, in such active layer, photo generated electron-hole pairs, called exciton, are separated at the donar acceptor interface and the free charge carriers are collected by the respective electrodes.

And the free carriers are collected by respective electrodes. Bulk heterojunction films constructed from a glass substrate such as ITO are processed from solutions mainly through spin coating method, which is quite easy and cheap.

1.1 The origin of semiconducting behavior [6]

Since carbon atom (C-atom) is the main building block of most polymers, the type of bonds that its valence electrons make with other C-atoms or other elements

determines the overall electronic properties of the respective polymer. Polymers can, in general, be categorized as saturated and unsaturated based on the number and type of the carbon valence electrons involved in the chemical bonding between consecutive C-atoms along the main chain of the polymers. Saturated polymers are insulators since all the four valence electrons of C-atom are used up in covalent bonds, whereas most conductive polymers have unsaturated conjugated structure. π -Conjugated polymers are excellent examples of unsaturated polymers whose electronic configuration from their alternate single and double carbon-carbon bonds. The fundamental source of semiconducting property of conjugated polymers originates from the overlap of the molecular orbitals formed by the valence electrons of chemically bonded C-atoms. Two different hybridizations are shown in Fig2.1, the sp^3 hybrids allow a strong degree of overlap in bond formation with another atom and this produces high bond strength and stability in the molecules. In most carbon compounds containing σ -bonds are sp^3 hybrid orbital, which is saturated bond and high band gap and classified as insulator. And the sp^2 hybridization has one unpaired electron (π -electron) per C-atom. The three sp^2 hybrid orbitals of a C-atom arrange themselves in three-dimensional space to attain stable configuration. And the residue Pz orbital exhibit π -overlap, which results into a delocalization of an electron along along the polymer chain. Therefore, the π -bonds are considered as the basic source of



transport band in the conjugated systems[7, 8].

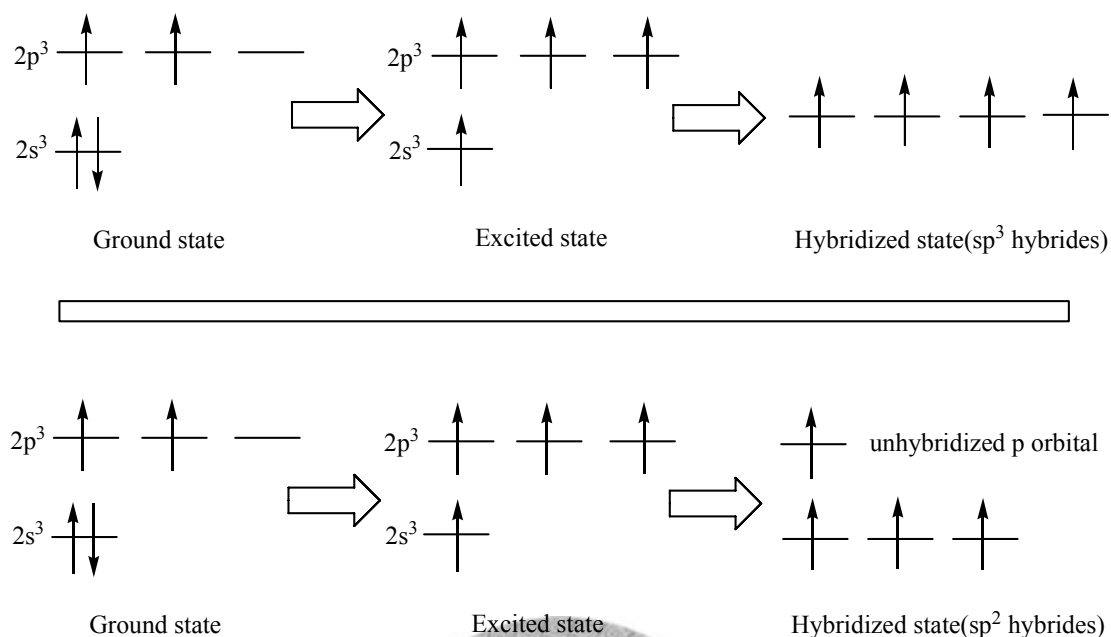


Fig2.1 The hybridizations of the valence shell electrons of a carbon atom. The upper and lower panels show sp^3 and sp^2 hybridization, respectively[6].

Some polymers have semiconducting properties due to their unique structural behavior such as formation of alternating single and double bonds between the adjacent backbone carbon atoms. These conducting polymers are known as π -conjugated polymers. The semiconducting polymers have attracted considerable attention due to their wide range of applications. And a typically π -conjugated polymer poly(3-alkylthiophene)(P3ATS) had been discussed for several years due to its good performance in organic solar cell.

Poly(3-alkylthiophenes) belong to the most extensively studied conductive polymers in the past decade due to their solubility, which is rare in polyconjugated systems, and their interesting electrochemical and physical properties make a lot of tension recently

year. And we will have a simple introduce in P3AT about its history and some photovoltaic properties.

1.2 History and synthesis of Poly (alkyl-thiophene)

The study of polythiophene has intensified in 1980. The maturation of the field of conducting polymers was confirmed by the awarding of the 2000 Nobel Prize in Chemistry to Alan Heeger, Alan MacDiarmid, and Hideki Shirakawa “for the discovery and development of conductive polymers.” The most notable property of these materials, electrical conductivity, results from the delocalization of electrons along the polymer backbone. But, conductivity is not the only interesting property resulting from electron delocalization. But the optical properties of these materials, with dramatic color shifts in response to changes in solvent, temperature, applied potential[9]. But the development was restricted in solubility, at 1985, Elsenbaumer develops a new polythiophene derivative Poly (3-alkylthiophene) (P3AT) which contains alkyl side chain to solve the problem of solubility. After that, a lot of relative research had been investigated, there are many way to synthesize P3AT, such as electrochemical polymerization(Sato1991) and oxidative polymerization by iron(III) chloride(Sugimoto 1986) had been reported in early time[10], and the configuration was regiorandom which the photovoltaic property will decrease, the regioregular

P3AT had been synthesized at 1993 by McCullough who used Grignard reaction and nickel complex($\text{Ni}(\text{dppp})\text{Cl}_2$) to synthesis a highly head-to tail configuration P3AT, and another way to synthesis highly head-to-tail P3AT was reported by Rieke at 1995[11], who used highly reactive “Rieke zinc(Zn^*)” to activate the monomer and nickel complex($\text{Ni}(\text{dppp})\text{Cl}_2$) as a initiator, also synthesize a highly H-T regioregular P3AT up to 98%^[10].

1.3 Configuration of Poly(alkyl-thiophene)

There are four possible configuration in P3AT: 1.head-to-tail head-to-tail(HT-HT) 2.head-to-tail head-to-head(HT-HH) 3.tail-to-tail head-to-tail(TT-HT) 4.tail-to-tail head-to-head(TT-HH), as shown in Figure2.2, and the real configuration inside the P3AT can be analysed by H NMR, there are different chemical shift on the proton of the thiophene ring(H1) and α -methylene-H of the side chain, as shown in Table2.1.

The best configuration for the photovoltaic property is HT-HT, due to the arrangement of alkyl side will be more regular than other three configurations, otherwise, the HT-HT configuration also help the arrangement of polymer backbone, and it will increase π - π stacking to form a coplanar structure. it can be proved by X-ray diffraction(XRD)[12], the morphology of HT-HT P3AT is lamellar[13] which appears more regularity than others. The 2-D lamellar structure with interlayer

spacing of H-T P3ATs[14] are shown in Fig2.4.

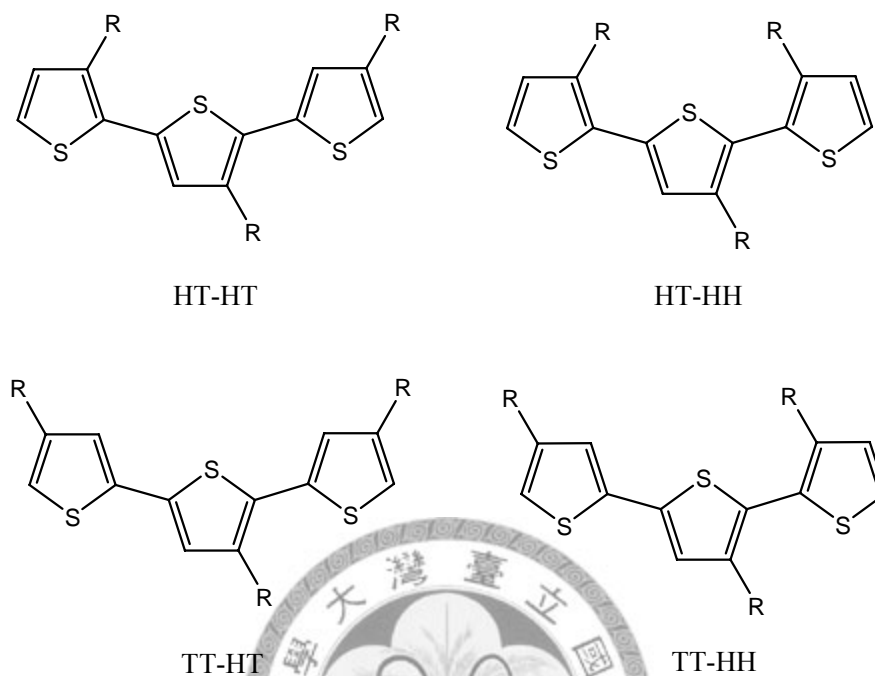
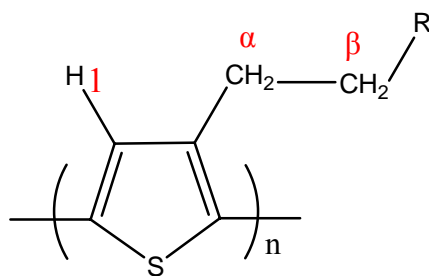


Figure2.2 Four configuration of P3AT[10]



	HT-HT	TT-HT	HT-HH	TT-HH
H1	6.98	7	7.02	7.05
	head-to tail		head-to-head	
α -methylene-H		2.8		2.58
β -methylene-H		1.72		1.63

Table2.1 H NMR Chemistry Shift (ppm) of 'H in Different Regiostmctures[15]

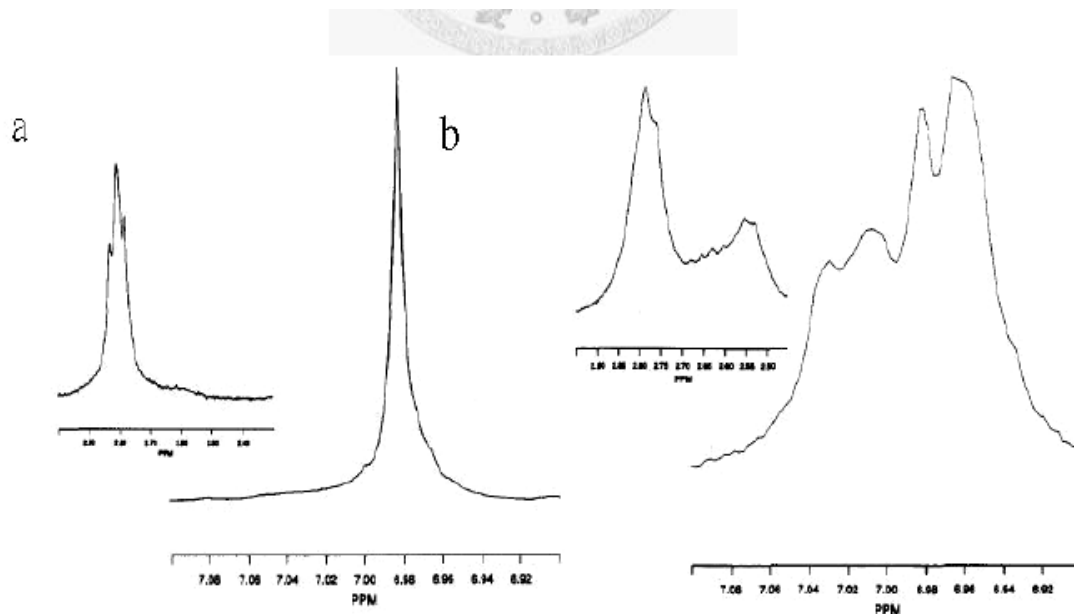


Figure 2.3 NMR spectra of (a) HT-P3AT and (b) regiorandom P3AT[15]

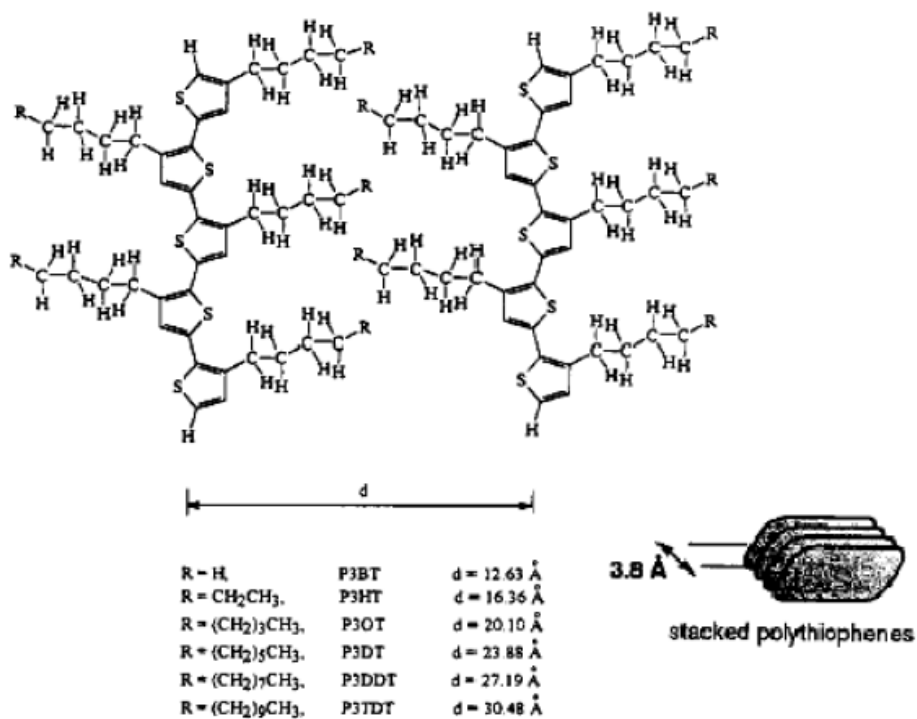


Figure 2.4 2-D lamellar structure with interlayer spacing of H-T P3ATs[15]

1.4 Mechanism of the Nickel-Initiated Grignard reaction

Scheme 1. Proposed Mechanism for the Nickel-Initiated Cross-Coupling Polymerization

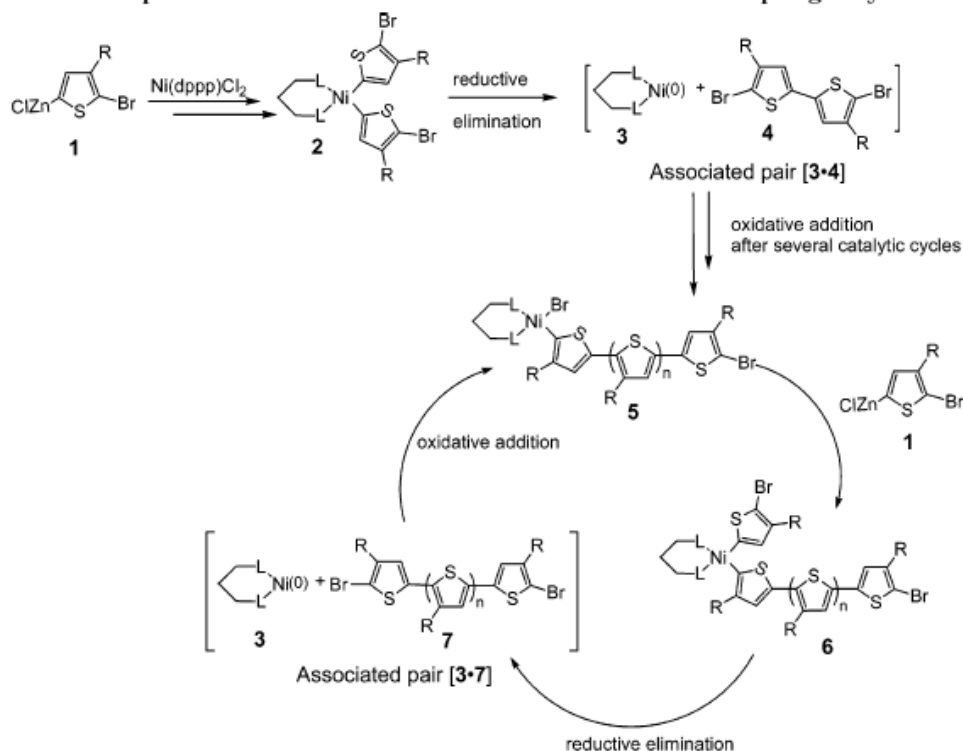


Figure 2.5 Proposed Mechanism for the Nickel-Initiated Cross-Coupling Polymerization[16]

The chain growth mechanism had been discussed extensively in recently years, at 2004, Mccullough report an credible mechanism on Macromolecules, and also proved it by a lot of experiments, the assumption is shown in Fig2.5. First of all, 2,5,dibromo-3-hexlythiophene react with Grignard reagent(RMgX) to form 2-bromo-5-bromomagnesium-3-hexylthiophene, and two 2-bromo-5-bromo magnesium-3-hexylthiophene react with Ni(dppp)Cl_2 to yield a new organonickel compound, then reductive elimination occurs, the organonickel compound transfer to an associated pair quickly, which is consist of the tail-to-tail aryl halide dimer and nickel(0). The dimer undergoes fast oxidative addition to nickel center generating

nickel complex which on the terminal C-Br bond react with a new monomer to form a organonickel compound, and the reductive elimination occurs quickly and the next following steps are the same as before, growth of the polymer chain occurs by insertion of one monomer at a time in the reaction cycle.

After a lot of experiment, they defined Grignard method as a living nature polymerization, and also found that the molecular weight of polymer can be predicted by the molar ratio of monomer to Ni(dppp)Cl₂, which means that 1mol of Ni(dppp)Cl₂ initiates one polymer chain. Therefore, the polydispersity index(PDI) is quite narrow[16]

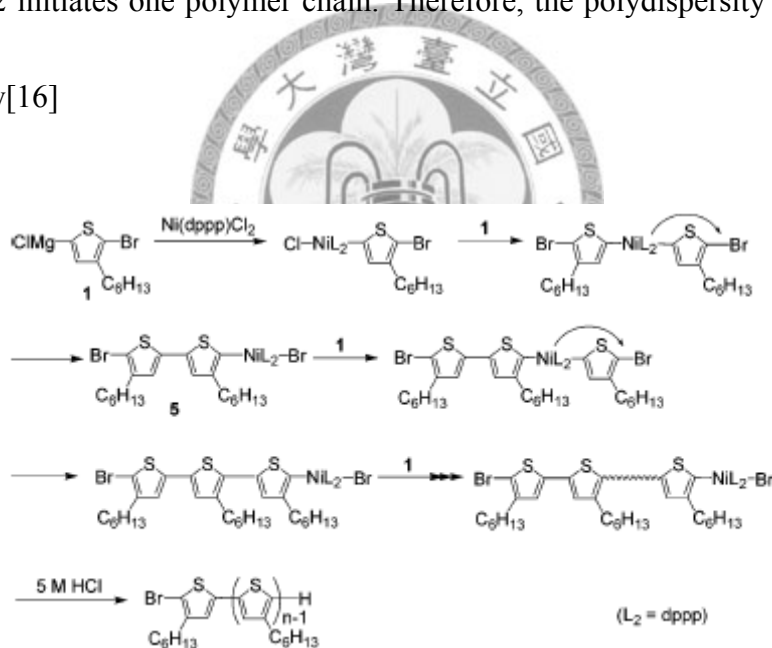


Figure 2.6 Mechanism of Chain-Growth Polymerization[17]

In 2005, Mccullough had another report “Catalyst-Transfer Polycondensation. Mechanism of Ni-Catalyzed Chain-Growth Polymerization Leading to Well-Defined Poly(3-hexylthiophene)”, which is published on JACS. They use matrix-assisted laser desorption ionization time-of-flight (MALDI-TOF) mass spectrometry to prove all

polymer have the same end group with one bromine atom and one hydrogen atom, and the hydrogen end group is generated from nickel complex upon quenching, based on the result and another experiments, they propose the Grignard reaction as a new mechanism of chain-growth polycondensation. First of all, Ni(0) generated by the formation of the bithiophene, then Ni(0) transferred from intramolecule to the C-Br bond of the bithiophene. And growth continues with the coupling reaction followed by the transfer of Ni(0) to the terminal C-Br bond. The scheme is shown in Fig2.6[18]

1.5 Photovoltaic properties of poly (3-alkyl thiophene)

The conjugation length is defined as the distance that charge can delocalize. Longer conjugation length in polymer backbone results in small energy gap. And the HT-P3ATs had a larger adsorption λ_{\max} than that of reiorandom P3ATs, the HT P3HT had a λ_{\max} in 456nm, and reiorandom in 427nm, a 29nm red-shift as shown in Fig 2.7, due to the arrangement of HT-P3AT is more regular, the packing between polymer chain will be more close, increasing the π - π interaction and low the π - π transition energy, this phenomenon is favor for charge transition and decrease the band gap.

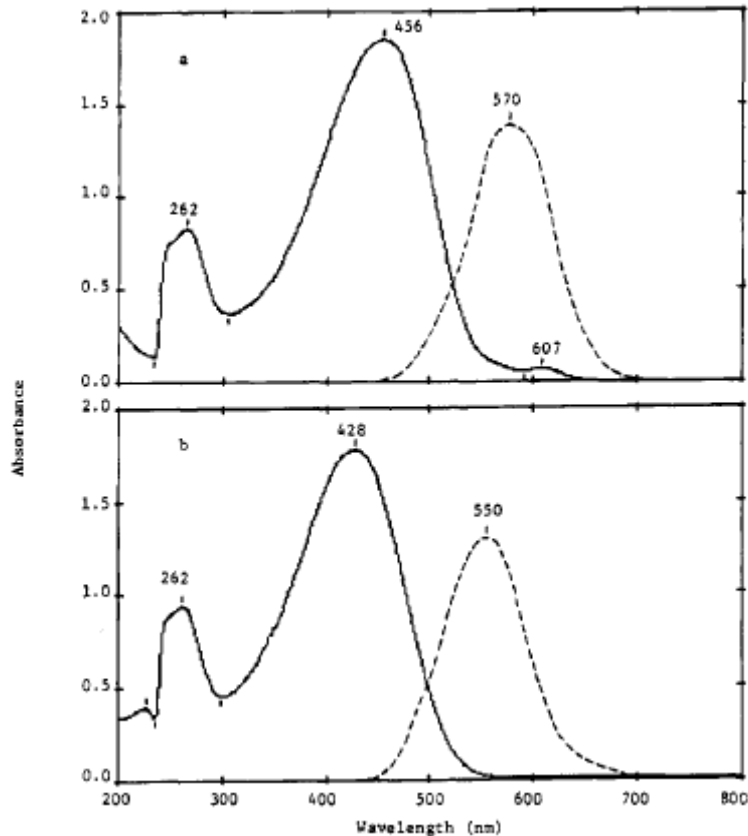


Figure 2.7. UV-vis and fluorescence spectra of (a) regioregular HT-P3HT and (b) regiorandom P3HT of CHCl₃ solution. (—):UV-vis; (- - -): fluorescence[15].

1.6 Working principles of organic solar cell[6]

Organic solar cell is activated by shining light to produce excitons. But excitons have a binding energy of several tenths of electron volts. And the diffusion length of an exciton is quite low in most conducting polymers. This makes solar cell to charge generation more difficult as it leads to a lot of recombination within the bulk of the active layer. To improve this bad phenomenon in polymer solar cell, the most efficient improved way was blend some electron acceptor molecules with bulk heterojunction method[18]. The bulk heterojunction of donar/acceptor blend which are suitable for efficient exciton dissociation. At donar/acceptor interfaces, the driving force for

exciton dissociation is generated by the electrochemical potential difference between the LUMO of the donor and the LUMO of the acceptor. The electrodes collect the photogenerated free carriers; the anode collects holes and the cathode collects the electrons, and we can separate this mechanism into four steps, which are 1. exciton creation. 2. exciton migration. 3. exciton dissociation 4. free charge carrier transfer, as shown in Figure 2.8.

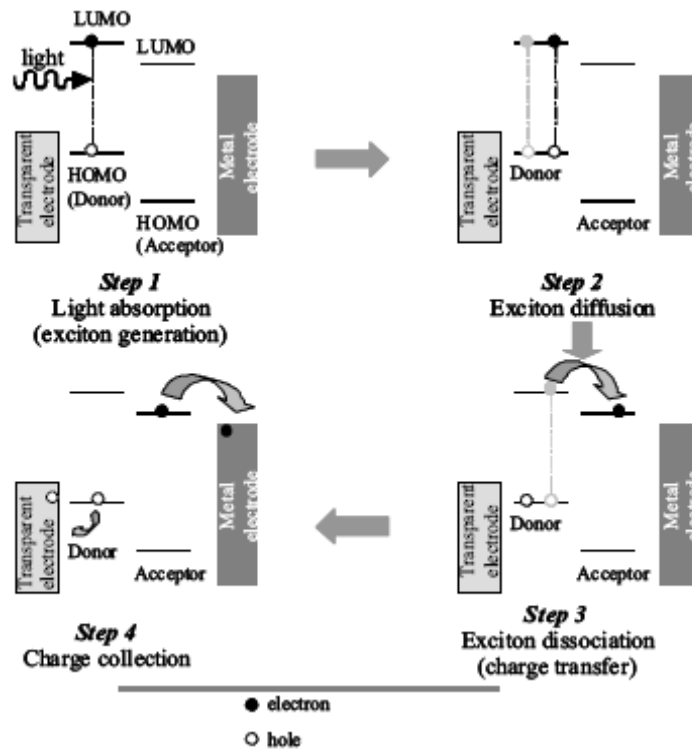


Figure 2.8 The simplified four basic steps of photocurrent generation in bulk heterojunction based solar cells.[6]

The typical I-V curve is shown in Figure 2.9, which is measured under full sun illumination immediately gives several photovoltaic parameters including V_{oc} , short-circuit current density (J_{sc}), fill-factor (FF), and overall power conversion

efficiency (η). Each of these parameters is shortly described in this section. The spectral response of a solar cell is also defined.

(a) The open-circuit voltage (V_{oc}) of a solar cell under light is defined as a voltage at which the net current in the cell is equal to zero. In a well behaving device, the current measured in the dark and under illumination conditions should be the same when the voltage is exceeding the V_{oc} , so the V_{oc} corresponds to the net internal electric field of the device.

(b) The short-circuit current (J_{sc}) is the photogenerated current of a solar cell, which is extracted at zero applied voltage. Photocurrent is directly related to optical and electrical material properties. As observed from Figure 3.3, in the region of the voltage between 0 to V_{oc} , the current is dominated by a photo-generated current.

(c) The fill factor (FF) of a solar cell is the measure of the power that can be extracted from the cell and is defined as

$$FF = \frac{(JV)_{max}}{J_{sc}V_{oc}}$$

where the $(JV)_{max}$ represents the maximum power that can be extracted from the cell.

In Figure 2.8, the $(JV)_{max}$ is defined by the area of the filled rectangle. The shape of the I-V curve is a measure of the FF; rectangular shapes is the best shape for high efficiency solar cell.

(d) The power conversion efficiency (η) is simply the ultimate measure of the device

efficiency in converting photons to electrons, which is defined as

$$\text{Efficiency} = \frac{J_{sc} V_{oc}}{f_{in}} \text{ FF}$$

where f_{in} accounts for the flux of light incident on the solar cell.

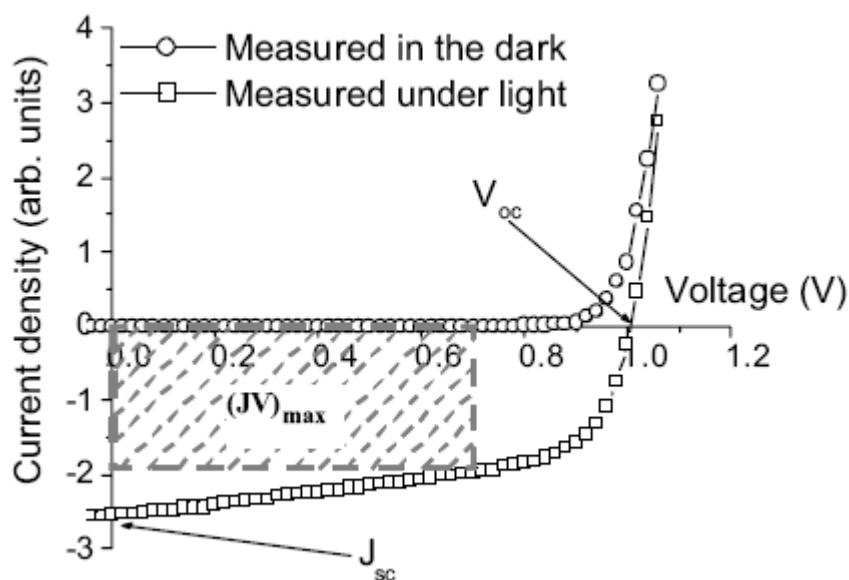


Figure 2.9 Typical current-voltage characteristics of a polymer/acceptor based solar cell. Which is measured in the dark and under white light illumination[6]

1.7 Solar cell performance of P3HT-PCBM bulk heterojunction

system

P3HT-PCBM system have been report in 2003, Niyazi S.Sariciftci reported the I-V behavior of P3HT-PCBM has $V_{oc} \sim 300\text{mV}$, J_{sc} of $\sim 2.5 \text{ mA cm}^{-2}$ and a calculated filling factor of 0.4 and the overall efficiency for this soalr cell is therefore 0.4%. But if solar cell heated to 75°C for 4min and the V_{oc} rises to 500mV, and J_{sc} increase to 7.5 mA cm^{-2} and filling factor has a value of 0.57, the overall efficiency rises to 2.5%, they proved thermal annealing is useful in these system, and they also make another

solar cell heated to 75°C plus an external voltage about 2.7V, and the Voc had a value 550 mV, a Jsc of 8.5mA cm⁻², a FF of 0.6 and efficiency of 3.5%. it prove that an addition of external voltage when annealed the solar cell will give rise to the efficiency[19]. The I-V curve are shown in Figure 2.10

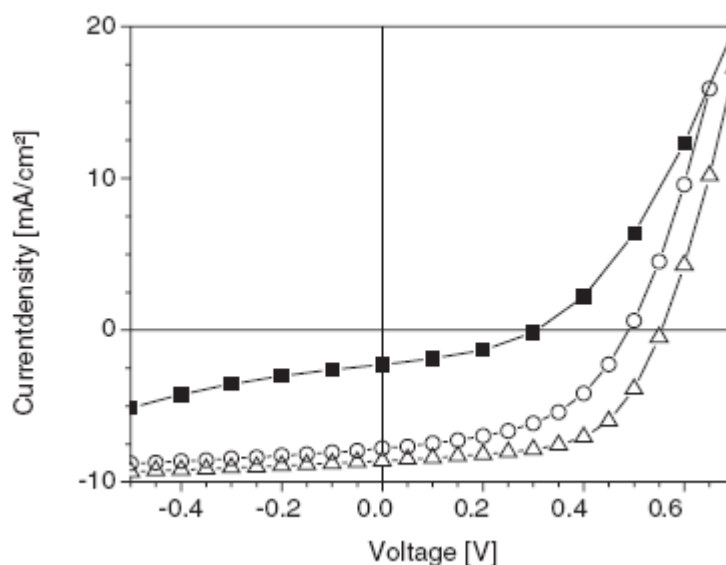


Figure 2.10 I-V curves of P3HT-PCBM solar cell under illumination with white light at an irradiation of 800 W m⁻², as-produced solar cell(filled squares), anneal cell(open circles), and cell simultaneously treated by annealing and applying an external electric field(open triangles)[19]

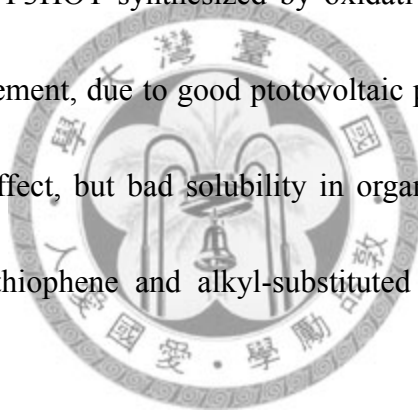
In 2007, Alan J. Heeger reported a breakthrough invention called “Tandem cell”[20], which combined with two linked solar cells with different absorption region. The tandem cell was fabricated by the front cell and back cell with were processed from solution. And the active layers of the back and front cell are PCPDTBT-PCBM and P3HT-P₇₀CBM respectively (PCPDTBT is a kind of low band gap polymer). Furthermore, a transparent titanium oxide (TiOx) layer separates and connects the

front cell and the back cell. The TiO_x layer serves as an electron transport and collecting layer for the first cell and as a stable foundation that enables the fabrication of the second cell to complete the tandem cell architecture. and tandem cell had a performance in Voc~1.24V, Jsc of 7.8 mA cm⁻², FF of 0.67 and the overall efficiency is up to 6.5%.which was an extensively high efficiency than before[20].

1.8 Development on poly(3-alkoxythiophene)

Polythiophenes with substitutes other than alkyl groups have also been investigated[21, 22], among which those with electron-donating alkoxy groups have displayed promising electrical and optical properties, at 1991, M. Leclerc had synthesized a series of alkoxy-substituted polythiophene such as poly(3-butoxythiophene(PBT)) by chemical polymerization using iron(III) chloride as oxidizing agent[23], but the polymers were regioirregular oligomers with low molecular weight. He also found PBT had a good electrical transport property, and a relatively low oxidation potential (0.60-0.64V). also another research on alkoxy-substituted thiophene at 2000 was reported by Xiao Hu[24]. They found chemical polymerization of 3-alkoxythiophene by oxidative polymerization (FeCl₃) under lower temperature and controlled addition of monomer helps to obtain polymers with relatively higher molecular weight. They also had a comparison with different length of alkoxy group to their thermal properties and the crystallinity. They

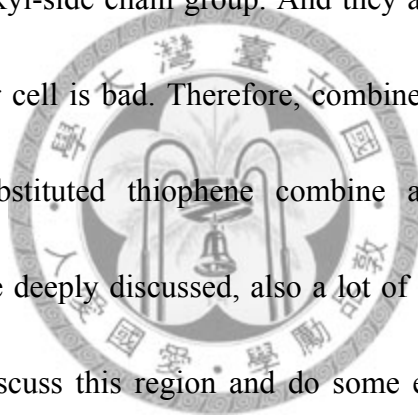
found alkoxy-substituted thiophene was worse than alkyl-substituted thiophene in thermal stability and crystallinity. In 2005, McCullough report a new synthesis method on alkoxy-substituted polythiophene rather than origin oxidative polymerization[25]. He use GRIM method to get a larger molecular weight and regioregular polymers such as Poly(3-hexyloxythiophene) (P3HOT) according to its mechanism[26], which $M_n=7.2k$, $PDI=1.7$ in P3HOT, the breakthrough of GRIM method-synthesized P3HOT is the intensively increment of molecular weight (2k to 7k) compare to the origin P3HOT synthesized by oxidative polymerization, and the highly head-to-tail arrangement, due to good photovoltaic property by the alkoxy side chain electron-donating effect, but bad solubility in organic solvent. Some research about alkoxy-substituted thiophene and alkyl-substituted thiophene copolymer had been discussed.



1.9 Development on poly (alkoxythiophene-co-alkylthiophene)

In 2006, Yang Yang and Qibing Pei report a random copolymer consist of alkyl and alkoxy side chain thiophene Poly(3-octylthiophene-co-3-decyloxythiophene) (POT-co-DOT)[27], they had synthesized poly(3-decyloxythiophene) (P3DOT) with molecular weight(M_n) 10.7k and polydispersity index(PDI) 1.48 and POT-co-DOT with M_w 14.5k and PDI 1.75, which is slightly larger P3DOT, and the solubility of

POT-co-DOT is also larger than P3DOT. they also verified by H NMR that the alkoxy-substituted thiophene is more reactive than alkyl-substituted thiophene during GRIM copolymerization. And a lot of photovoltaic properties detection, they detected that P3DOT soluted in chloroform have a maximum adsorption in 565nm and POT-co-DOT in 538nm, which a lot blue shifted when copolymer contains alkyl side chain. And verified the exact position of HOMO and LUMO by cyclic voltammetry, they find HOMO of P3DOT locate at -4.47eV and POT-co-DOT at -4.55eV, which is effected by addition of alkyl-side chain group. And they also make solar cell device, but the efficiency of solar cell is bad. Therefore, combine all of result in these area, we think the alkoxy-substituted thiophene combine alkyl-substituted thiophene copolymer still need to be deeply discussed, also a lot of characterization need to be built. So we decide to discuss this region and do some experiments to know more about it.



Chapter 2 Experimental Part

2.1 experiment materials

All procedures involving air-sensitive reagents were carried out under an atmosphere of high purity argon. All starting organic compounds were purchased from Acros, Sigma- Aldrich and used without further purification. THF and DMF were dried before use by sodium and CaH_2 , respectively. Column chromatography was performed on silica gel (230-400 mesh ASTM, Merck silica gel).

1. Ether, anhydrous, stabilized, ACS reagent (Acros, UK)
2. Tetrahydrofuran, 99+%, pure, stabilized with BHT (Merck, USA)
3. Methanol, 99+%, pure (Acros, UK)
4. Hexane, 95+%, pure (Acros, UK)
5. Magnesium, turnings 99.9+% (Acros, UK)
6. 1-Bromohexane, 99+% (Acros, UK)
7. $\text{Ni}(\text{dppp})\text{Cl}_2$, 99% (Acros, UK)
8. NBS(N-Bromosuccinimide), 99% (Acros, UK)
9. Cyclohexyl magnesium chloride, 1.3M in THF (Acros, UK)
10. Copper(I) bromide, 98% extra pure (Acros, UK)
11. Ammonium chloride, 99.5%, extra pure (Acros, UK)



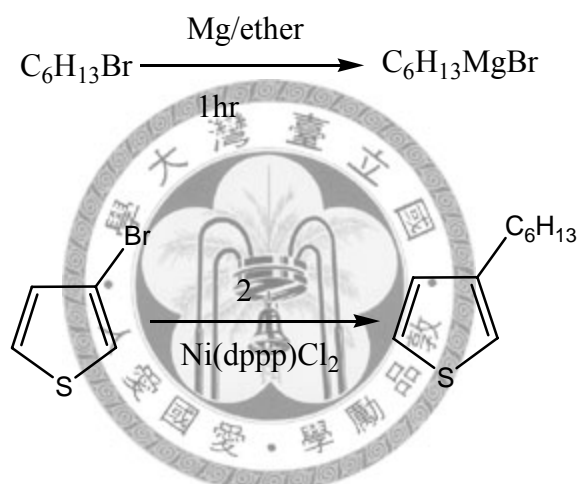
12. 1-Hexanol alcohol, 98% (Acros, UK)
13. CaH₂, 0-2 mm grain size ca. 93% (Acros, UK)
14. Diiodomethane, 99+%, stabilized (Acros, UK)
15. 3-Bromothiophene, 97% (Acros, UK)
16. Chlorotrimethylsilylamine, 98% (Acros)
17. Chloroform, 99+%, pure (Acros, UK)
18. Sodium hydride, dry, 95% (Aldrich)
19. N,N-Dimethylformamide(DMF),99.8+% (Acros, UK)

2.2 Experiment instrument

Instrument name	Instrument model	Company/ Origin country
Nuclear magnetic resonance (NMR)	AVANCE 400 (400MHz)	BURKER/USA
Fourier transform infrared spectroscopy (FT-IR)	Excalibur series FTS 3000	VARIAN/USA
UV-vis spectroscopy (UV)	Jasco V-570	JASCO/UK
Photoluminescence (PL)	Jasco FP-6300	JASCO/UK
Thermal Gravimetric Analysis (TGA)	PYRIS 1	Perkin-Elmer/ SA

Gel Permeation Chromatography (GPC)	Waters 2695	Waters/USA
Cyclic Voltammetry (CV)	CHI instrument	CHI/USA
ROTA VAPOR	ROTAVAPOR R-114	BUCHI/Sweden

2.3 Synthesis of 3-hexylthiophene

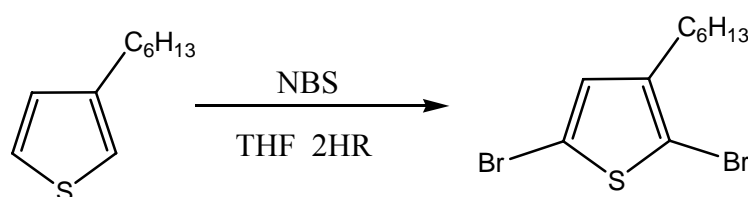


Synthesis of 3-hexylthiophene (Zimmer 1986)

Magnesium was added in a two-neck round bottom flask and charged with anhydrous ether, then 1-bromohexane was added dropwise into the flask via syringe and reacted for 1 hr. After reaction, the mixture was purged into a new flask with 3-bromothiophene and Ni(dppp)Cl_2 inside and reacted for 1 day. After reaction, the flask was poured into water and stirred for 10 min, the organic phase was extracted with ether and the aqueous phase was extracted with 1M NaCl solution, then dried over anhydrous

magnesium sulfate(MgSO₄), After the product was filtered, the solvent was removed by rotary evaporation. The crude product was purified by reduced pressure distillation (65-70°C (0.28 Torr)), the final product was a colorless oil.

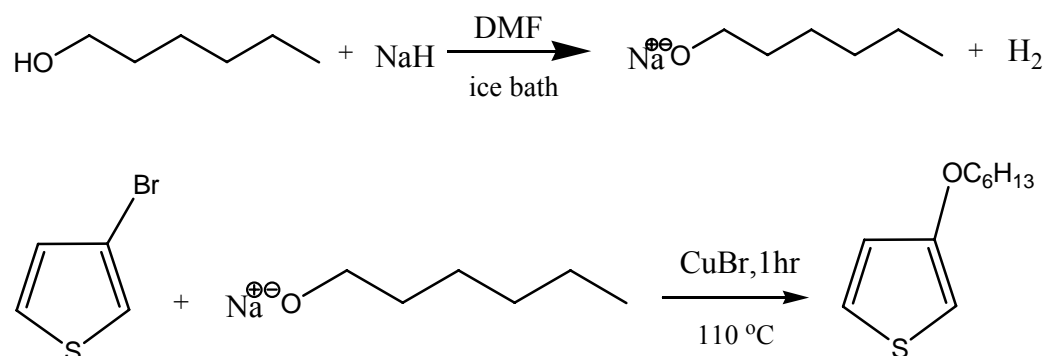
2.4 synthesis of 2,5-dibromo-3-hexylthiophene .



Synthesis of 2,5-Dibromo-3-hexylthiophene
(McCullough 1999)

A three-neck round bottom flask was flushed with nitrogen and charged with distilled 3-hexylthiophene and anhydrous THF, then the anhydrous n-bromo succinimide(NBS) was added and react for 1 day, after 1 day, the solution change from light yellow to orange . The solvent was removed by rotary evaporation. The resulting residue was washed with hexanes, filtered, and purified using column chromatography on silica gel with hexanes as the eluent . The product was dried over anhydrous MgSO₄, After filtration, the solvent was removed by rotary evaporation. The product was purified under reduced pressure distillation(145°C ,0.021torr), finally we got a light yellow oil, the product was flushed with N₂ and stored in a dark cool place (~ 0 °C).

2.5 Synthesis of 3-hexyloxythiophene

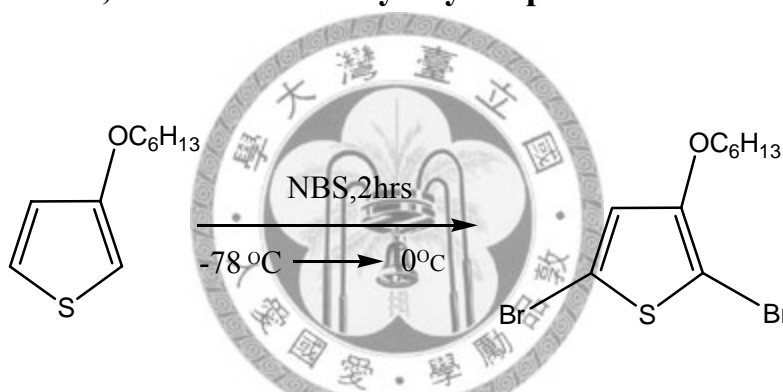


Synthesis of 3-hexyloxythiophene
(McCullough2005)

A three-neck round bottom flask equipped with a condenser and a funnel, which was flushed with nitrogen and NaH (gray powder) was added into the flask, then anhydrous DMF was added via syringe. The reaction flask was cooled down to 0 °C, then anhydrous 1-hexanol (0.48mol) was added dropwise via syringe over a 30 minute time period. The solution was stirred for 1.5 hour to assure complete consumption of NaH, while the temperature was maintained at 0 °C, 3-bromothiophene (16.3 g, 0.10 mol) and CuBr (1.44 g, 0.01 mol) were added quickly into the flask, and the ice bath was replaced with oil bath and heated up to about 110 °C. After 30 minutes, an equimolar amount of CuBr was added and the reaction was allowed to proceed for an additional 30 minutes to ensure the reaction was completed. The flask was then poured into a 1 M aqueous solution of NH₄Cl

(100mL) and stirred for 10 minutes. The organic phase was extracted with hexanes and dried over anhydrous magnesium sulfate (MgSO₄). After the product was filtered, the solvent was removed by rotary evaporation. The crude product was purified by reduced pressure distillation (60-70 °C (1Torr)), and then used column chromatography on silica gel with hexanes to remove the residual radical, the final product was a colorless oil.

2.6synthesis of 2,5-dibromo-3-hexyloxythiophene .

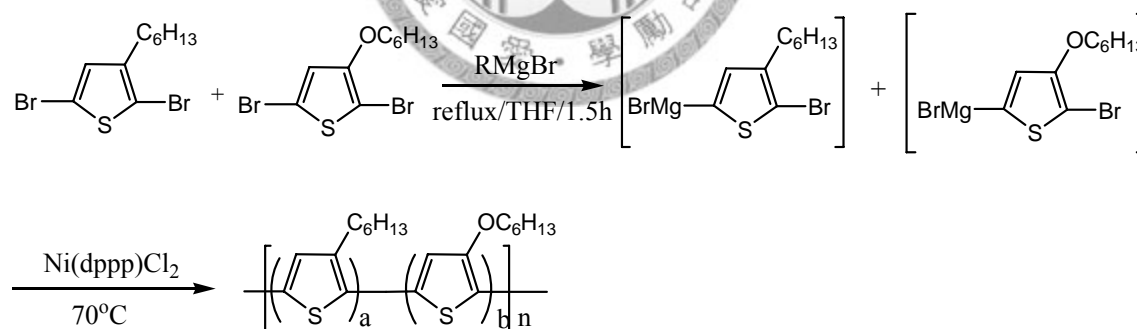


Synthesis of 2,5-Dibromo-3-hexylthiophene
(McCullough2005)

A three-neck round bottom flask was flushed with nitrogen and charged with distilled 3-hexyloxythiophene and anhydrous THF. The reaction flask was cooled down to -78 °C to stabilize the reaction, the anhydrous n-bromo succinimide (NBS) was added. The reaction mixture was stirred for 30 minutes at -78 °C. The ice bath was removed and the reaction was allowed to slowly warm up to ambient temperature. The reaction was stopped in two hours, after which the solution became dark green. The solvent

was removed by rotary evaporation. The resulting residue was washed with hexanes, filtered, and purified using column chromatography on silica gel with hexanes as the eluent. The product was dried over anhydrous MgSO_4 , The solution had a distinct color change from a yellow color to almost colorless. After filtration, the solvent was removed by rotary evaporation. The compound was dried under vacuum, finally an yellow color oil was left, the flask was flushed with N_2 and stored in a dark cool place ($\sim 0\text{ }^\circ\text{C}$).

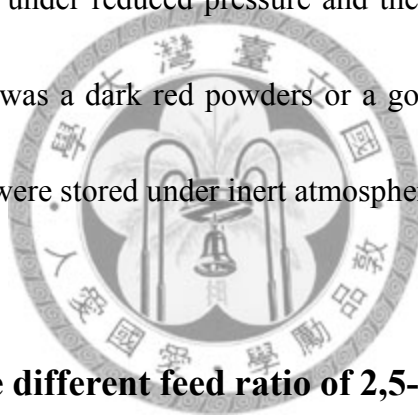
2.7 Synthesis of poly(-3-hexylthiophene)-co-poly (-3-hexyloxy thiophene) by the Grignard Metathesis method.



Synthesis of poly(-3-hexylthiophene)-co-poly (-3-hexyloxythiophene)

A three-neck round bottom flask equipped with a condenser and a funnel was flushed with N_2 and charged with different fraction of 2,5-dibromo-3-hexyloxythiophene and 2,5-dibromo-3-hexylthiophene. Anhydrous THF and cyclohexylmagnesium chloride

were added to the flask via syringe. The reaction mixture was allowed to stir for 120 minutes at gentle reflux (~75°C), then Ni(dppp)Cl₂ was added into the funnel first and previously dissolved by some anhydrous THF. Then the mixture was flushed into the flask as fast as possible, the polymerization was allowed to proceed for 30 mins at gentle reflux. Then, the reaction mixture cool down to ambient conditions and precipitated into a mixture of methanol (CH₃OH). The polymers were filtered, purified by Soxhlet extraction in sequence with hexanes, CH₃OH, and CHCl₃. Chloroform was removed under reduced pressure and the residues were dried under vacuum. The final product was a dark red powder or a golden chip depend on your procedure. The polymers were stored under inert atmosphere.



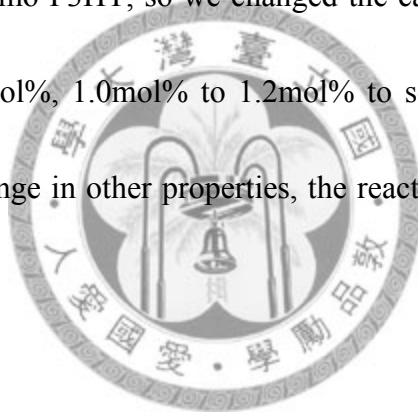
2.8 Experiment in the different feed ratio of 2,5-Br-3HOT and add the same molar ratio of catalyst.

First, we did five different molar feed fraction of 2,5,Br-3-HT and 2,5,Br-3-HOT but with the same molar ratio of catalyst, according to the chain growth mechanism of Grignard reaction, the molecular should be the same no matter which kind of monomer is or what molar fraction in a comonomer system polymerization is, therefore, we did five different fraction of 2,5,Br-3-HT and 2,5,Br-3-HOT copolymerization, which are 100%, 70%, 50%, 30%, 0% in 2,5,Br-3-HOT feed ratio

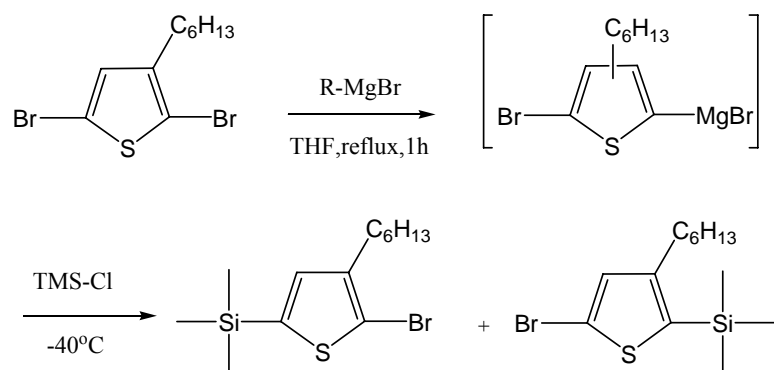
and all reaction is added 0.2mol% of catalyst, and the other condition are all the same, the detail condition are shown in Table2.1

2.9 Experiment of different molar ratio of catalyst in equal molar fraction of two monomers system (P3HT-P3HOT[5:5])

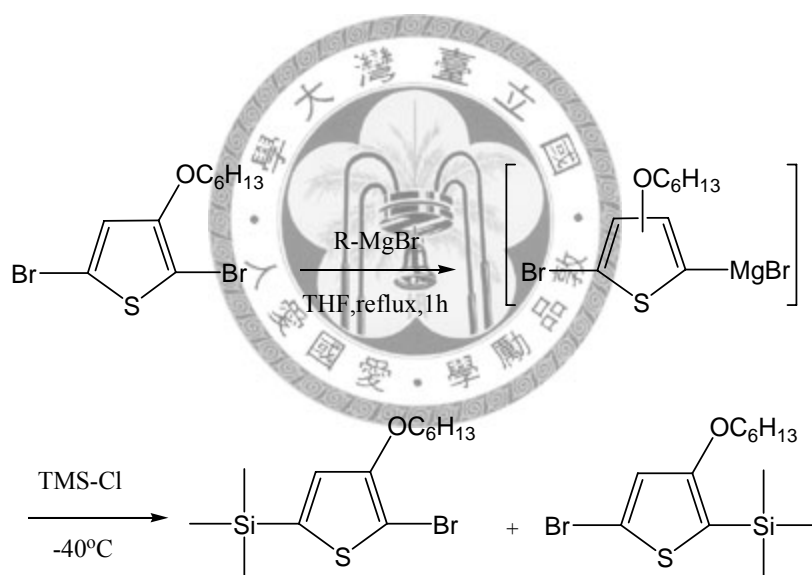
Molecule weight was an significance property of polymer, it could effect many properties to polymer, based on the mechanism of P3HT, we expect P3HT-P3HOT had similar result with homo-P3HT, so we changed the catalyst/monomer ratio from 0.2mol%, 0.5mol%, 0.7mol%, 1.0mol% to 1.2mol% to see the change of molecule weight, also anything change in other properties, the reaction condition are shown in Table2.2



2.10 Quenching result of Grignard metathesis reaction of 2,5-dibromo-3-hexylthiophene and 2,5-dibromo-3-hexyloxythiophene



Quenching experiment of Grignard metathesis reaction of 3-hexylthiophene.

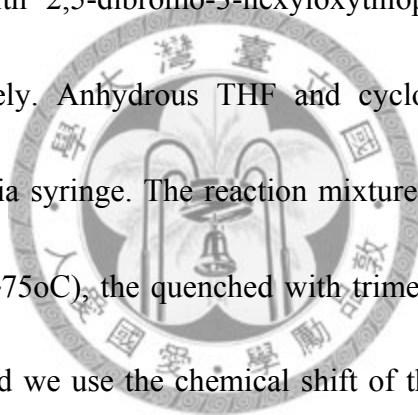


Quenching experiment of Grignard metathesis reaction of 3-hexyloxythiophene

In Grignard reaction of 2,5,Br-3-hexylthiophene, both 2-bromomagnesio-3-hexyl-5-bromothiophene and 2-bromo-3-hexyl-5-bromomagnesio thiophene are formed. But the catalyst only reacts with 2-bromo-3-hexyl-5-bromomagnesiothiophene due to steric hindrance. To test this hypothesis, McCullough did a quenching experiment of

Grignard metathesis reaction by 2,5-dibromo-3-hexylthiophene[28], and they found the Grignard exchange occurs with a large degree of regiocontrol (80:20 distribution of isomers, regardless of the Grignard reagent employed). Since the result could effect the molar fraction in P3HT-P3HOT copolymerization. We decide to do the same experiment on 2,5-dibromo-3-hexyloxythiophene, also on 2,5-dibromo-3-hexylthiophene to double check the result

A three-neck round bottom flask equipped with a condenser and a funnel was flushed with N₂ and charged with 2,5-dibromo-3-hexyloxythiophene and 2,5-dibromo-3-hexylthiophene respectively. Anhydrous THF and cyclohexylmagnesium chloride were added to the flask via syringe. The reaction mixture was allowed to stir for 90 minutes at gentle reflux(~75oC), the quenched with trimethylsilyl chloride(TMS-Cl) at -40°C for 120mins. And we use the chemical shift of the proton on the thiophene ring to calculate the result.



Chapter 3 Result and discussion

3.1 Synthesis of 3-hexylthiophene

The product is a colorless oil, and the yield is about 65% to 70%, The ^1H NMR of 3-hexyl thiophene shown in Figure 3.1. the product has six peaks at 0.88 ppm (f) ; 1.25 ppm (e) ; 1.61 ppm (d) ; 2.61 ppm (c) ; 6.91 ppm (b) ; 7.21 ppm (a), and the proportion of the integral area in each peak is accord with the theoretically number except peak (a) and (b), this phenomenon is caused by the byproduct $\text{C}_{12}\text{H}_{26}$, this byproduct forms in the reactions and also distilled with our product, but we can't separate them because two boiling points are too close, but we can separate it in the next step, so it is acceptable to do the next reaction



3.2 synthesis of 2,5-dibromo-3-hexylthiophene .

The product is an yellow oil and has a good yield (>90%), in Fig 4.4, we can see peak 7.21 ppm disappear compare with Fig 3.2, that means the reaction is success, and the proportion of peak 0.88 ppm (e) and 1.25 ppm (d) are accord with the thorry number, the byproduct $\text{C}_{12}\text{H}_{26}$ is removed because the different boiling point between 2,5-dibromo-3-hexyl thiophene and $\text{C}_{12}\text{H}_{26}$, the product is flushed with N_2 and stored in a dark cool place ($\sim 0\text{ }^\circ\text{C}$).

3.3 Synthesis of 3-hexyloxythiophene

The product is a colorless oil, and the yield is about 60% to 65%, the crude will accompanied some reactant 1-hexanol and be found a unique peak 3.69ppm, this reactant can be eliminated by column chromatography on silica gel with hexanes as the eluent, 1-hexanol will be stock on the top of the gel and removed, The ¹H NMR of 3-hexyloxythiophene shown in Figure3.3 has seven peaks at 0.93ppm(f) 1.47ppm(g) 1.47ppm(f) ; 1.79ppm(e) ; 3.95ppm(d) ; 6.23ppm(c) ; 6.76ppm(b) ; 7.25ppm(a), and the proportion of the integral area in each peak is accord with the theoretically number, the product is flushed with N₂ and stored in a dark cool place (~ 0 oC).

3.4 synthesis of 2,5-dibromo-3-hexyloxythiophene .

The product is an yellow oil and has a good yield(>90%), in Fig3.4, we can see peak 7.25ppm and 6.23ppm disappear compared with Fig4.6, that means the reaction is success, it is unstable at bright place, so the product needs to be flushed with N₂ and stored in a dark cool place (~ 0 oC).

3.5 Experiment in the different feed ratio of 2,5,Br-3HOT and add the same molar ratio of catalyst.

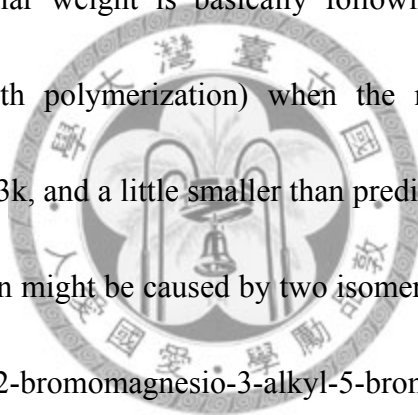
The results are summarized in Table3.1. First of all, we detect the real ratio of 3-HOT in copolymer by H NMR. The H NMR of each copolymer shows one sharp peak at

4.16ppm, which is for the $-OCH_2-$ group, and one at 2.79ppm for the $-CH_2-$ group, on the basis of the relative areas of the peaks at 4.16ppm and 2.79ppm[27], the mole fraction of 3-hexyloxythiophene(3-HOT) and 3-hexylthiophene(3-HT) units in P3HT-P3HOT can be estimated. The H NMR of five copolymers is shown in Fig 3.5, Fig3.6, Fig3.7, Fig3.8 and Fig3.9. We find the molar fraction of 3-HOT in copolymer is a little higher (6%~10%) than the molar fraction of comonomers no matter what fraction of 3-HOT is. Then we detect the molecular weight by GPC with Polystyrene as the standard. Surprisingly, the result of the molecular weight is totally different to the expected number, and the molecular weight decrease when molar fraction of 3-HOT increase in feed ratio. The number-average molecular weight (M_n) decrease from 40k to 6k when the mole fraction of 3-HOT increase. If reaction followed the GRIM chain growth polymerization, the molecular should be the same no matter what molar fraction of 3-HOT is. Therefore, we decide to discuss the copolymer mechanism synthesized by GRIM method.

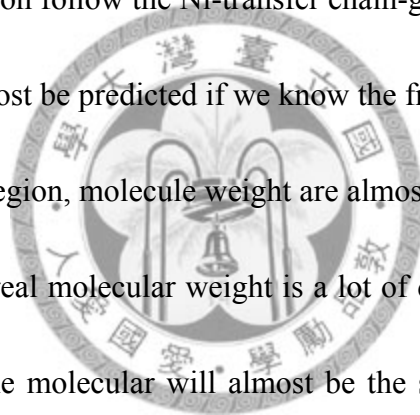
3.6 Experiment of different molar ratio of catalyst in equal molar fraction of two monomers system (P3HT-P3HOT[5:5])

It is known that the mechanism of poly(3-hexylthiophene) had been proved to be a catalyst-transfer polycondensation[26], also considered as nickel-catalyzed

Chain-Growth Polymerization, that is, one Ni catalyst molecule forms one polymer chain. But the result is quite different at P3HT-P3HOT copolymer system, so we decide to study on the relationship between catalyst and molecular weight in 3-HT and 3-HOT system. We did a series of experiments on equal molar ratio of 3-HT and 3-HOT which added 1.2mol%, 1.0mol%, 0.7mol%, 0.5mol% and 0.2mol% of nickel catalyst. And the results are shown in Table3.2, and we plot the relationship of M_n and mol% of Ni-catalyst, which is shown in Fig3.10. According to Fig3.10, We find the increment of molecular weight is basically following the GRIM mechanism (Ni-catalyzed chain-growth polymerization) when the number-average molecular weight (M_n) is low than 23k, and a little smaller than predicted molecular weight. The reason for the phenomenon might be caused by two isomers formed during the GRIM reaction. (Both 2-bromomagnesio-3-alkyl-5-bromo thiophene and 2-bromo-3-alkyl-5-bromomagnesiothiophene are formed). Also, due to the selectivity of the Ni(dppp)Cl₂, 2-bromomagnesio-3-alkyl-5-bromothiophene is almost unreact by the effect of steric hindrance. Therefore, a part of reactant can't be reacted and the molecular weight will be lower than prediction, we will have more detail explanation in GRIM quenching experiment. After 23k, the molecular weight didn't increasing when the molar ratio of Ni(dppp)Cl₂ become lower. And we find the reason of this phenomenon might be caused from the solubility of the copolymer according to the



GPC diagram, which is shown in Fig 3.11. The curve of the peak becomes different when molecule weight reaches higher molecular weight. And the slope of curve at left part, which means higher molecule weight part in one polymerization, becomes steeper than those curve at lower molecule weight, it means these higher molecular polymers might be limited by the solubility and stop growing. Base on these results, we can define two regions in 3HT-3HOT copolymer system. One region call “GRIM-obeyed region”, the other call ”solubility –limited region”, In GRIM-obeyed region, the copolymerization follow the Ni-transfer chain-growth mechanism. And the molecular weight can almost be predicted if we know the fraction of unreact reactants. At the solubility-limited region, molecule weight are almost the same caused by factor of the solubility, and the real molecular weight is a lot of different with the predicted number, in this region, the molecular will almost be the same no matter what mole fraction of catalyst we added. Figure3.12 is draw by all experiments of the relationship between the mole percentage of catalyst and the derived Mn at Table3.6. We can realize the GRIM-obeyed region becomes smaller and the solubility limited region becomes larger when alkoxy group increase, This is a obvious evidence that the copolymerization is affected by the solubility. Base on these conclusions, we can explain the weird result in the before-mentioned experiment of different feed ratio of 2,5,Br-3HOT with the same molar ratio of catalyst (0.2mol%). Because every



copolymerization is located on the “solubility-limited region”, the molecular weight can't be predicted by GRIM method. Therefore, the alkoxy-side chain thiophene will decrease the solubility and limit the larger molecule formed.

3.7 Quenching experiment of Grignard metathesis reaction of 2,5,dibromo-3-hexylthiophene and 2,5,dibromo-3-hexyloxythiophene

The H NMR of 2,5,Br-3HT quenching result is shown in Fig3.13. Basically, there should be two product form during quenching reaction, which are 2-TMS-5-bromo-3-hexyl thiophene (6.86ppm) and 2-bromo-5-TMS-3-hexyl thiophene (6.78ppm) respectively, but we find that there is still another product form, which are 5-bromo-3-hexyl thiophene (6.799ppm) and 2-bromo-3-hexyl thiophene (6.875ppm). We guess the result was effected by reactant TMS-Cl. TMS-Cl has good volatility and it may volatilize during the reaction, but we only add equal molar of TMS-Cl compared with 2,5,Br-3HT. Therefore, some Grignard reagent didn't react with the TMS-Cl and finally react with water and form 2-bromo-3-hexyl thiophene (6.875ppm) and 5-bromo-3-hexyl thiophene(6.799ppm), but base on the theory of GRIM theory[29]. Due to the only bromide end group doesn't react with water, we still can figure out that the 5-bromo-3-hexyl thiophene is formed by 2-bromomagnesio-3-hexyl-5-bromothiophene, and 2-bromo-3-hexyl thiophene is

formed by 2-bromo-3-hexyl-5-bromomagnesium thiophene. Based on the theory, we can calculate the fraction by the integral of the proton area. We find 5% of 2,5-dibromo-3-hexyl thiophene(6.768ppm) doesn't react, 76% reactants form 2-bromomagnesium-3-hexyl-5-bromothiophene and 19% reactant form 2-bromo-3-hexyl-5-bromomagnesium thiophene. And this result is very similar to the result of McCullough reported at 1999[28]. and the result of 2,5,Br-3HOT is shown in Fig3.14, the ¹H NMR shows 5% of 2,5-dibromo-3-hexyloxythiophene(6.750ppm) doesn't react, 89% reactants form 2-bromomagnesium-3-hexyl-5-bromothiophene (6.736ppm) and 6% reactant form 2-bromo-3-hexyl-5-bromomagnesiumthiophene. And we get important information from these. The regiocontrol of alkoxythiophene(94:6) is better than alkyl thiophene(80:20) in Grignard methathesis. In other, the useful intermediate of 2,5,Br-3-HOT is more than 2,5,Br-3-HOT during equi-molar fraction feed ratio copolymerization.

3.8 Adjustment of the ideal molecular calculation in P3HT-P3HOT[5:5] system based on the quenching experiments

According to the results of quenching experiments, we know 5% unreact reactant and 19% unreact Grignard methathesis in the 2,5-dibromo-3-hexylthiophene system, and 5% unreact reactant and 6% unreact Grignard metathesis in 2,5-dibromo-3-hexyloxy

thiophene system, which means 17% of reactant doesn't react in the P3HT-P3HOT [5:5] copolymerization. Therefore, we build another ideal molecular curve which reduce the unreact material, as shown in Fig3.15. And we can see the ideal molecular weight is more close to the real molecular weight, also intensify the chain growth properties of P3HT-P3HOT[5:5] system which is the same with the mechanism of P3HT.

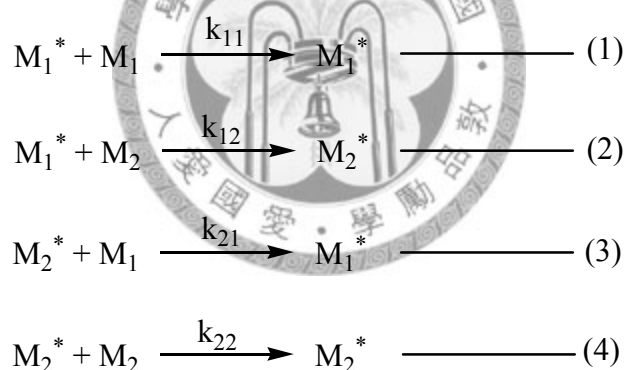
3.9 Mechanism prediction of P3HT-P3HOT[5:5] system

Base on a series of experiments. We make an assumption on P3HT-P3HOT[5:5] system, the scheme are shown in Fig3.16. first ,equal molar fraction of 2,5,Br-3-HT and 2,5,Br-3-HOT both are added to the flask, during the Grignard metathesis intermediate reaction, 44.5% of 2,5,Br-3-HOT become 2-Br-5-MgBr-3HOT and 38% of 2,5,Br-3-HT become 2-Br-5-MgBr-3HT, which means only 82.5% of reactant is involved in the copolymerization, and we assume if two monomers were totally reacted. it would be 56% of 3-hexyloxythiophene in the copolymer, and the predicted molar fraction of 3-hexyloxythiophene is coincide with the experiment results, which intensify the assumption of our prediction.

3.10 Calculation of the reactivity ratio in 2,5,Br-3-HT and 2,5,Br-3-HOT copolymerization base on the copolymerization equation

Since we have proved the P3HT-P3HOT[5:5] obey the GRIM chain growth rule in certain region, the reaction can be considered as a chain copolymerization just like the others. Therefore, the monomer reactivity ratio of 2,5,Br-3-HT and 2,5,Br-3-HOT can be calculated by copolymerization equation[30]. The equation assumed that the reactivity of the propagating species was dependent only on the monomer unit at the end of chain. Thus, four possible propagation reactions (1),(2),(3) and (4) are shown

as followed



This assumption is acceptable for GRIM reaction, which only react on the Ni-catalyzed group during reaction. And in order to simplify the equation. A steady-state concentration is assumed for each of the reactive species M1* and M2* separately.

Finally, we derive an equation

$$F_1 = \frac{r_1 f_1^2 + f_1 f_2}{r_1 f_1^2 + 2f_1 f_2 + r_2 f_2^2} \quad \text{where } r_1 = \frac{k_{11}}{k_{12}} \quad \text{and} \quad r_2 = \frac{k_{22}}{k_{21}}$$

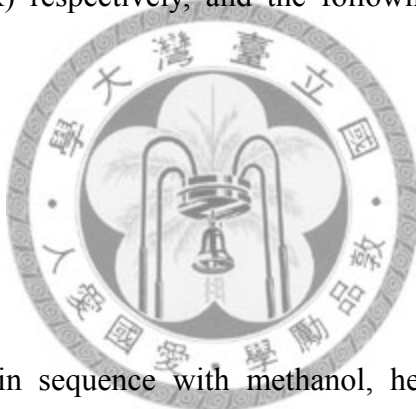
f_1 and f_2 are the mole fractions of monomers M₁ and M₂ in the feed, and F_1 and F_2 are

the mole fractions of M_1 and M_2 in the copolymer. Base on the copolymerization equation, we consider 1 as 3-hexyloxythiophene and 2 as 3-hexylthiophene. And put our experiment data into the copolymerization equation to derive r_1 and r_2 , which are 1.2 and 0.8 respectively. Therefore, we plot a diagram between the copolymer composition F_1 and the comonomer feed composition f_1 based on the r_1 value of 1.2 and r_2 value of 0.8. The diagram is shown in Fig3.17. And the value of r_1 and r_2 can also be a prediction of which type of copolymerization is. When the multiple of r_1 and r_2 is equal to zero, the copolymerization is referred to as ***alternating copolymerization***.

When the multiple of r_1 and r_2 is equal one, the copolymerization is referred as ***random copolymerization***. When the multiple of r_1 and r_2 is larger than one, the copolymerization is referred as ***block copolymerization*** [30]. In other words, as the $r_1 r_2$ product decreases from one toward zero, there is an increasing tendency toward alternation, as the value of $r_1 r_2$ are greater than one, there is an increasing tendency to form a block copolymer, as the value of $r_1 r_2$ is closer to one, there is a tendency to form a random copolymer[30]. The value of $r_1 r_2$ in P3HT-P3HOT copolymer system is equal to 0.96, which can almost be referred as a random copolymerization. Therefore, we can define P3HT-P3HOT copolymerization as a random copolymerization by experiment data and copolymerization equation.

3.11 Characteristic of five different molar fraction of P3HT-P3HOT

Although there are some research on alkyl and alkoxy side chain copolymers[27], but are all short and brief. Thus, we would like to do more deeply discussion to each different molar fraction of P3HT-P3HOT on photovoltaic and thermal properties. We select five different molar fraction of P3HT-P3HOT as our samples, which are P3HT($M_w=62k$, $M_n=40k$), P3HT-P3HOT[7:3]($M_w=54k$, $M_n=30k$), P3HT-P3HOT[5:5]($M_w=49k$, $M_n=23k$), P3HT-P3HOT[3:7]($M_w=15.8k$, $M_n=10k$) and P3HOT($M_w=10k$, $M_n=6k$) respectively, and the following result are all based on these five samples.

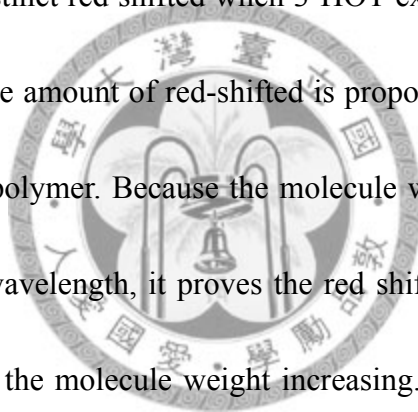


3.12 Appearance

After soxhlet extraction in sequence with methanol, hexane, chloroform, we get different color of powders, and they appear distinct color change in organic solvent, the outlook of five copolymers which dissolved in chloroform are shown in Fig3.18, which are orange(P3HT), berry red(P3HT-P3HOT[7:3]), purple (P3HT-P3HOT[5:5]), navy blue(P3HT-P3HOT[3:7]) and dark blue(P3HOT) respectively. And it represent that each copolymers have different UV adsorption. and we will discuss in the next section.

3.13 UV-Visible Absorption of P3HT-P3HOT in different molar fraction

We can see obviously color change between five copolymers. So we decide to start at the UV-vis detection. Optical absorption spectra detection were measured in dilute chloroform solution, also measured in thin films state by spin coating, the spectra of solution condition and in thin film condition are shown in Fig3.19 and Fig3.20 respectively, and the spectroscopic data of five copolymers are summarized in Table3.3, we can see a distinct red shifted when 3-HOT exist in copolymer no matter which condition is, and the amount of red-shifted is proportional to the mole fraction of 3-HOT exist in the copolymer. Because the molecule weight was lower when the absorption reach higher wavelength, it proves the red shift phenomenon is effect by the alkoxy side chain but the molecule weight increasing. The absorption maximum of homogeneous P3HOT is approximately 150nm red-shifted compared to that of homogeneous P3HT in dilute chloroform solution, and a 90nm red-shifted in thin film state, the red-shift may be due to the strong electron-donating alkoxy side groups which intensify the π - π^* interaction on the thiophene rings, which are more effective in lowering the band gap of the polymer than the alkyl side chain. It is a good phenomenon in organic solar cell device, which means more photon can be absorbed from the sunshine, and further improve the efficiency theoretically.



3.14 Electrochemical Characterization of P3HT-P3HOT in different molar fraction

We can use the result of UV-vis spectroscopic data to define the energy gap by the UV onset point. The onset point of optical absorption can be verified by the UV-onset and PL-offset cross point, and the band gap (E_g) was calculated by equation

$$E_g = 1240 / \lambda_{ONSET}$$

based on the result of calculation, the band gap is smaller when the mole fraction of 3-HOT increase, the band gap of homogeneous P3HOT is 1.58eV, which is lower than that of homogeneous P3HT ($E_g=1.94$) of 0.36eV, and the high occupied molecular orbital(HOMO) are determined by cyclic voltammetry (CV), The polymer is coated on Pt electrode in thin film, and detected in a 0.1M TBAP solution in acetonitrile, the scan rate is 100Mv/s, and the oxidation potentials (E_{ox}) are derived from the onset point in the cyclic voltammograms, which is shown in Fig3.24. We find the oxidative potential of P3HT is 0.97eV, P3HT-P3HOT[7:3] is 0.77eV, P3HT-P3HOT[5:5] is 0.52eV, P3HT-P3HOT[3:7] is 0.40eV and P3HOT is 0.25eV. The oxidative potential becomes smaller when alkoxy group increase in the copolymer, which is caused from the electron-donating property of the alkoxy group. This result is coincide with the theory. And the HOMO level can be calculated by the following equation[31].

$$E_{HOMO} = E_{ox}(complex) - E_{12}(reference)$$

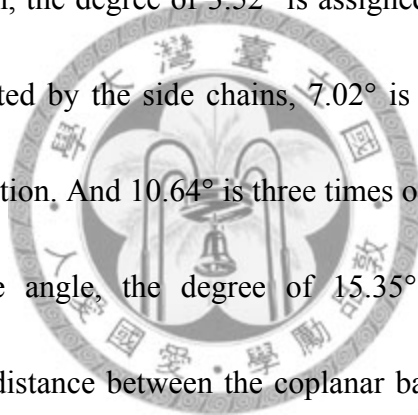
$$HOMO = -(E_{12} + 4.8eV)$$

$$LUMO = HOMO - Bandgap$$

And the HOMO value of P3HOT is calculated to be -4.56eV, which is lower than P3HT of 0.71eV. The phenomenon is because of the presence of the hexyloxy group, which intense the electro-donating property and makes polymer more oxidizable, Therefore, the oxidation potential decrease when alkoxy side chain is inside of the polymer. And the potential decrease more when fraction alkoxy side chain increase. That is, the HOMO level decrease when alkoxy side chain increase. And the result is coincide with the other reports[24]. As to the detection of the reduction potential, because no obviously reduction potential is observed in cyclic voltammograms, the LUMO levels is estimated from the HOMO values and values of optical band gaps by equation. And the LOMO level of P3HOT is calculated to be -3.33eV, which is a little higher to the calculated value of P3HT -2.98eV, but not so big compare to the HOMO difference. Therefore, the addition of alkoxy group almost effect the HOMO level rather than LUMO level, this is because the oxygen atom provide more free electronics from its long-pair-electron, which makes the electro-donating property is larger than the electro-withdrawing property[27], the results of all electrochemical properties are summarized in table3.3.

3.15 X-ray diffraction (XRD) of P3HT-P3HOT in different molar fraction

The polymer films to be analyzed are made by solvent-casting in chloroform. The concentration of the solvent is 1wt%, and the solvent casting rate is limited to ensure that the crystallization is formed gradually. The XRD results are shown in Figure3.21 and table3.4. We can see the degree of 3.38° , 6.94° , 10.61° , 15.24° are present in P3HT. The arrangement of P3HT is shown in Figure3.22 according to the previous study. At low angle region, the degree of 3.52° is assigned to a distance between the polymer backbone separated by the side chains, 7.02° is two times of 3.52° , which might be the second reflection. And 10.64° is three times of 3.52° , which might be the third reflection. At wide angle, the degree of 15.35° is considered to be the layer-to-layer π -stacking distance between the coplanar backbones. Expect of P3HT, which only shows a highly crystallinity, each of the other four polymers has bad crystallinity. In low angle region, polymers which contain hexyloxy side chain have one peak larger than homogeneous P3HT. When the mole fraction of 3-HOT in copolymer increase, the distance of polymer backbone separated by side chain become shorter from P3HT of 16.9A to P3HOT of 12.7A. It might be the alkoxy group is more flexible than alkyl group, therefore, the distance of polymer backbone separated by side chain is shorter than homogeneous P3HT. In wide angle region, we



find a unique peak at 12.18° only appears when alkoxy side chain exist, and this peak is not distinct in some copolymers. We still can not find a proper explanation to the peak, only know the peak is formed because of the alkoxy side chain. And it also shows a peak in homogeneous P3HT at 15.24° , which is assign to the layer-to-layer π -stacking distance. And we also find a broad amorphous peak at 14.6° when polymers contain alkoxy group, and we assume the peak is the layer-to-layer π -stacking distance, which is smaller than homogeneous P3HT. it means the layer-to-layer π -stacking distance will become larger from 3.7Å to 3.9Å. Therefore, we find the arrangement becomes looser when polymer contains alkoxy group.

3.16 Thermal analysis (TGA)

The polymers are placed in the oven for one day to eliminate the water. And the TGA curves of five polymers are shown in Fig3.23. it shows that polymers were decomposed by two or three major steps, the first step is ascribable mainly to the loss of the hexyloxy side chain if the hexyloxy side chain existed, the second step is ascribable to the loss of the hexyl side chain if the hexyl side chain existed, but the difference between two steps are hard to recognized, the result is coincide with the other reports[24]. The onset temperature of 5% weight loss(T_d) for the polymer is found to decrease with the increasing of hexyloxy side chain, which means the

thermal stability will decrease with the increasing of hexyloxy side chain. This is attributed to the presence of hexyloxy groups which makes the system more reactive and easily to be oxidized. The third weight loss step, which took place in the temperature range of 400–700°C corresponds to the degradation of polymer backbone[24]. Since the backbone of each polymer is thiophene ring, the degradation temperature is the same theoretically. The difference is assigned to be the different molecule weight.

3.17 FT IR

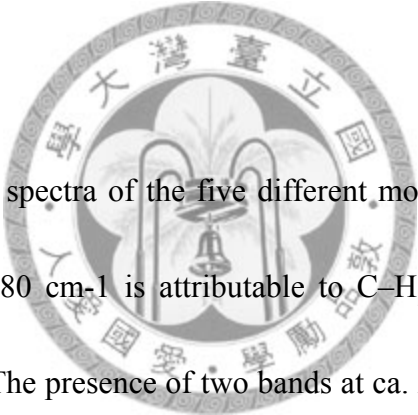


Fig3.26 depicts the FT-IR spectra of the five different molar fraction P3HT-P3HOT. The vibrational band at 880 cm⁻¹ is attributable to C–H_β out-of-plane deformation mode of thiophene rings. The presence of two bands at ca. 2850, 2950 and 3020 cm⁻¹ suggests that the alkoxy chain remains intact after polymerization(–CH₂– and –CH₃ groups), Ring vibrational modes are seen at 1510, 1436 and 1345 cm⁻¹. The band at 1180 cm⁻¹ is assigned to C–O–C stretching, which exist in polymers which contain alkoxy group. Therefore, this peak can be a evidence that alkoxy side exist in FT IR spectra.

3.18 Organic solar cell performance

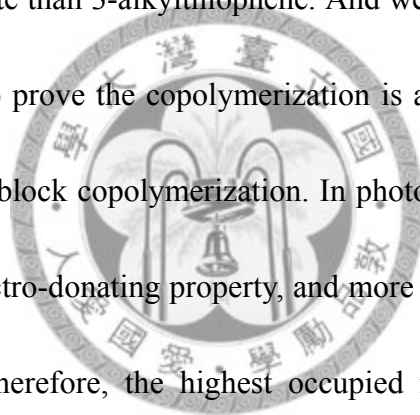
The polymer solar cells had a layered structure of glass/ITO/PEDOT-PSS/polymer-PCBM blend/Al. It was spin-coated from a solution containing the polymer and PCBM in chlorobenzene onto an ITO/glass substrate covered by poly(3,4-ethylenedioxythiophene)/poly(styrenesulfonate) (PEDOT-PSS). Thin layers aluminum were thermally deposited onto the device. Representative characteristics of the solar cells are listed in Table 3.5. All data were obtained under white light illumination from a solar simulator. The current-voltage characteristics of the solar cells based on the three blends P3HOT/PCBM, P3HT-P3HOT[3:7]/PCBM, P3HT-P3HOTP[5:5]/PCBM, P3HT-P3HOT[7:3]/PCBM and P3HT/PCBM are shown in Figure 3.27. the cell based on P3HOT/PCBM as the active layer has a short circuit current density (J_{sc}) of 0.3 mA/cm², an open circuit voltage (V_{oc}) of 0.020 V, a fill factor (FF) of 0.58% and efficiency of $3.48 \times 10^{-5}\%$. The low efficiency may be resulted from these two factors: the polymer blend layer was not uniform due to poor film-forming ability of P3HOT and that P3HOT have a HOMO at -4.56 eV, which is lower than P3HT at -5.27 eV, it is known that the V_{oc} is basically determined by the HOMO of the donar and the LUMO of the acceptor. The decreasing of HOMO actually effect the V_{oc} of the device. Therefore, it is not a ideal solar cell design although it is a low band gap polymer which can harvest more photon. By Table3.5,

the P3HT-P3HOT/PCBM efficiency is still low , and we can see that Voc decreasing obviously as the molar fraction of alkoxy side chain increasing, expect for the P3HT/PCBM system, the best performance of P3HT-P3HT/PCBM system is the P3HT-P3HT[5:5]/PCBM system. a short circuit current density (J_{sc}) of 2.27 mA/cm², an open circuit voltage (V_{oc}) of 0.25 V, a fill factor (FF) of 31.17% and efficiency of 0.18%. Annealing has been effective in enhancing the performance of the P3HT/PCBM bulk. Preliminary study showed that annealing has no effect on the PCEs of P3HT-P3HOT based solar cell.



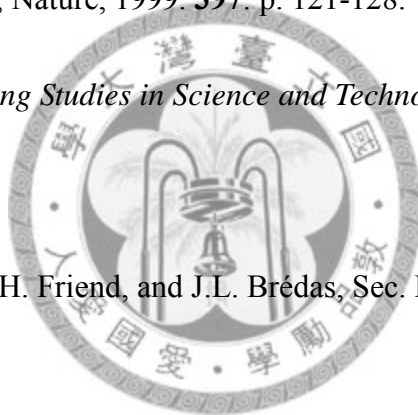
Chapter4 Conclusion

We have successfully synthesized the Poly(3-hexylthiophene-co-3-hexyloxythiophene) (P3HT-P3HOT) by Grignard reaction, and confirm the inert structure by ¹H NMR. And, due to the effect of solubility, the chain-growth phenomenon is occurred only below certain molecular weight, after this number the molecular won't grow up. And we find the real ratio of 3-alkoxythiophene is always 6~10% higher than feed ratio in different molar fraction of comonomer experiment because the 3-alkoxythiophene form more react Grignard intermediate than 3-alkylthiophene. And we also use copolymerization equation and our result to prove the copolymerization is a random copolymerization rather than alternating or block copolymerization. In photovoltaic properties, we find alkoxy side chain has electro-donating property, and more flexible and more oxidized than alkyl side chain. Therefore, the highest occupied molecule orbital (HOMO) increase and the band gap decrease when we increase the mole fraction of alkoxythiophene. And the thermal stability and crystallinity become worse when we increase the mole fraction of alkoxythiophene in copolymer. In the use of organic solar cell, due to the HOMO increasing, the Voc become smaller and affect the efficiency.

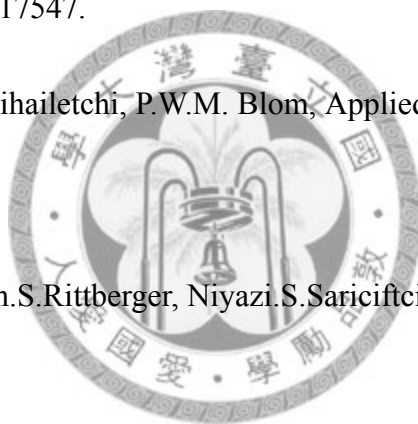


Chapter5 Reference

1. Shaheen, S.E., et al., Appl. Phys. Lett, 2001. **78**.
2. Svensson, M., et al., Adv. Mater, 2003. **15**: p. 988-991.
3. Bao, Z., A. Dodabalapur, and A.J. Lovinger, Appl. Phys. Lett, 1996. **69**: p. 4108-4110.
4. Meijer, E.J., et al., Nat. Mater, 2003. **2**: p. 678-682.
5. Friend, R.H., et al., Nature, 1999. **397**: p. 121-128.
6. Gadisa, A., *Linköping Studies in Science and Technology Dissertation*. 2006: p. 1056.
7. Salaneck, W.R., R.H. Friend, and J.L. Brédas, Sec. Phys. Lett, 1999(319): p. 231-251.
8. Heeger, A.J., Rev. Mod. Phys, 2001. **73**: p. 681-700.
9. wekipedia, *polythiophene*.
10. 顏惟哲, *Synthesis and characterization of Poly (3-hexylthiophene)-b-Poly (2-vinylpyridine)*. 2005.
11. Chen, T.-A., X. Wu, and R.D. Rieke, J. Am. Chem. SOC, 1995. **117**: p. 233-244.
12. Richard D. McCullough, t.S.T.-N., ;, t.R.D.L.a. Shawn P. Williams, and



- M.a.k.J.a. yaramant, J. Am. Chem. Soc. ,, 1993. **115**: p. 4910-4911.
13. Chen, S.-A. and J.-M. Ni, Macromolecules, Vol. 25, No. 23, , 1992. **25**(23): p. 6081-6089.
14. Chiang, C.K., et al., 1997. **39**: p. 1098-1101.
15. Richard.D.McCullough, Macromolecules, 1996. **29**: p. 3654.
16. Sheina, E.E., et al., Macromolecules, 2004. **37**: p. 3526-3528.
17. Miyakoshi, R., A. Yokoyama, and T. Yokozawa, J. AM. CHEM. SOC., 2005. **127**(49): p. 17542-17547.
18. Koster, L.J, V.D. Mihailetschi, P.W.M. Blom, Applied Physics Letters, 2006. **88**: p. 93511 .
19. Padinger, F, Roman.S.Rittberger, Niyazi.S.Sariciftci, Adv. Funct. Mater, 2003. **13**(1): p. 85-88.
20. Kim, J.Y., et al., *Efficient tandem polymer solar cells fabricated by all-solution processing*. Science, 2007. **317**(5835): p. 222-225.
21. Chen, S.-A. C.C. Tsai, Macromolecules, 1993. **26**: p. 2234-2239.
22. Leclerc', G.D.a.M., Macromolecules 1991. **24**: p. 455-459.
23. Leclerc', G.D.a.M., Macromolecules, 1991. **24**: p. 455-459.
24. Xiao Hu, L.Xiu, Polymer, 2000. **41**: p. 9147-9154.
25. Sheina, E.E., et al., Chem. Mater, 2005. **17**(13): p. 3317-3319.



26. Ryo Miyakoshi, A.Y. Tsutomu Yokozawa, J. AM. CHEM. SOC., 2005. **127**(49): p. 17542-17547.
27. Chenjun Shi, Yang Yang, and Qibing Pei, J. AM. CHEM. SOC., 2006. **128**: p. 8980-8986.
28. Robert S. Loewe, R.D. McCullough, Adv. Mater., 1999. **11**(3): p. 250-253.
29. Boymond, L., et al., Angew. Chem. Int. Ed., 1998. **37**(12): p. 1701-1703.
30. Odian, G., *Principles of polymerization, second edition*. p. 423-440.
31. Leeuw, D.M., et al., Synth. Met., 1997. **87**: p. 53.



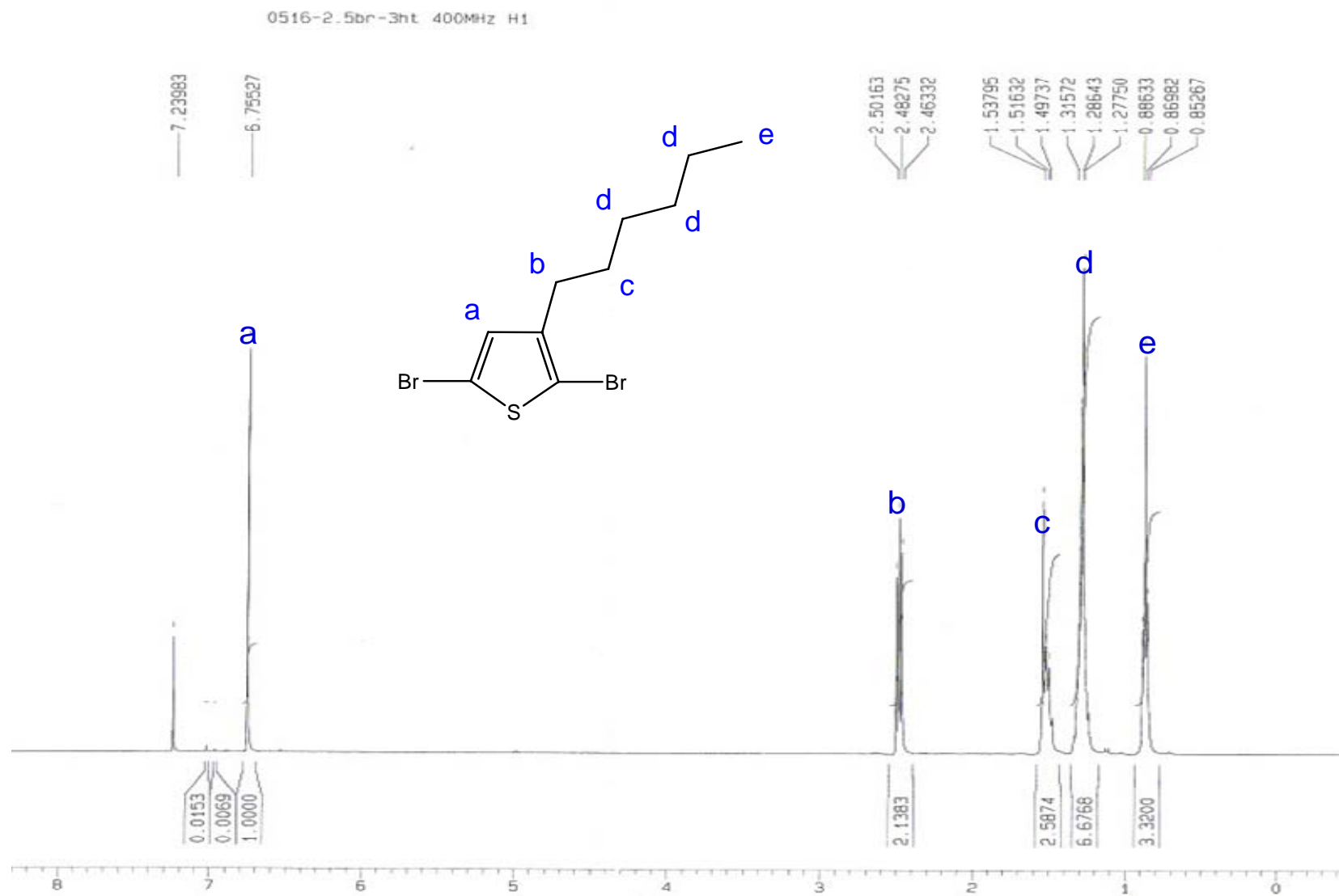


Figure 3.2 ¹H NMR of 2,5-dibromo-3-hexyl thiophene

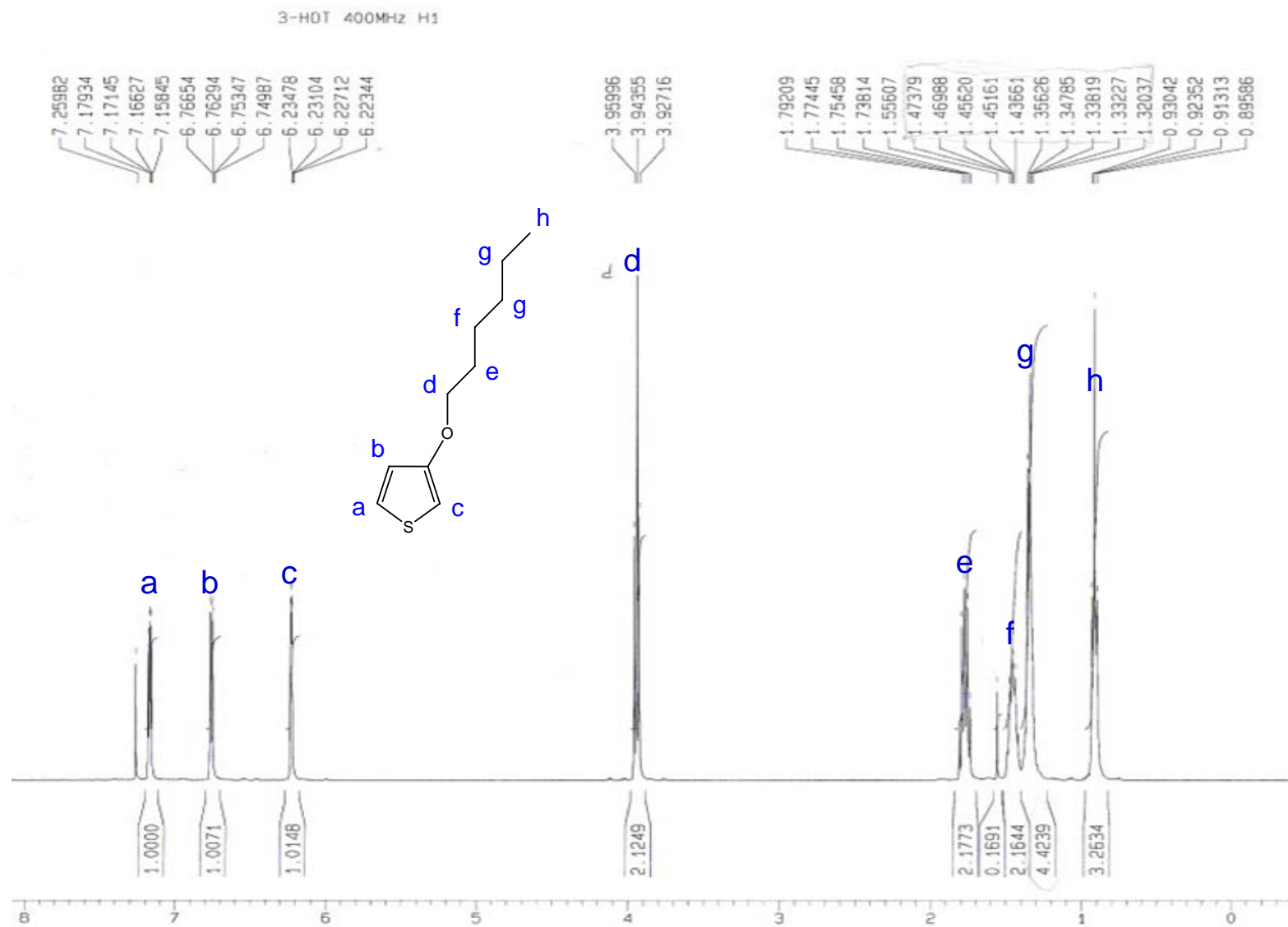


Figure 3.3 H NMR of 3-hexyloxy thiophene

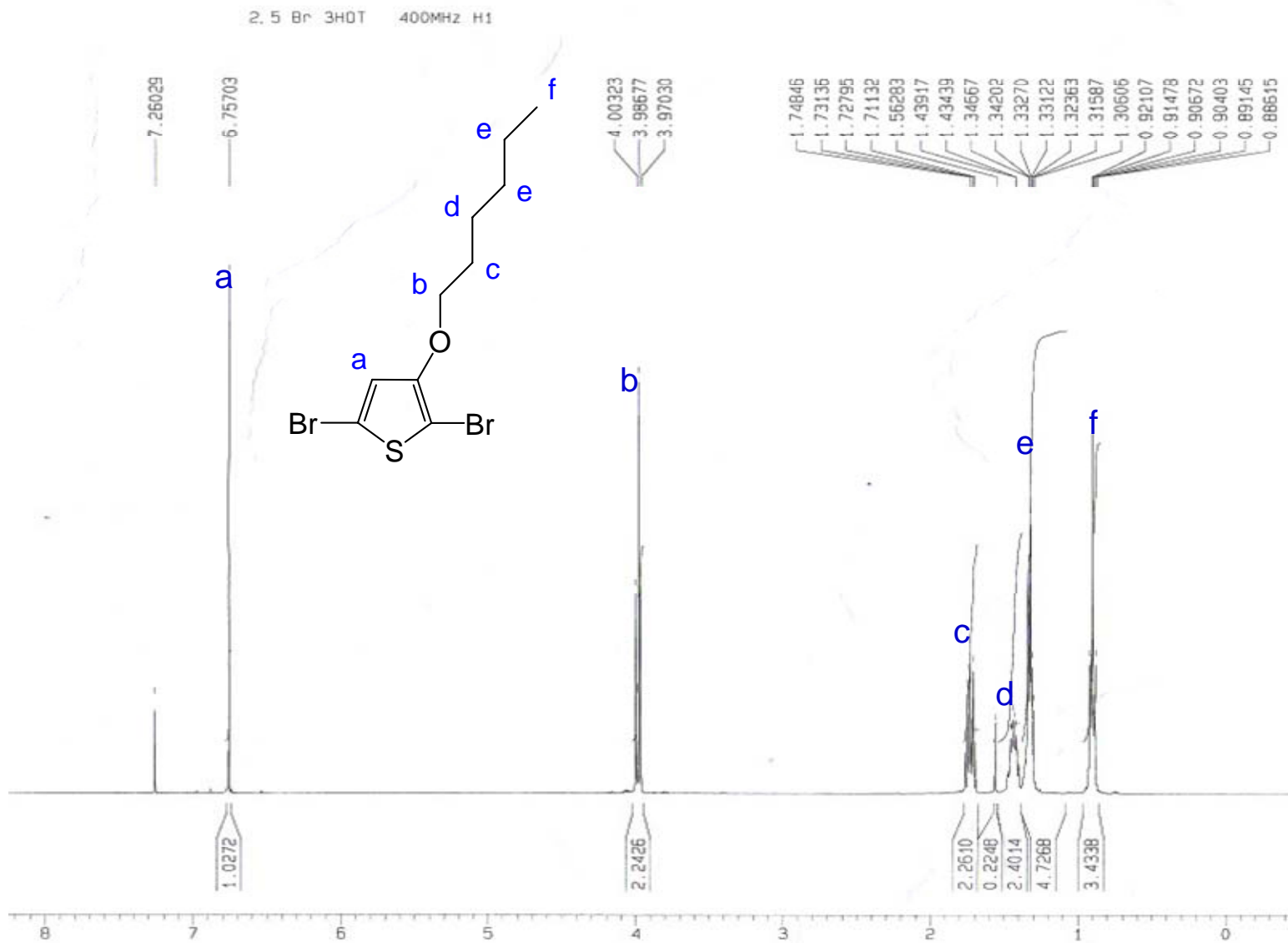


Figure 3.4 ^1H NMR of 2,5-dibromo-3-hexyloxy thiophene

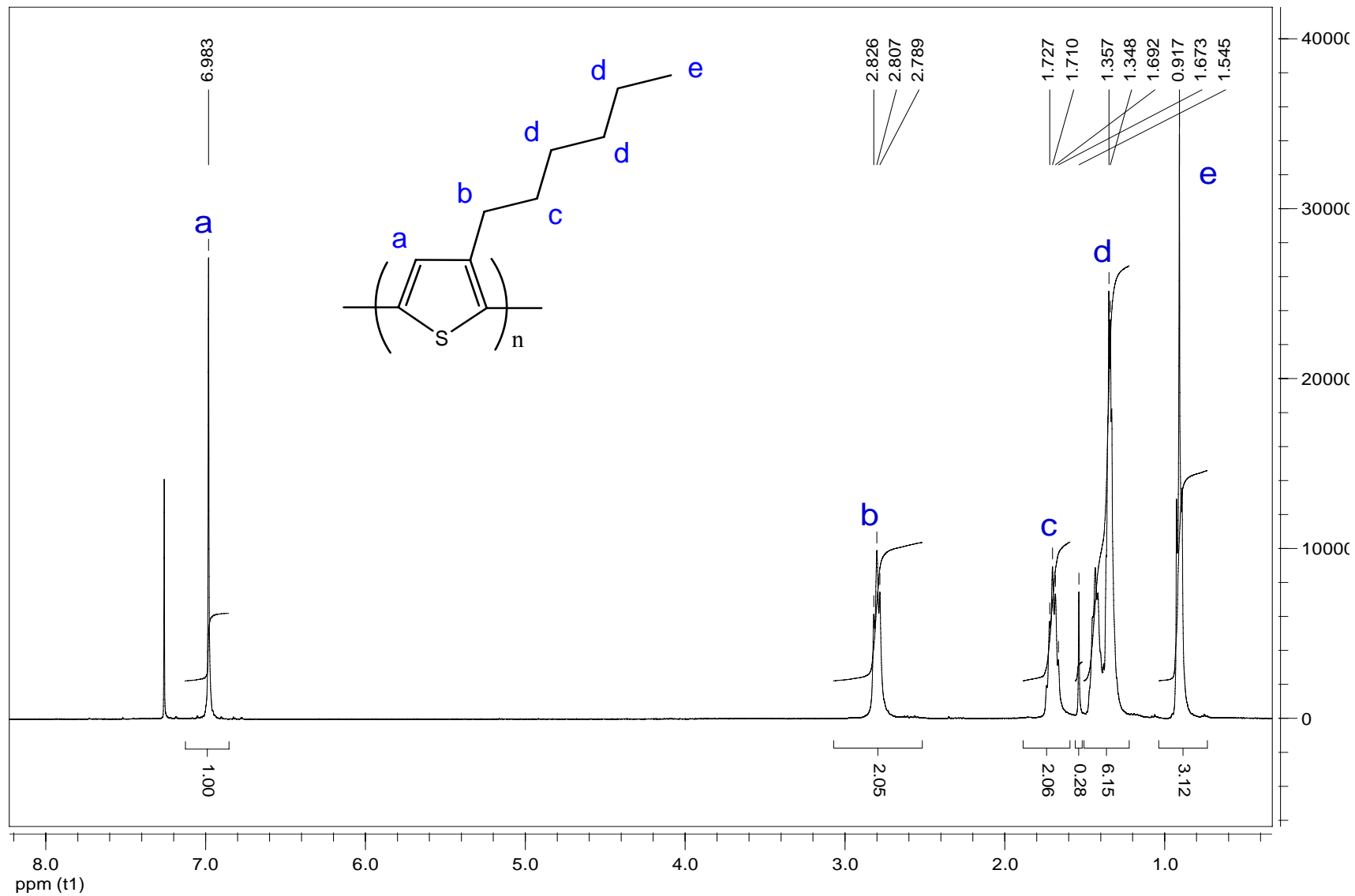


Figure 3.5 ¹H NMR of poly(3-hexyl thiophene)

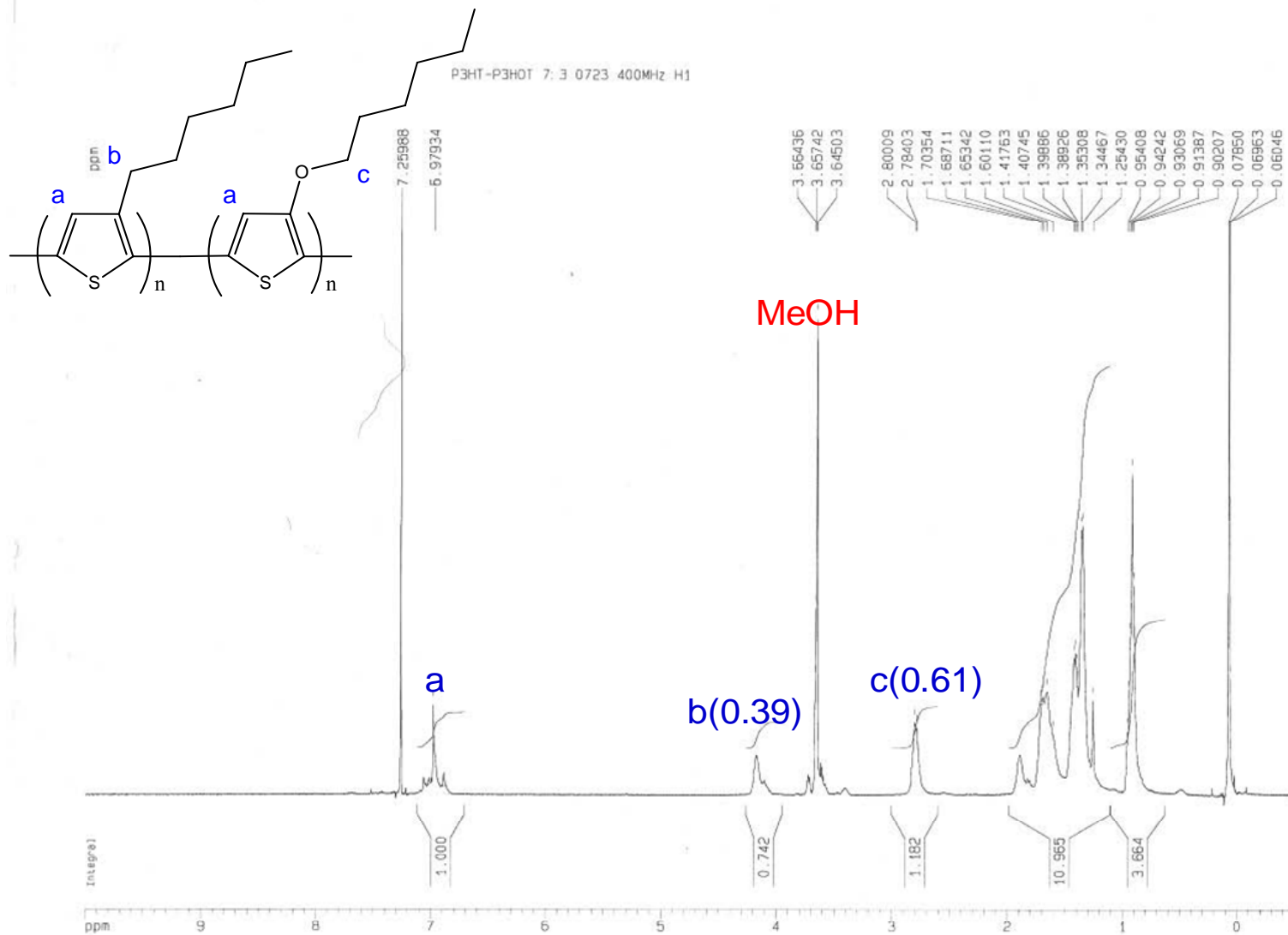


Figure 3.6 ¹H NMR of poly(3-hexyl thiophene)-co-poly(3-hexyloxy thiophene) Feed ratio: 7:3

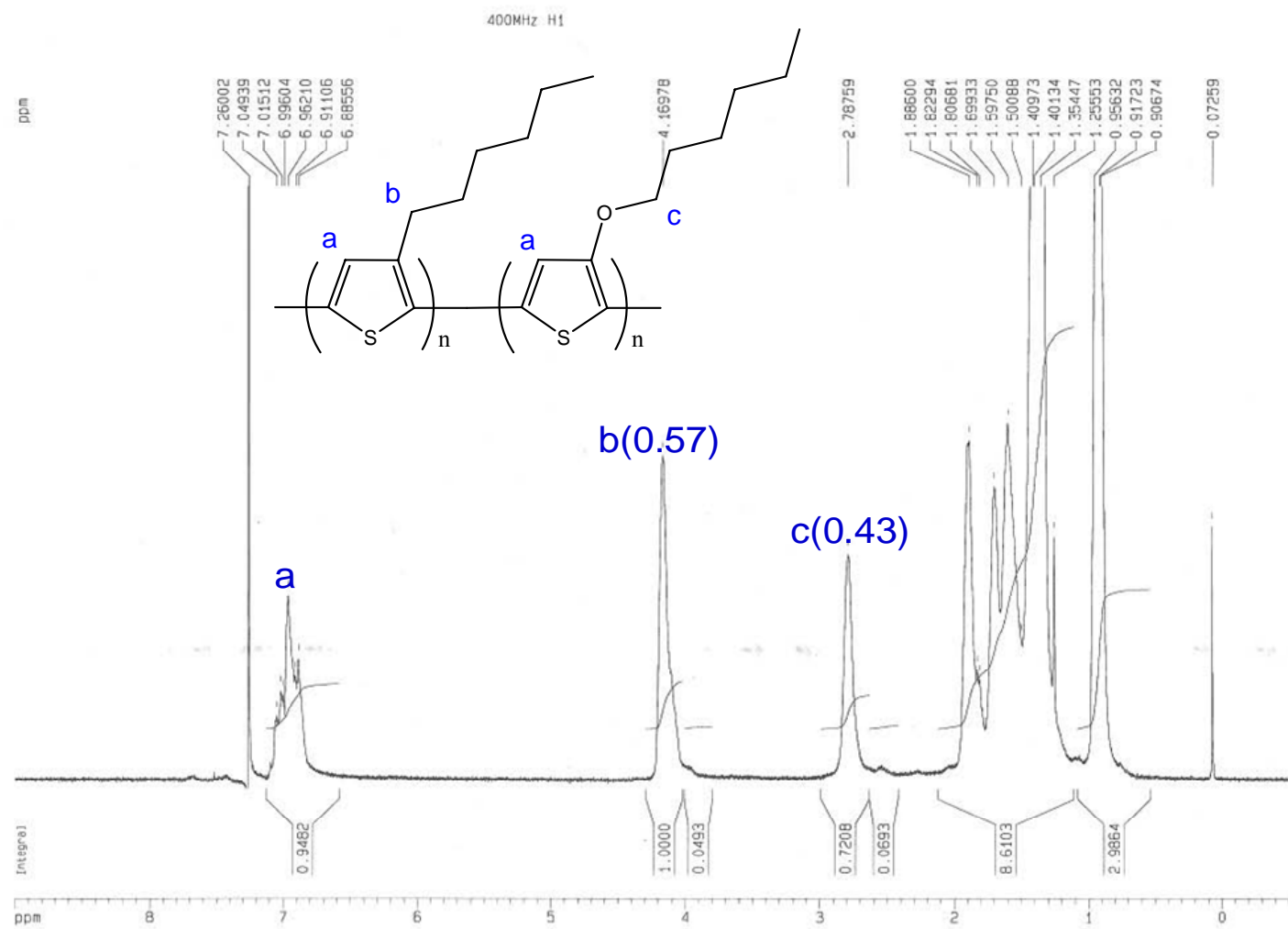


Figure 3.7 ¹H NMR of poly(3-hexyl thiophene)-co-poly(3-hexyloxy thiophene) **Feed ratio: 5:5**

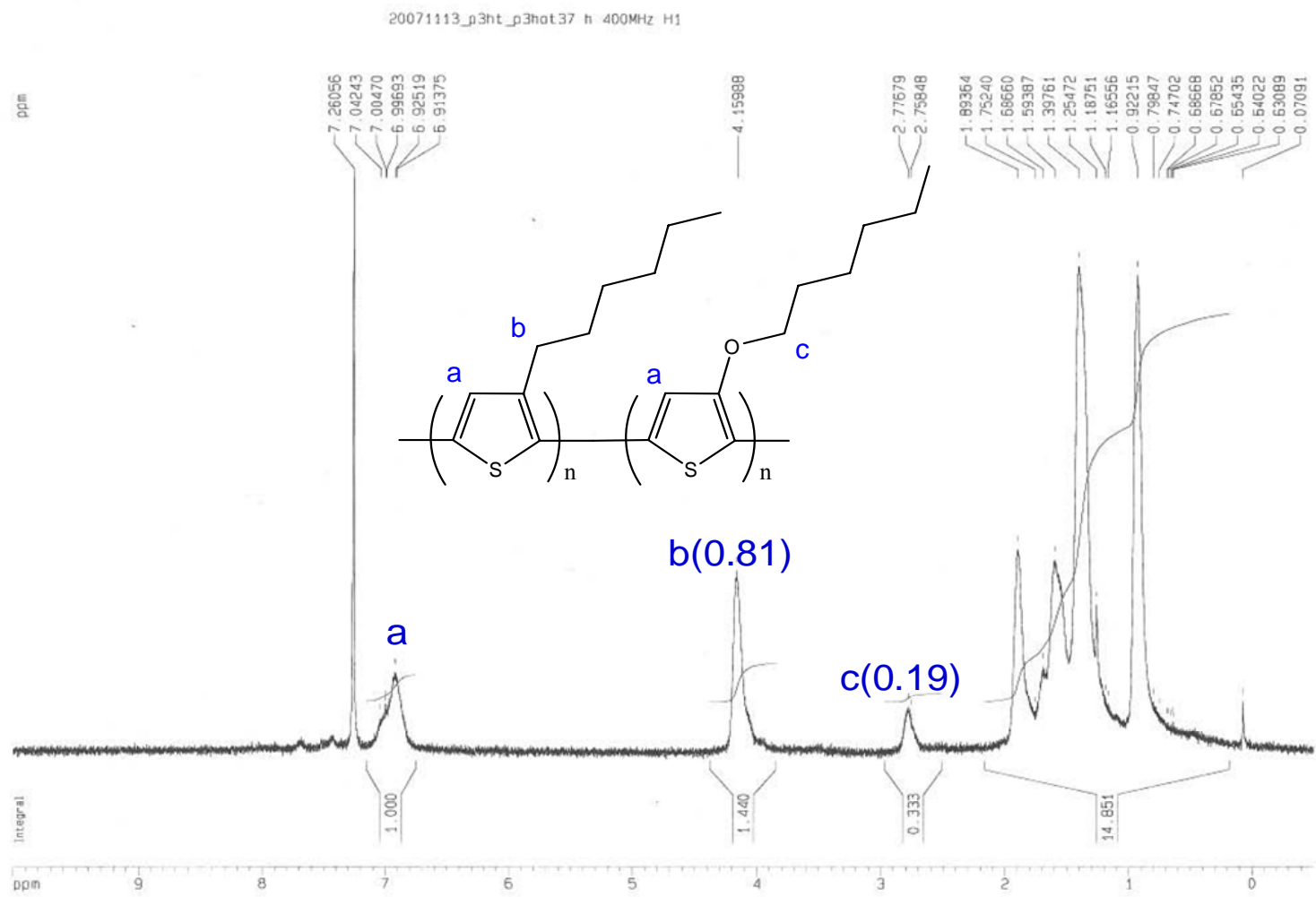


Figure 3.8 ¹H NMR of poly(3-hexyl thiophene)-co-poly(3-hexyloxy thiophene) **Feed ratio: 3:7**

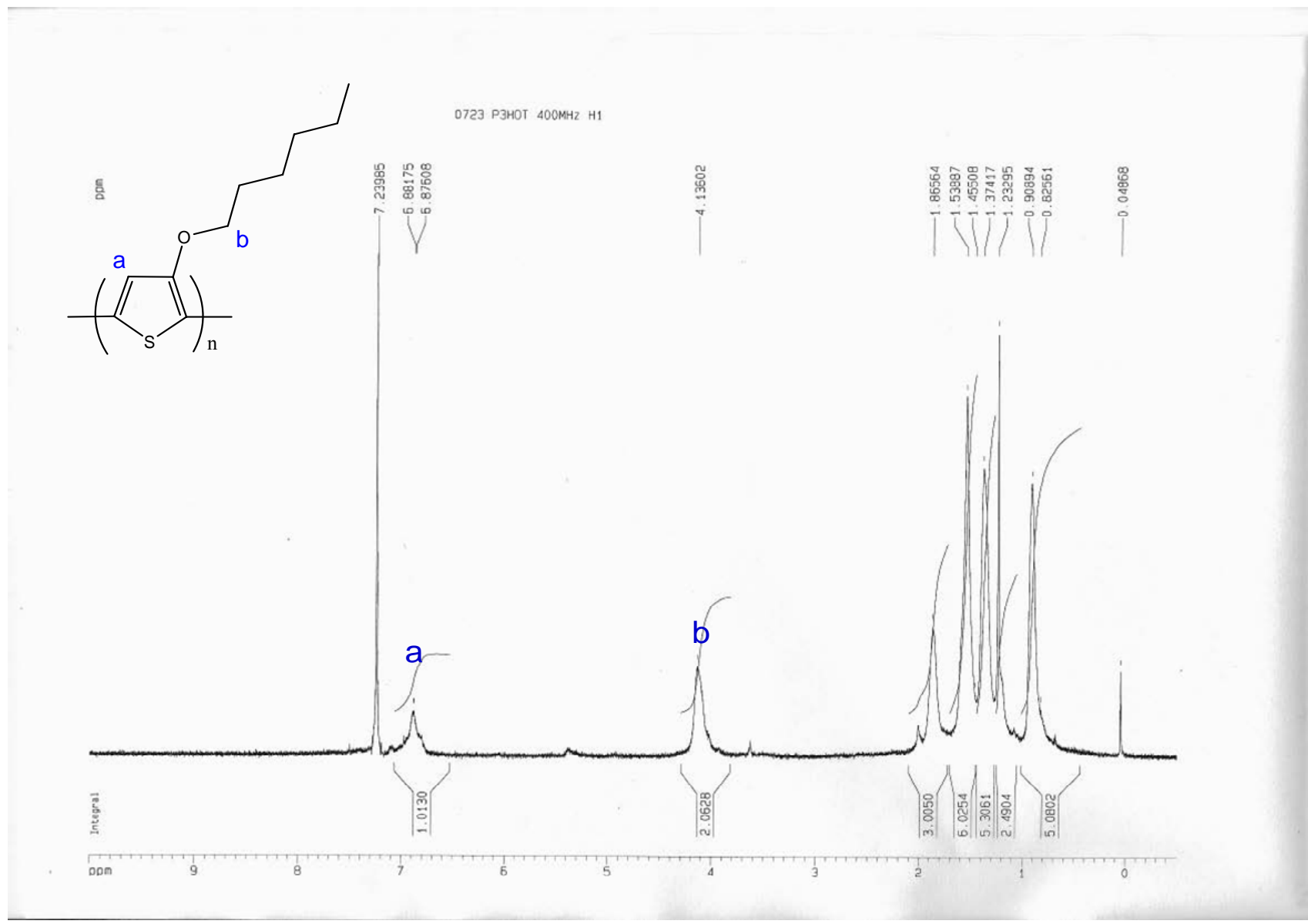


Figure 3.9 ¹H NMR of poly(3-hexyloxy thiophene)

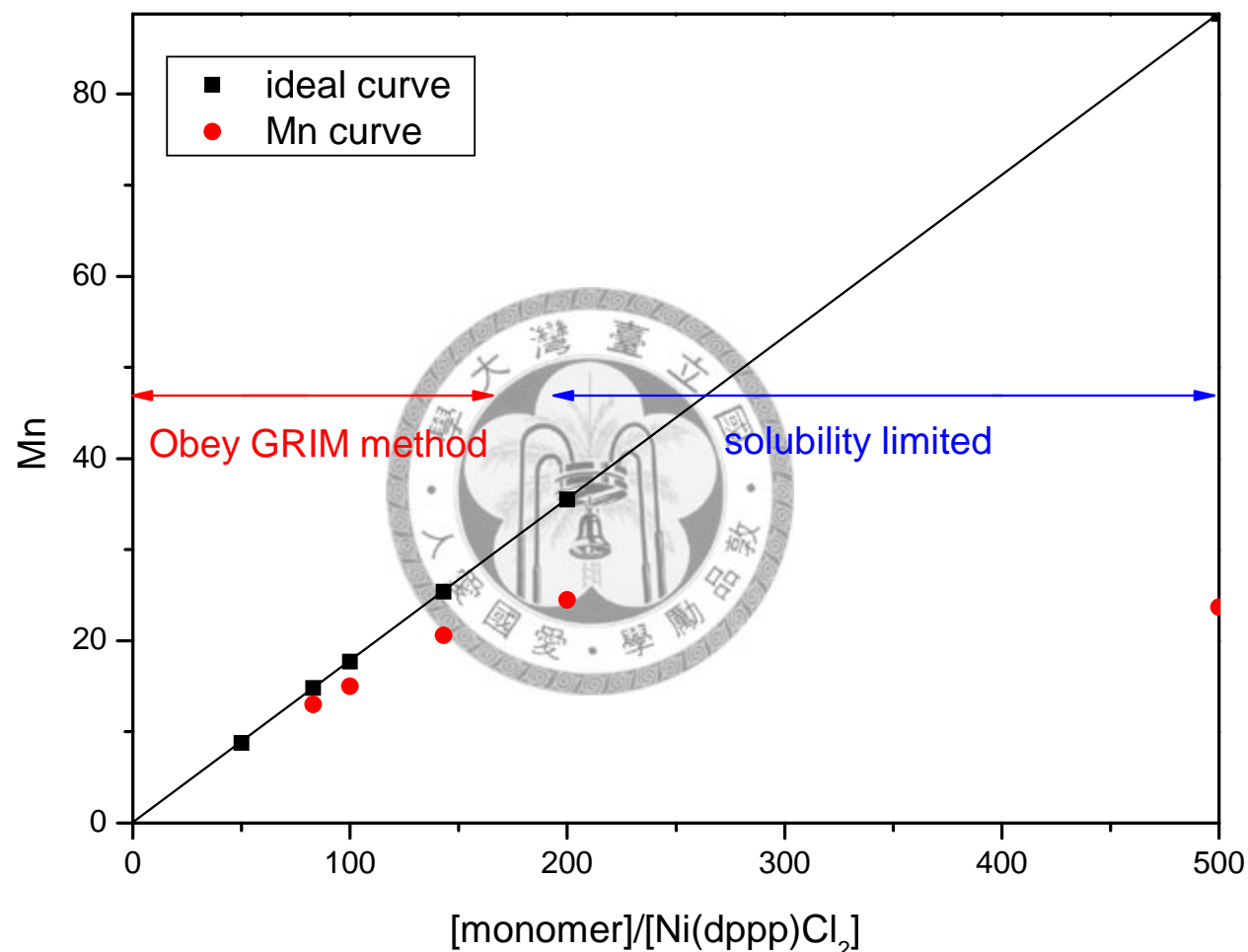


Figure 3.10 different ratio of monomer to Ni(dppp)Cl₂ results in equal molar of 3HT and 3HOT system(P3HT-P3HOT[5:5]), the solid line represent the ideal molecular weight calculated by the amount of feed, and the red dot represent the result of each experiment.

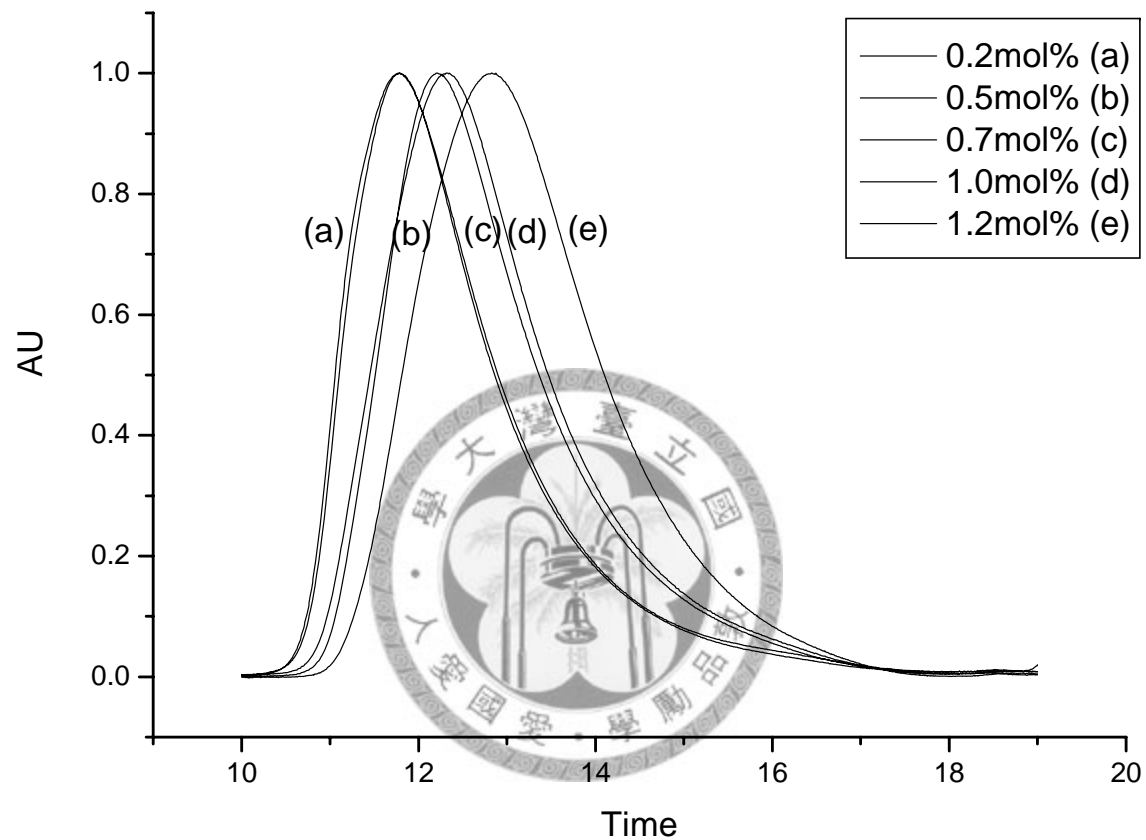


Figure 3.11 Five GPC peak of different ratio of monomer to Ni(dppp)Cl₂ results in equal molar of 3HT and 3HOT system(P3HT-P3HOT[5:5]), the slope of curve at left part has different number on high molecular weight(0.0986) is steeper than low molecular weight(0.0964), which means the reaction of high molecular weight in P3HT-P3HOT[5:5] system is restricted by the solubility

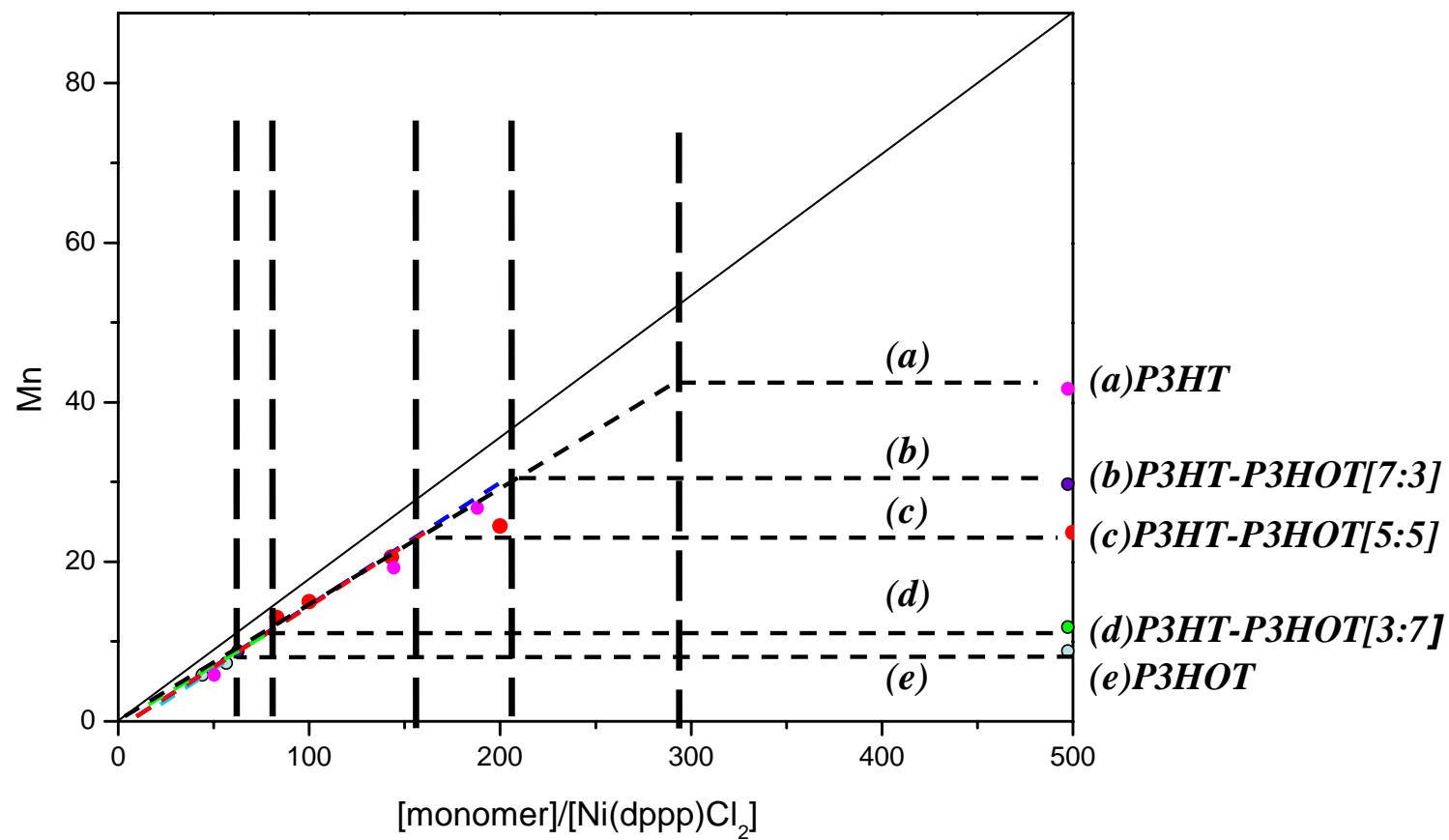


Figure 3.12 The relationship of Mn and [monomer]/[Ni(dppp)Cl₂] in different molar ratio of P3HT-P3HOT

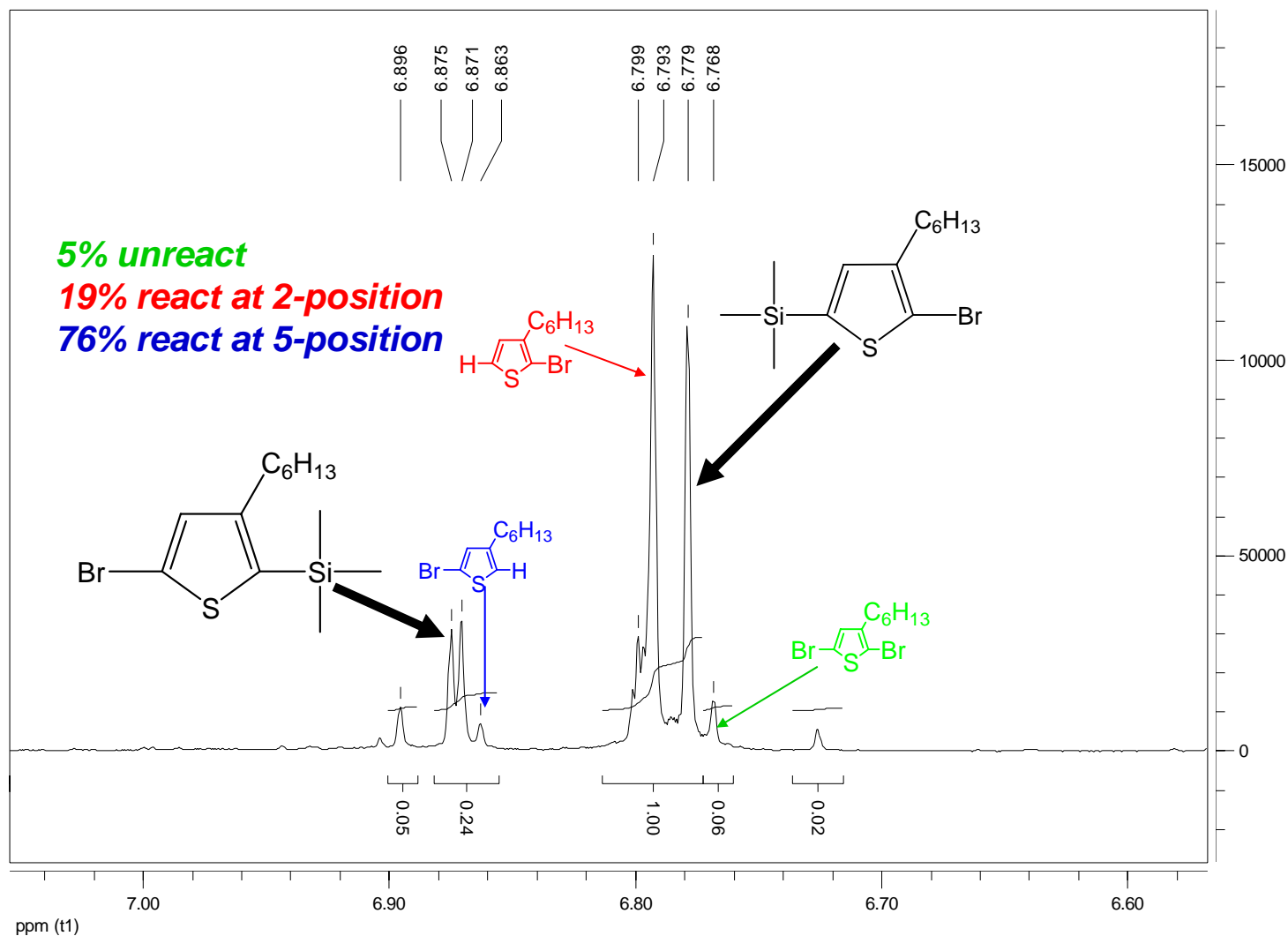


Figure 3.13 Quenching result of Grignard metathesis reaction of 3-hexylthiophene. The result shows that 5% of 2,5,Br-3-HT is unreact, 19% of 2,5,Br-3-HT react to the 2-position, 76% of 2,5,Br-3-HT react to the 5-position

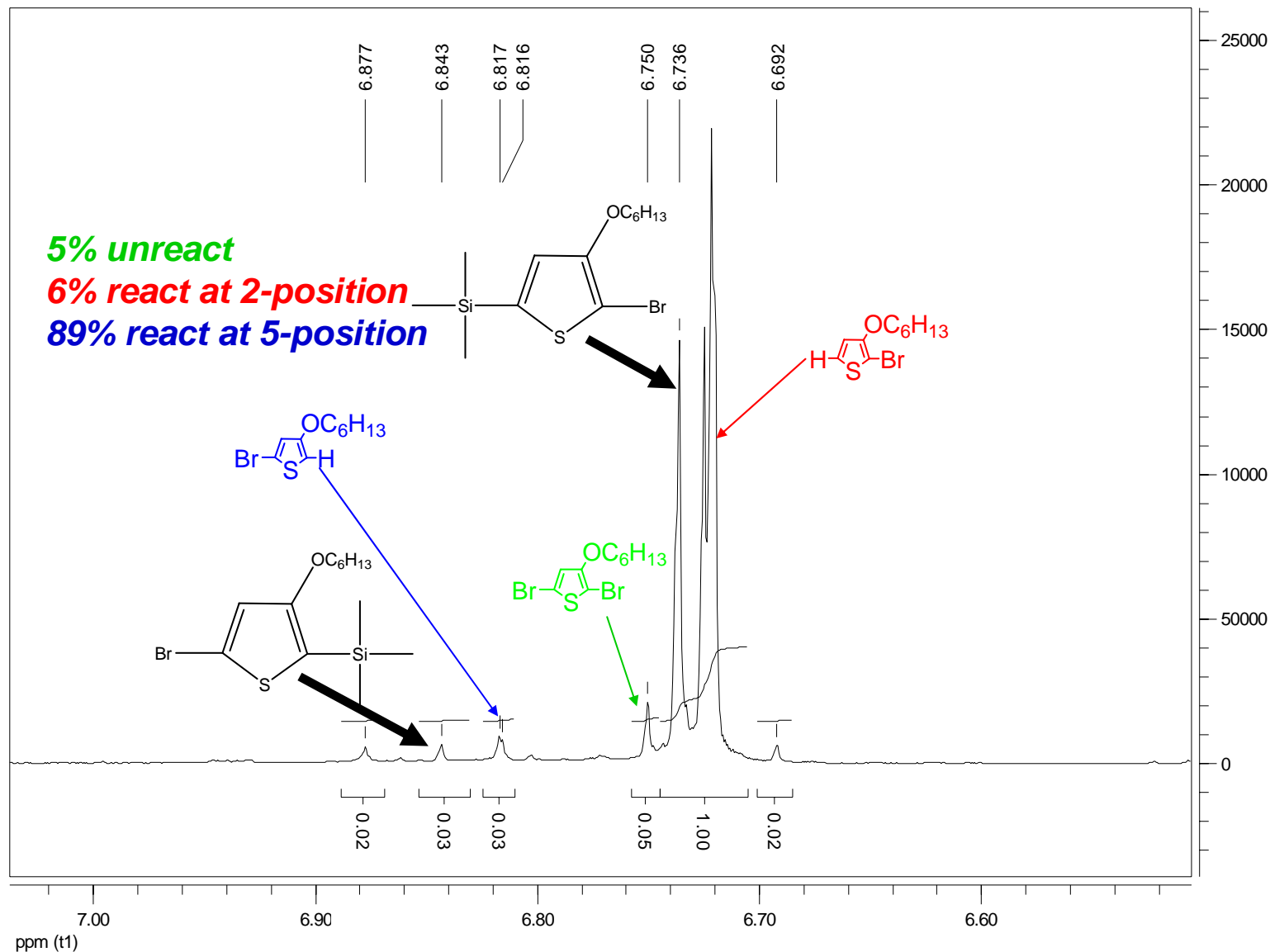


Figure 3.14 Quenching result of Grignard metathesis reaction of 3-hexyloxythiophene. The result shows that 5% of 2,5,Br-3-HOT is unreacted, 6% of 2,5,Br-3-HOT react to the 2-position, 89% of 2,5,Br-3-HOT react to the 5-position

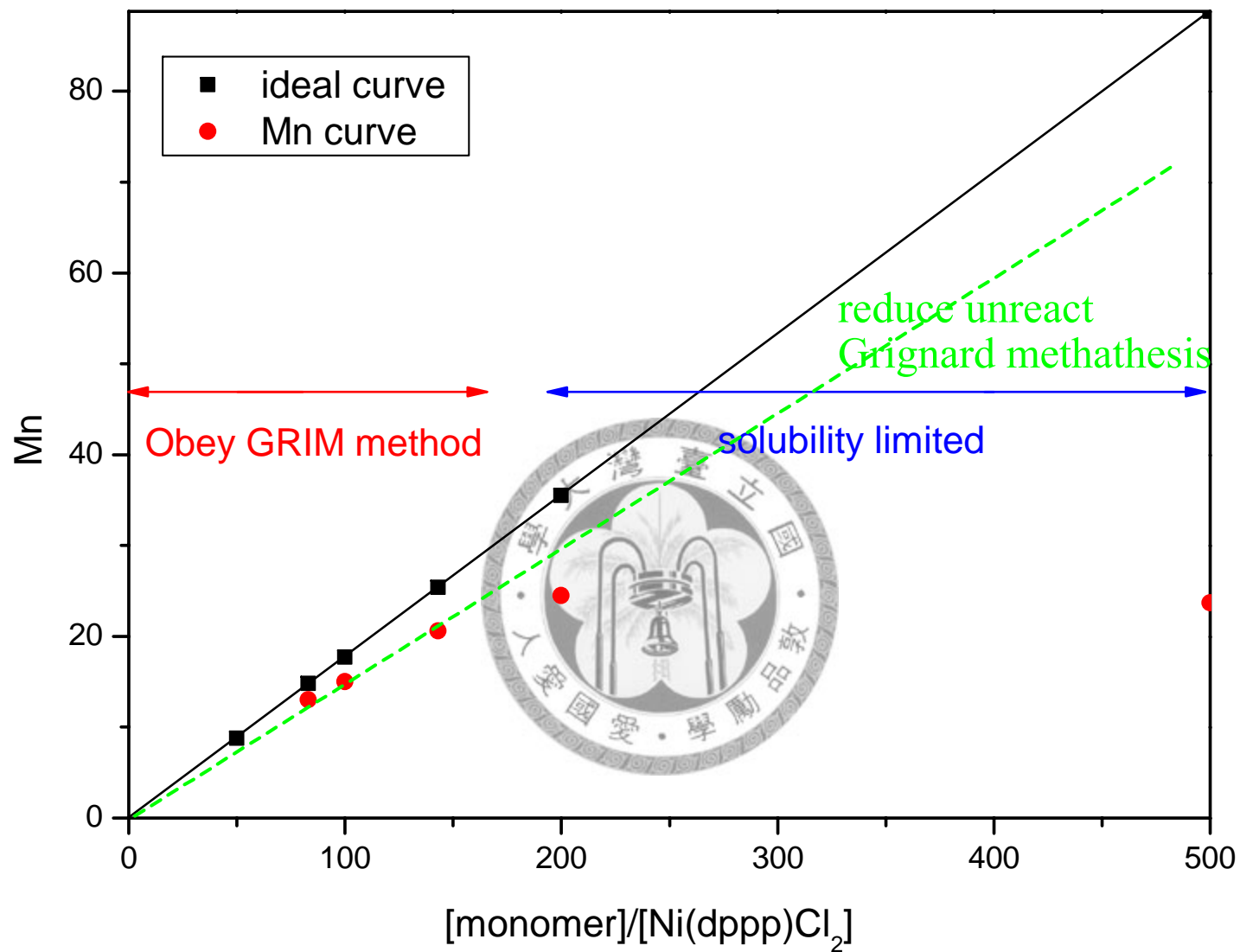


Figure 3.15 different ratio of monomer to Ni(dppp)Cl_2 results in equal molar of 3HT and 3HOT system (P3HT-P3HOT[5:5]), the green dash line represent the ideal molecular weight reduced to the unreact monomer plus the inreact Grignard methathesis

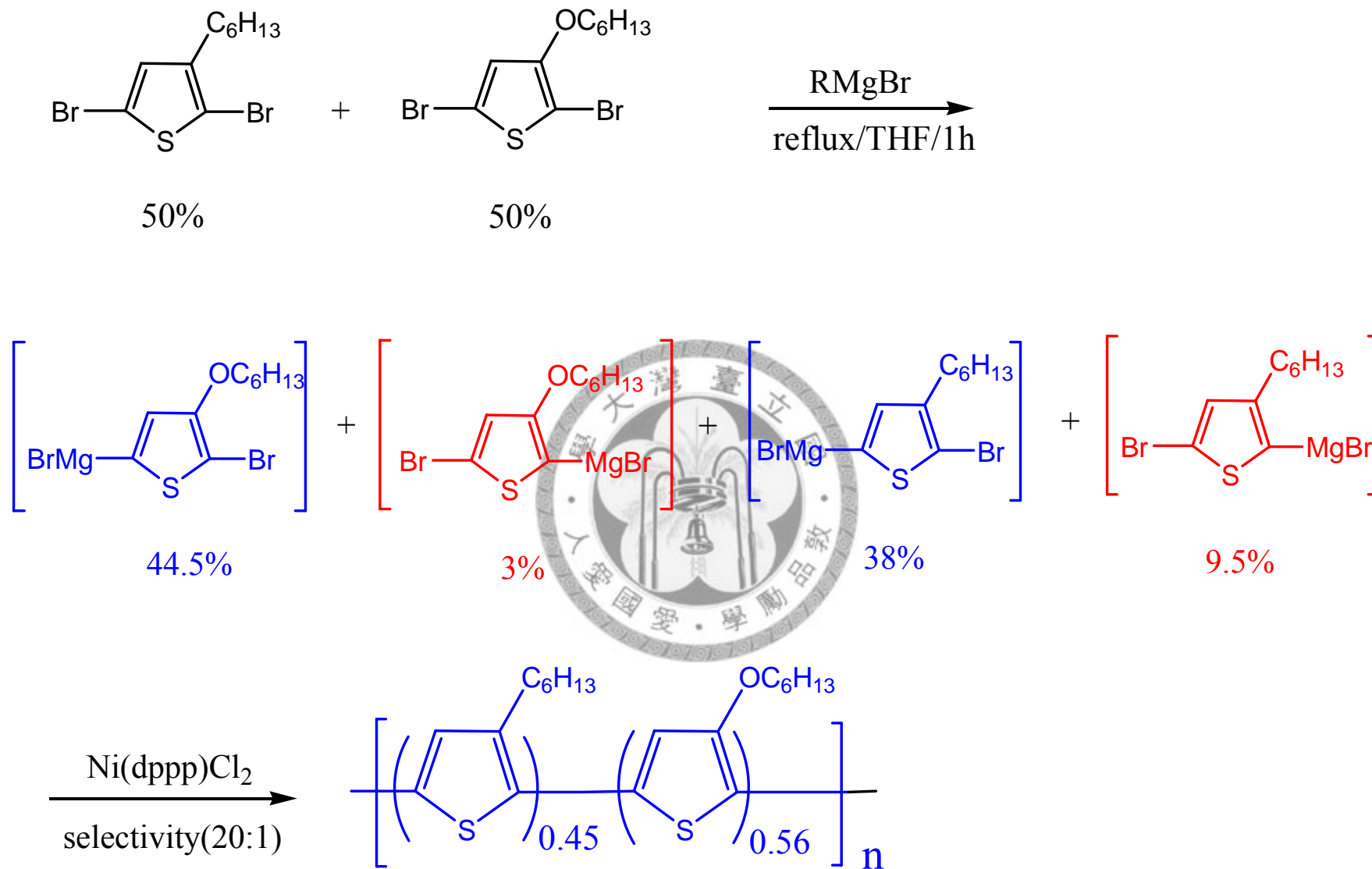


Figure 3.16 Mechanism prediction of equal molar of 3-HT and 3-HOT copolymerization(P3HT-P3HOT[5:5])

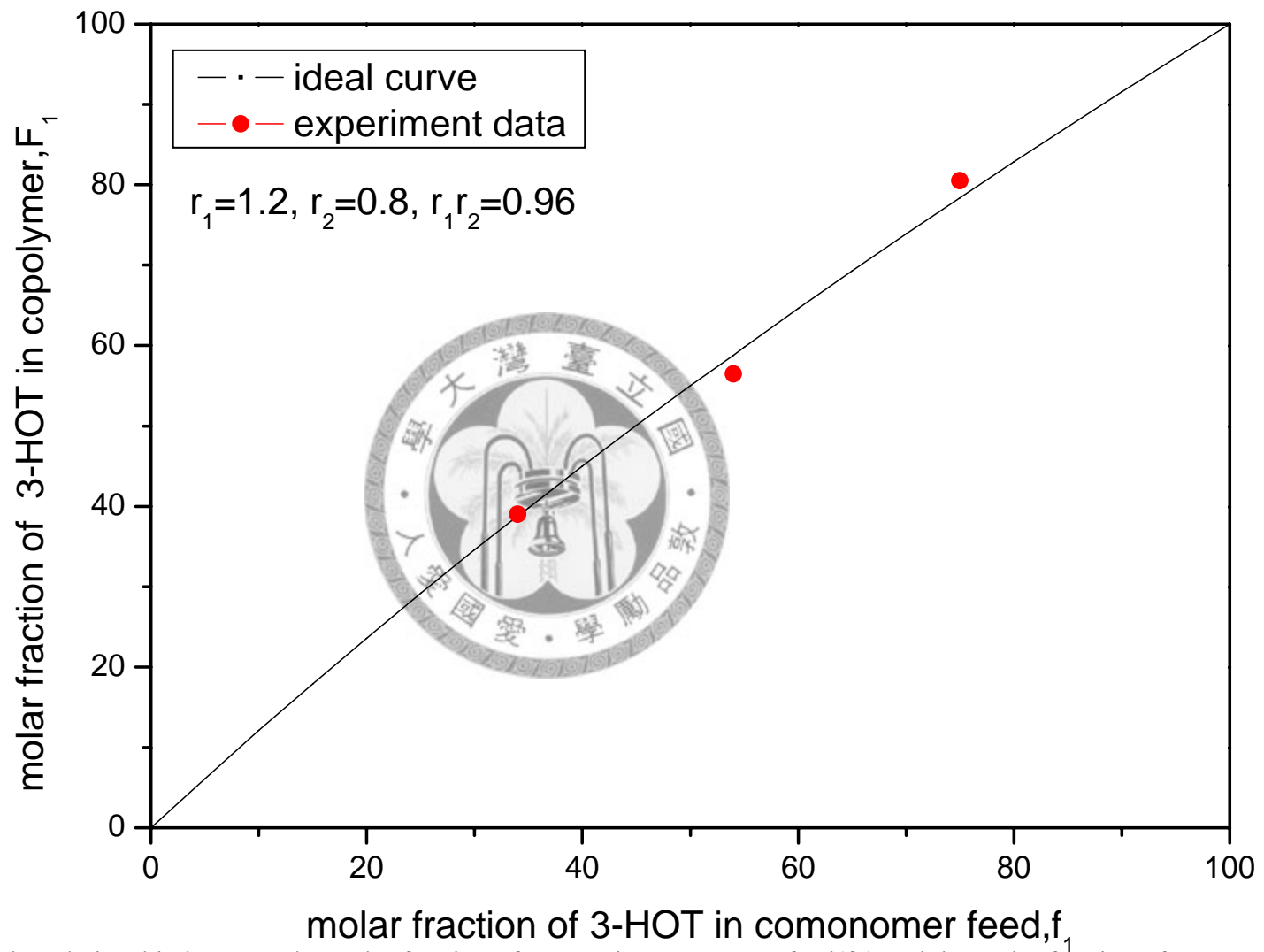


Figure 3.17 The relationship between the molar fraction of 3-HOT in comonomer feed(f_1) and the molar fraction of 3-HOT in copolymer(F_1), the black solid line was poltted by the copolymerization equation and the result of experiment

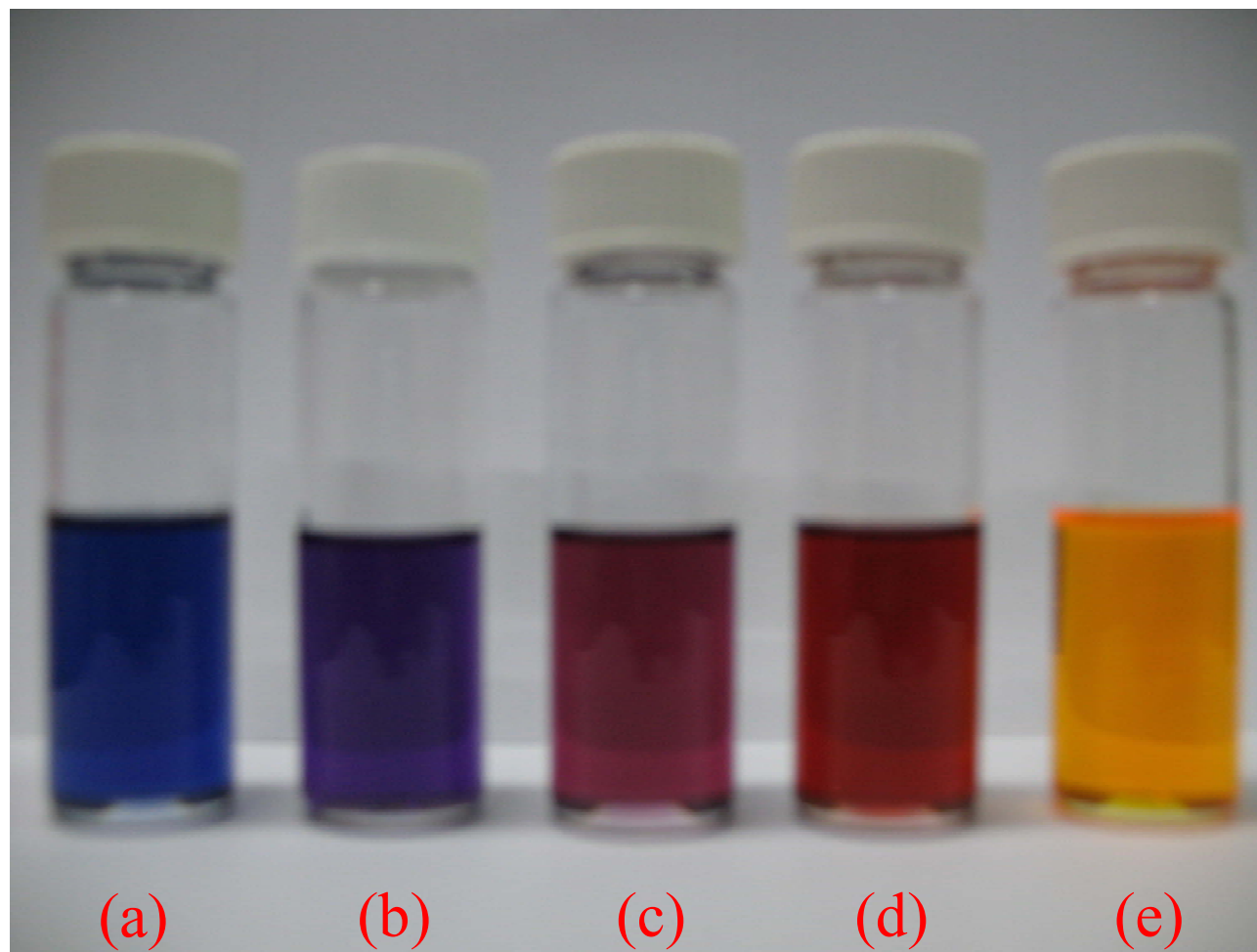


Figure 3.18 Outlook of five different molar fraction of P3HT-P3HOT, from left to right are (a)P3HOT, (b)P3HT-P3HOT[3:7], (c)P3HT-P3HOT[5:5], (d)P3HT-P3HOT[7:3], (e)P3HT respectively which are dissolved in Chloroform

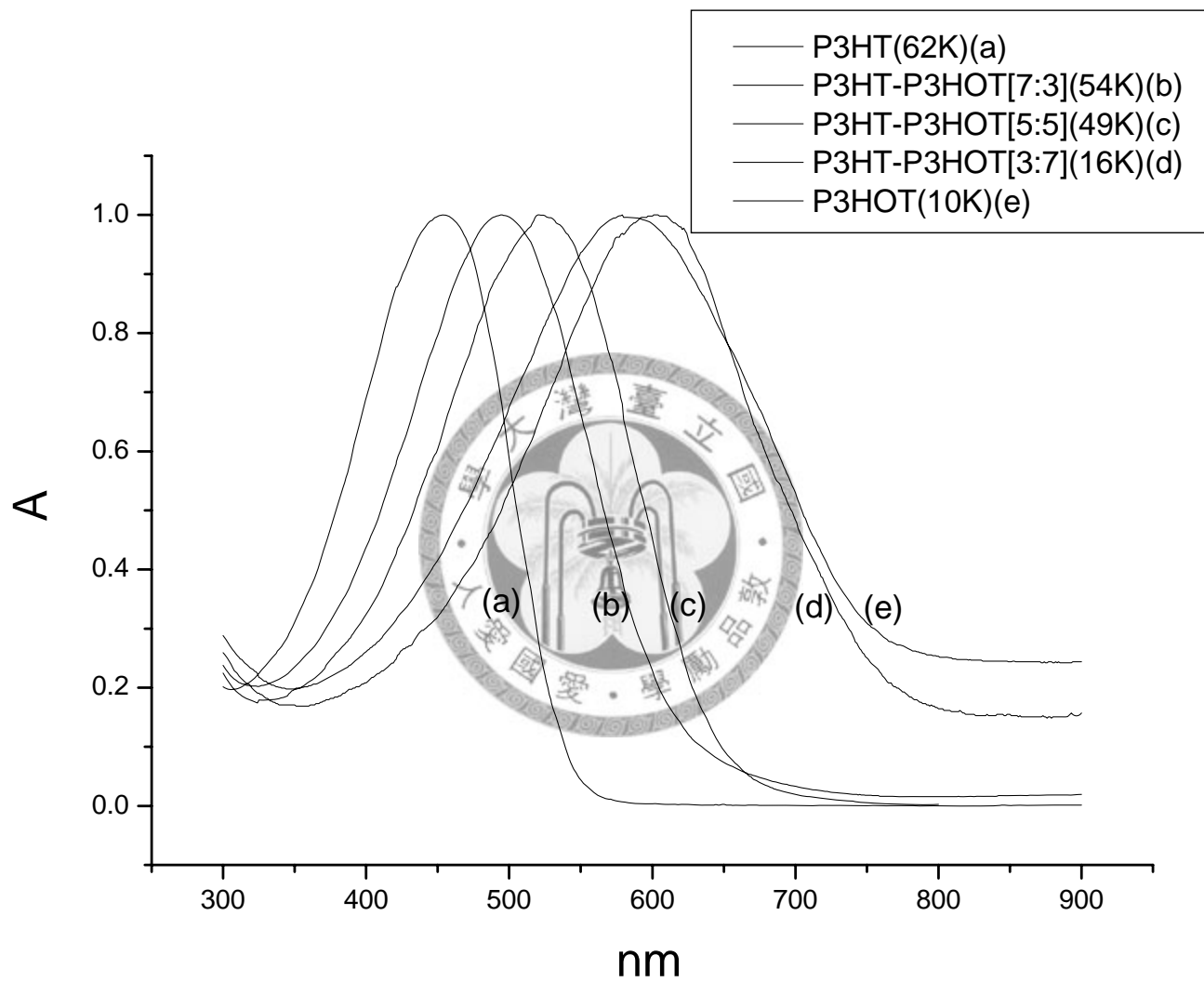


Figure 3.19 UV-absorption of five copolymers in chloroform solution

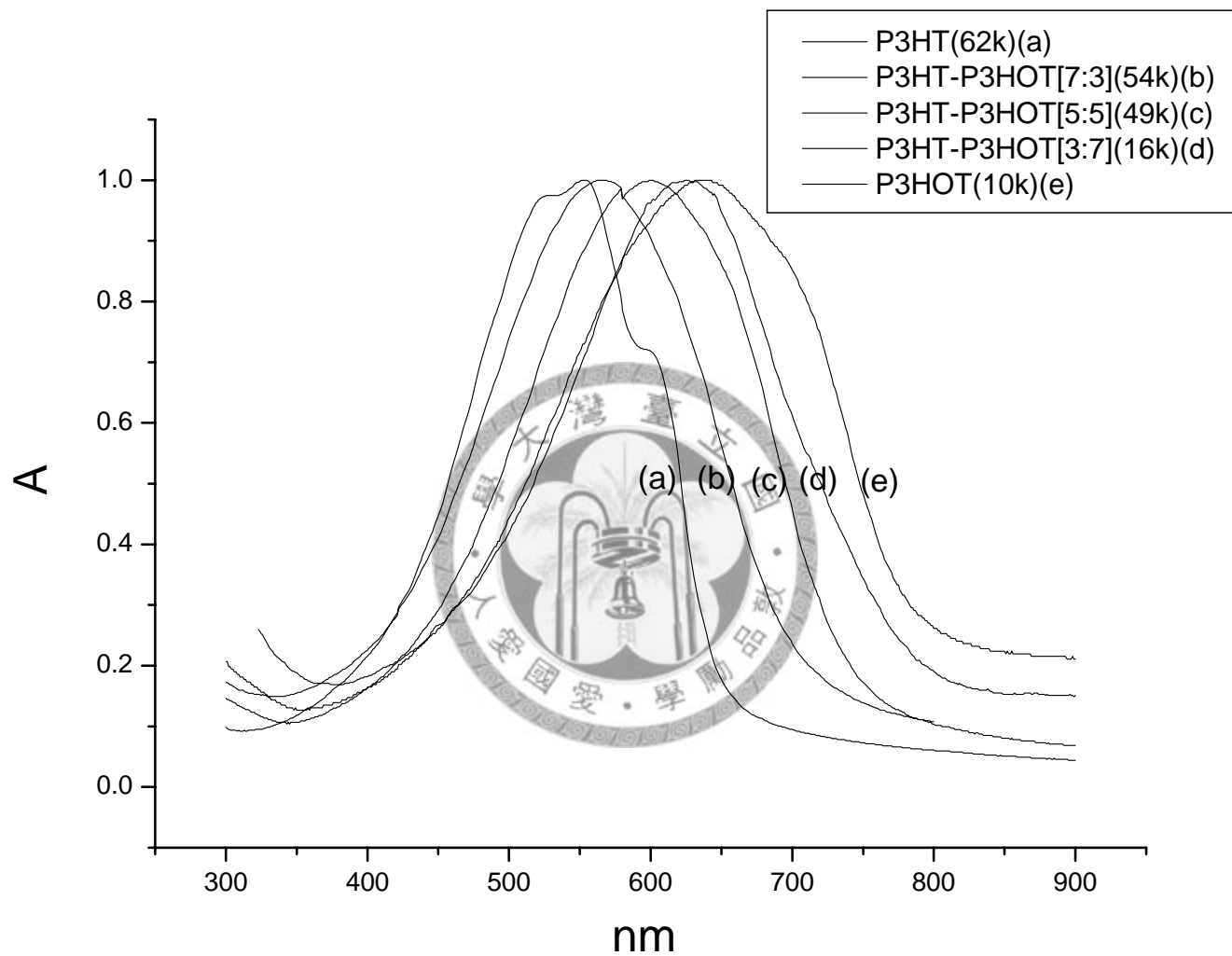


Figure 3.20 UV-absorption of five copolymers in thin film state

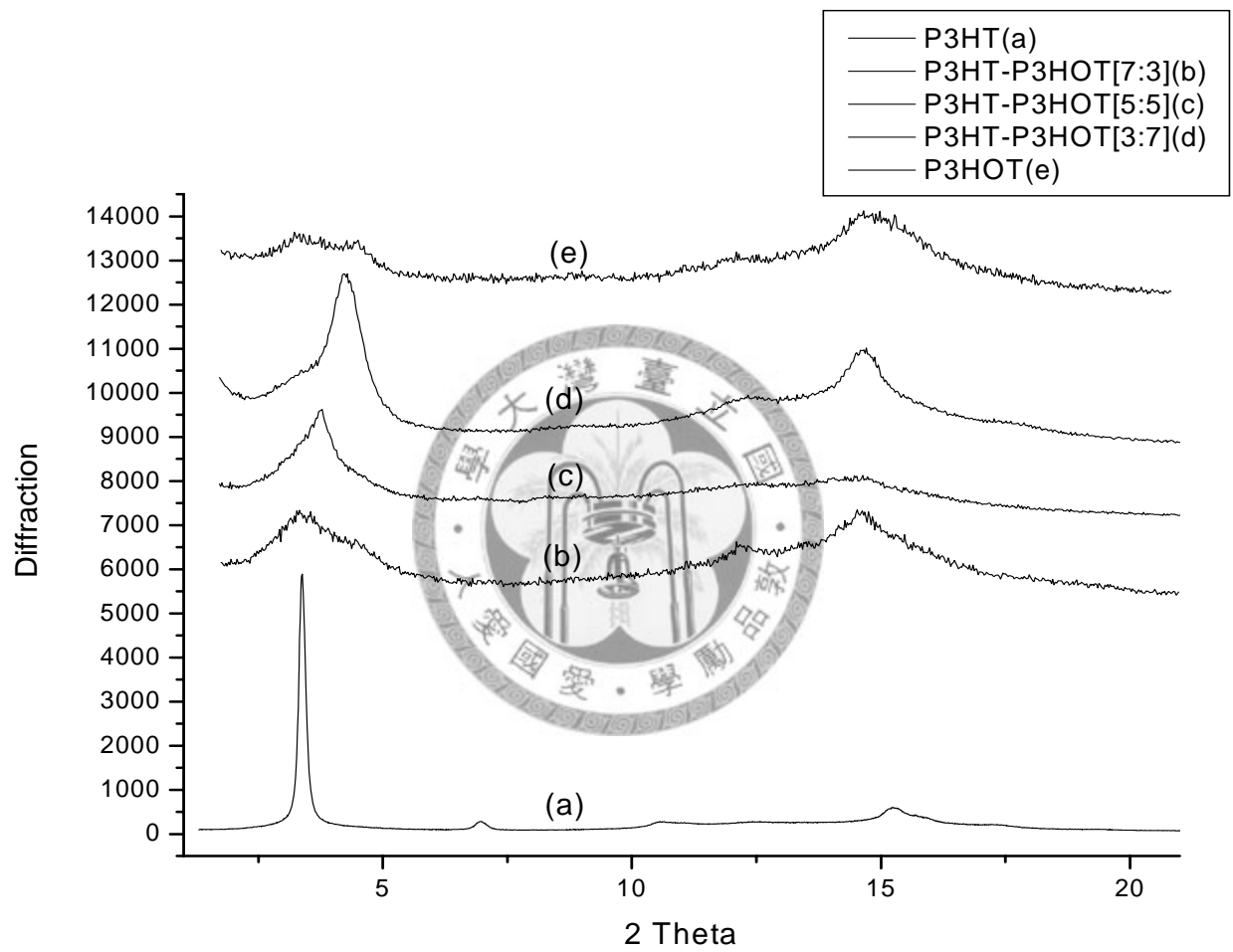


Figure 3.21 X-ray diffraction patterns of five polymer films cast from chloroform solutions

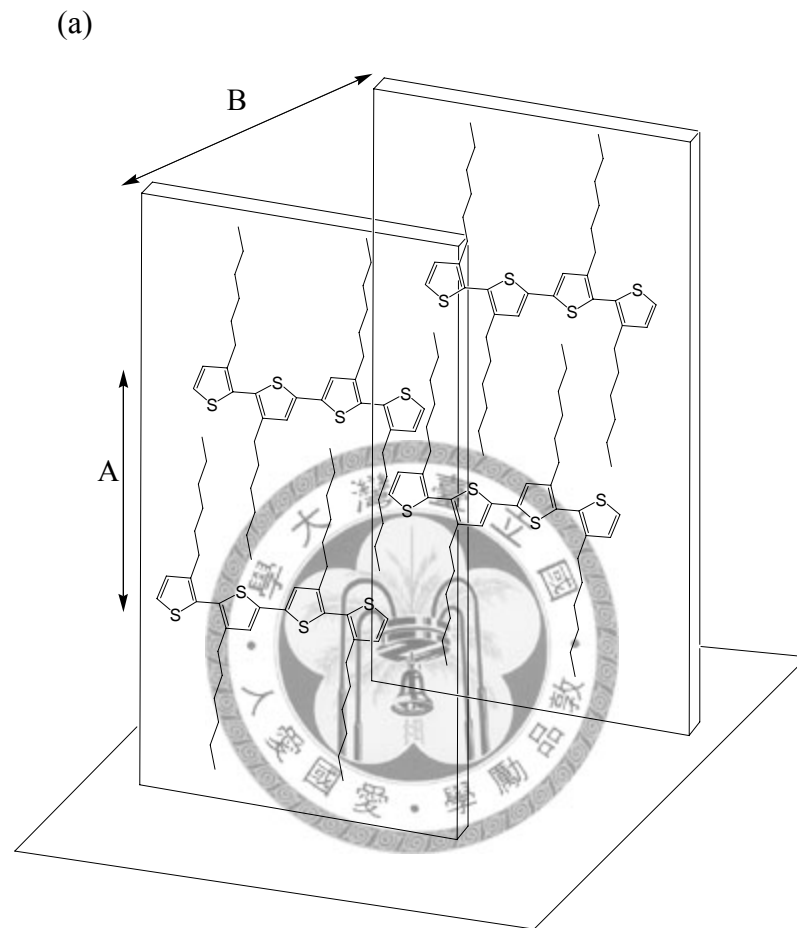


Figure 3.22 (a) simulate arrangement inside P3HT

since the hexyloxy group is more flexible than hexyl group, therefore, the distance of polymer backbone separated by hexyloxy side chain A is shorter than homogeneous P3HT. and the layer-to-layer π -stacking distance B will become larger, due to the packing is looser when polymer contains hexyloxy group

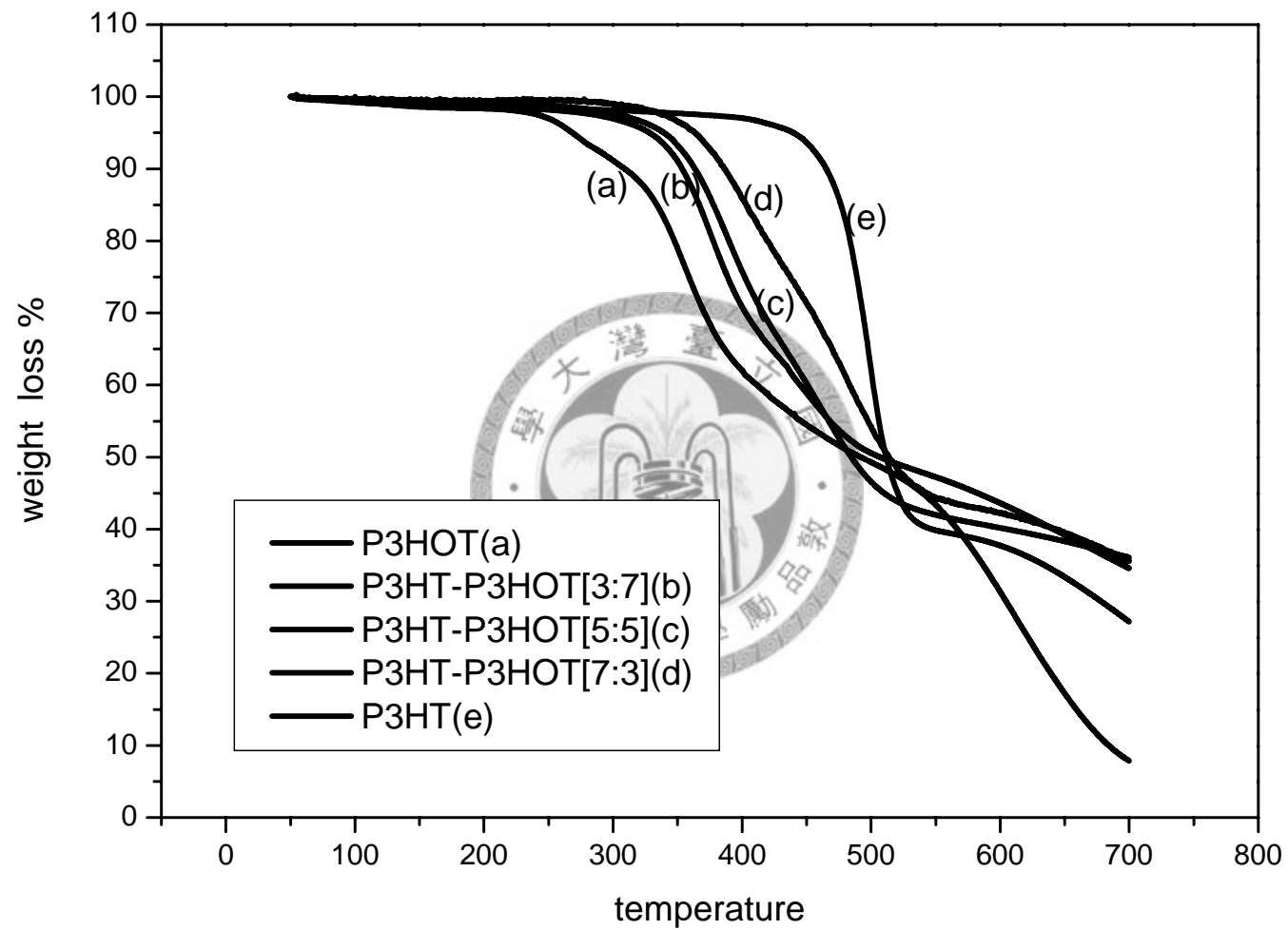


Figure 3.23 TGA curve of five polymer

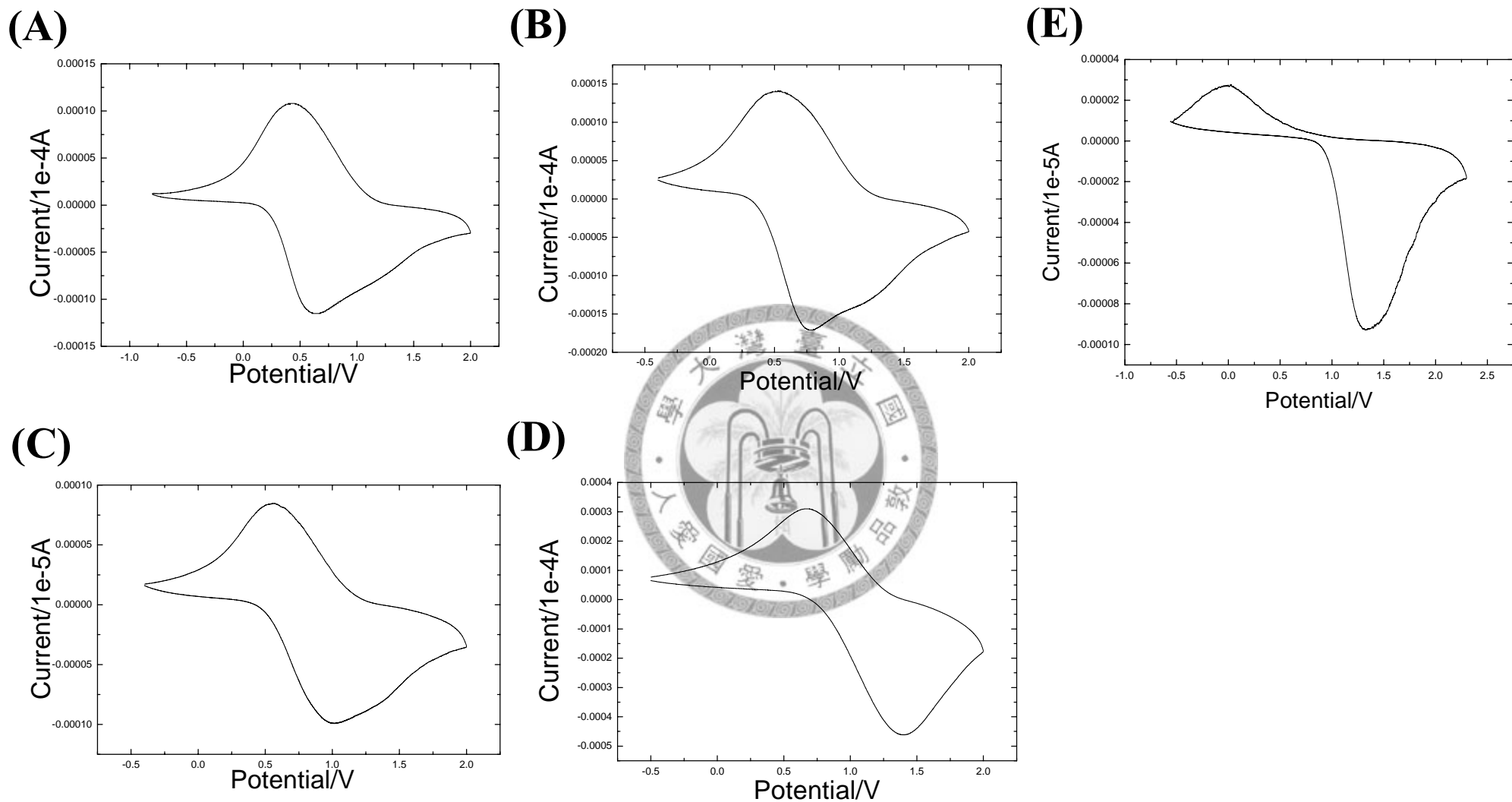


Figure 3.24 Cyclic voltammograms diagram(CV) of five different molar fraction of P3HT-P3HOT
 (A)P3HOT (B)P3HT-P3HOT[3:7] (C)P3HT-P3HOT[5:5] (D)P3HT-P3HOT[7:3] (E)P3HT

Vaccum level(Unit: eV)

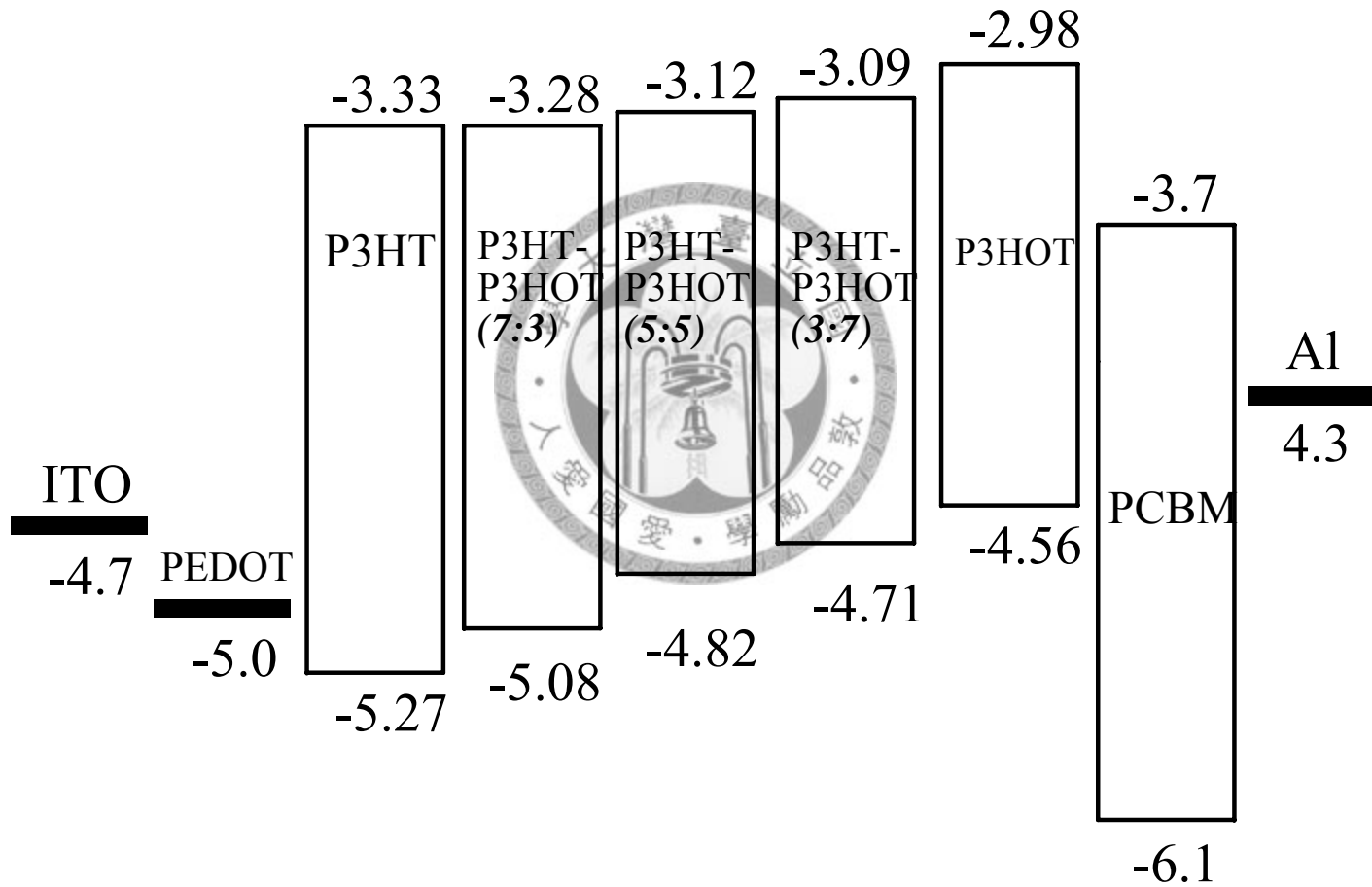


Figure3.25 Energy-level diagram of five different molar fraction of P3HT-P3HOT

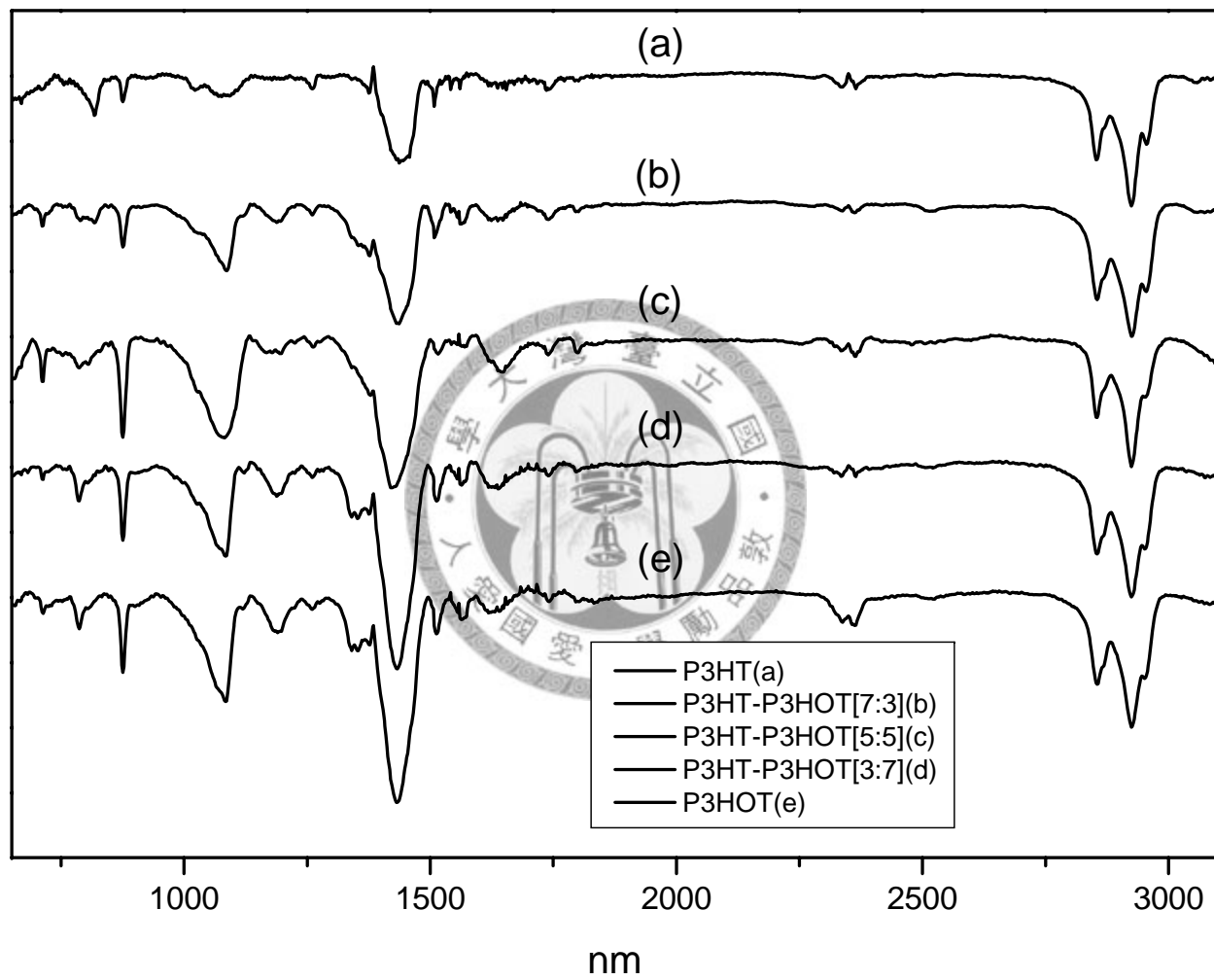


Figure 3.26 FT-IR of five different molar fraction of P3HT-P3HOT

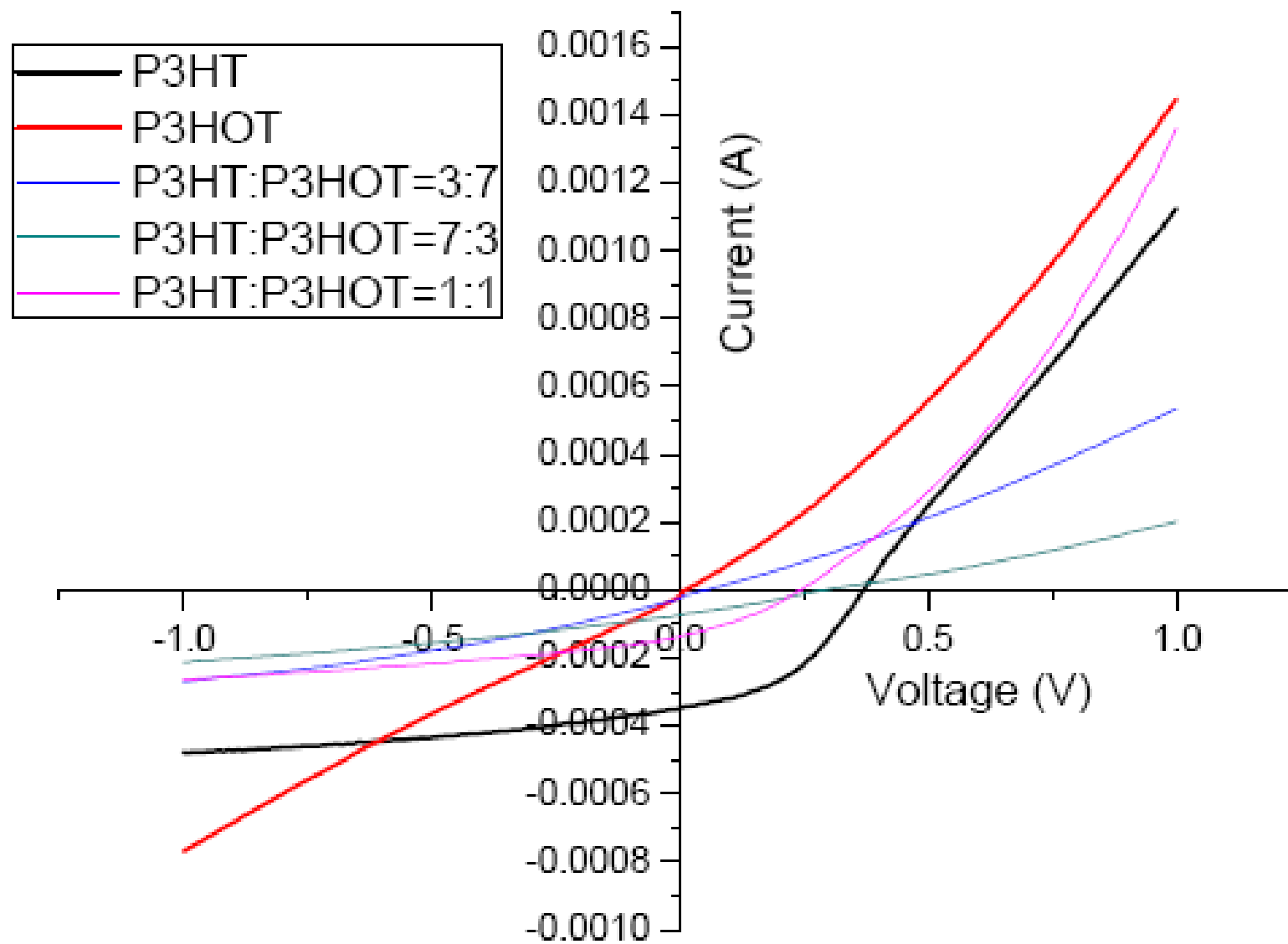


Figure 3.27 The current-voltage characteristics of a P3HT-P3HOT/PCBM bulk heterojunction solar cell

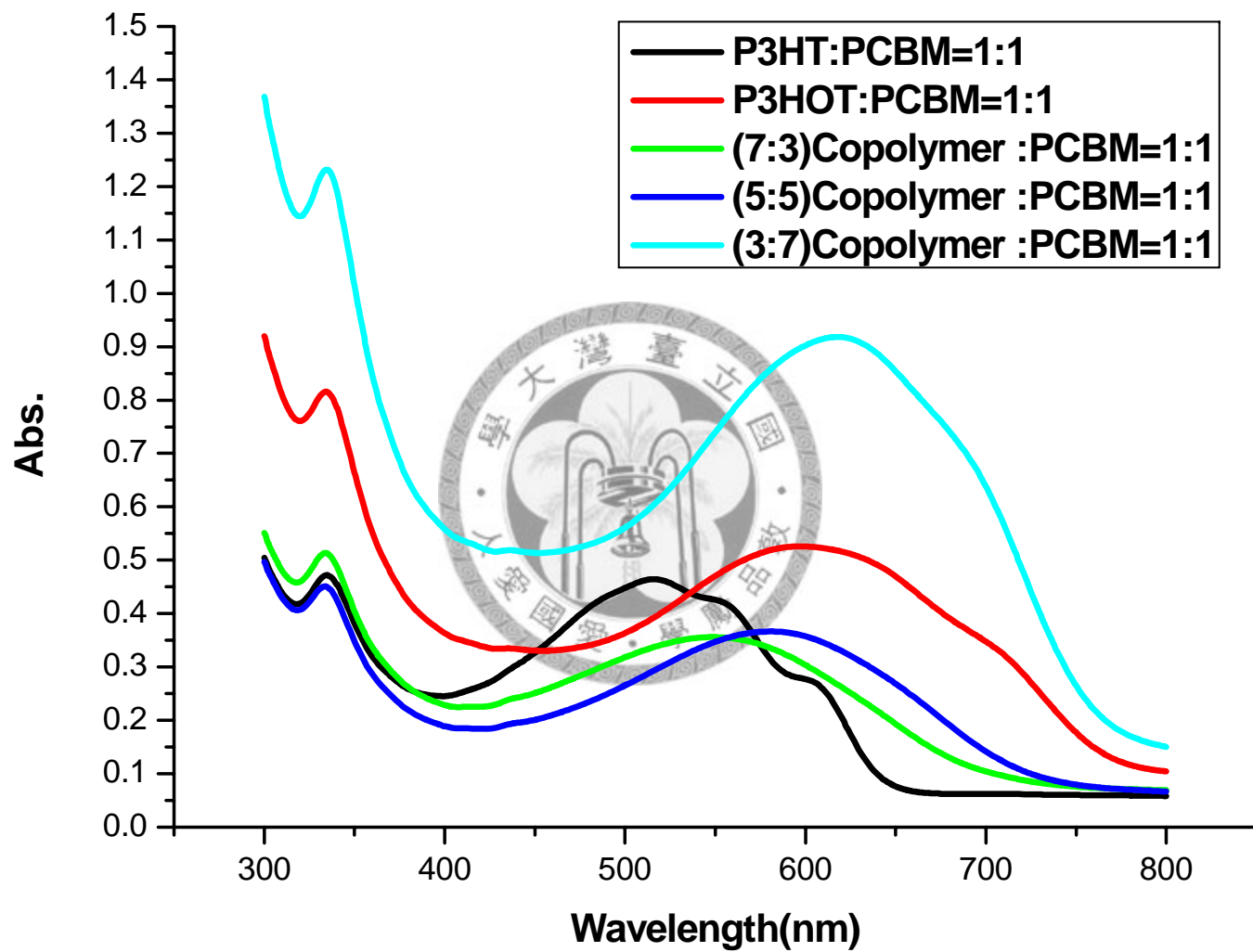


Figure 3.28 UV-vis of five different molar fraction of P3HT-P3HOT blend with PCBM in equal mole

NO	2,5-Br-3-HT	2,5-Br-3-HOT	Mol fraction of Ni(dppp)Cl ₂	Reaction Temperature (°C)	solvent	Reaction time
(1)P3HT	3.26g	0g	0.2	70	THF	60
(2)P3HT-P3HOT[7:3]	2.28g	1.03g	0.2	70	THF	60
(3)P3HT-P3HOT[5:5]	1.63g	1.71g	0.2	70	THF	60
(4)P3HT-P3HOT[3:7]	0.98g	2.39g	0.2	70	THF	60
(5)P3HOT	0g	3.42g	0.2	70	THF	60

Table2.1 Experiment in the different feed ratio of 2,5,Br-3HOT and add the same molar ratio of catalyst.

NO	2,5-Br-3-HT	2,5-Br-3-HOT	Mol fraction of Ni(dppp)Cl ₂	Reaction Temperature (°C)	solvent	Reaction time
(1)P3HT-P3HOT[5:5] 0.2mol%	1.63g	1.71g	0.2	70	THF	60
(2)P3HT-P3HOT[5:5] 0.5mol%	1.64g	1.72g	0.5	70	THF	60
(3)P3HT-P3HOT[5:5] 0.7mol%	1.63g	1.71g	0.7	70	THF	60
(4)P3HT-P3HOT[5:5] 1.0mol%	1.62g	1.70g	1.0	70	THF	60
(5)P3HT-P3HOT[5:5]	1.63g	1.71g	1.2	70	THF	60

Table 2.2 Experiment of different molar ratio of catalyst in equal molar fraction of two monomers system

NO)/Sample name	Mn	Mw	PDI	mol% of Ni(dppp)Cl ₂	Feed ratio of 3-HOT in comonomer	Real ratio of 3-HOT in copolymer
(1)P3HT	40.0k	62.8k	1.57	0.2	0%	0%
(2)P3HT-P3HOT[7:3]	30.6k	54.0k	1.76	0.2	30%	39%
(3)P3HT-P3HOT[5:5]	23.2k	49.6k	2.11	0.2	50%	57%
(4)P3HT-P3HOT[3:7]	10.3k	15.8k	1.52	0.2	70%	81%
(5)P3HOT	6.4k	10.2k	1.60	0.2	100%	100%

Table 3.1 Summary of five different molar fraction of 3-HT and 3-HOT experiment

NO/Sample name	mol% of Ni(dppp)Cl₂	Mn	Mw	PDI	Feed ratio of 3-HOT in comonomer	Real ratio of 3-HOT in copolymer
(1)P3HT-P3HOT[5:5]0.2mol%	0.2	23.5k	49.6k	2.13	50%	60%
(2)P3HT-P3HOT[5:5]0.5mol%	0.5	24.4k	49.0k	1.96	50%	57%
(3)P3HT-P3HOT[5:5]0.7mol%	0.7	20.5k	37.1k	1.89	50%	56%
(4)P3HT-P3HOT[5:5]1.0mol%	1.0	16.5k	30.4k	1.82	50%	55%
(5)P3HT-P3HOT[5:5]1.2mol%	1.2	14.4k	24.4k	1.65	50%	57%

Table 3.2 Summary of the different ratio of monomer to Ni(dppp)Cl₂ experiment results in equal molar fraction of 3HT and 3HOT system(P3HT-P3HOT[5:5])

NO/Sample name	λ_{MAX} (CHCl₃)	λ_{MAX} (Film)	UV_{film} onset (nm)	Band gap (eV)	HOMO (eV)	LUMO (eV)	Td (°C)
(1)P3HT	452	551	693	1.94	5.27	3.33	440
(2)P3HT-P3HOT[7:3]	495	568	690	1.80	5.08	3.28	362
(3)P3HT-P3HOT[5:5]	522	602	730	1.70	4.82	3.12	339
(4)P3HT-P3HOT[3:7]	579	627	765	1.62	4.71	3.09	328
(5)P3HOT	601	643	784	1.58	4.56	2.98	268

Table 3.3 Photovoltaic and thermal properties of five different molar fraction of 3-HT and 3-HOT copolymer

Polymer	2θ / (d-spacing, Å)			
	<i>low angle</i>			<i>wide angle</i>
(1)P3HT	3.38(16.9)	6.94(8.3)	10.61(5.4)	15.24(3.77)
(2)P3HT-P3HOT[7:3]	3.38(16.9)			12.18(4.71) 14.63(3.93)
(3)P3HT-P3HOT[5:5]	3.79(15.2)			14.63(3.93)
(4)P3HT-P3HOT[3:7]	4.28(13.4)			12.40(4.65) 14.70(3.91)
(5)P3HOT	4.50(12.7)			14.65(3.92)

Table 3.4 X-ray diffraction 2θ positions and calculated d spacing of P3HT-P3HOT

NO/Sample name	Voc (V)	Jsc (mA/cm²)	FF (%)	Efficiency (%)
(1)P3HT	0.38	5.83	41.5	0.92
(2)P3HT-P3HOT[7:3]	0.3	1.25	26.54	0.1
(3)P3HT-P3HOT[5:5]	0.25	2.27	31.17	0.18
(4)P3HT-P3HOT[3:7]	0.06	0.42	17.4	4.38*10 ⁻³
(5)P3HOT	0.02	0.3	0.58	3.48*10 ⁻⁵

Table 3.5 Summary of P3HT-P3HOT/PCBM bulk heterojunction solar cell performance

NO/Sample name	Mol% of Ni(dppp)Cl ₂ / Derived Mn				
(1)P3HT	2%/8.1k	0.67%/20k	0.5%/28k	0.2%/40k	
(2)P3HT-P3HOT[7:3]	2%/7.4k	0.2%/30k			
(3)P3HT-P3HOT[5:5]	1.2%/14k	1.0%/16k	0.7%/20.5k	0.5%/24k	0.2%/24k
(4)P3HT-P3HOT[3:7]	2%/8.2k	0.2%/11k			
(5)P3HOT	4%/4.1k	3%/5.8k	0.2%/6.1k		

Table 3.6 every experiment of the relationship between mole percentage and derived Mn